2012

Measurements of Reactive Trace Gases and Variable Ozone Formation Rates in South Carolina Biomass Burning Plumes

Sheryl Kashi Akagi
The University of Montana

MEASUREMENTS OF REACTIVE TRACE GASES AND VARIABLE O_3 FORMATION RATES IN SOUTH CAROLINA BIOMASS BURNING PLUMES

By

SHERYL KASHI AKAGI

M.S. Chemistry, University of Montana, Missoula, MT, 2011
B.S. Chemistry, University of Puget Sound, Tacoma, WA, 2007

Dissertation

presented in partial fulfillment of the requirements
for the degree of

PhD in Chemistry

The University of Montana
Missoula, MT

August 2012

Approved By:

Dr. Robert Yokelson, Committee Chair
Department of Chemistry

Dr. Christopher Palmer, Committee Member
Department of Chemistry

Dr. Anna Klene, Committee Member
Department of Geography

Dr. Garon Smith, Committee Member
Department of Chemistry

Dr. Richard Field, Committee Member
Department of Chemistry

Akagi, Sheryl K., PhD, Summer 2012 Chemisty

Measurements of reactive trace gases and variable O_3 formation rates in South Carolina biomass burning plumes

Advisor: Dr. Robert Yokelson, Department of Chemistry
Co-Chairperson: Dr. Chris Palmer, Department of Chemistry

ABSTRACT

Biomass burning (BB) is the second largest source of trace gases and the largest source of primary fine carbonaceous particles in the global troposphere. BB trace gases and particles are of both regional and global importance. In the US, prescribed fire and wildfire are the two major fire types and they occur frequently. Prescribed fires are ignited to improve and aid forest health, maintenance, and management. Land managers strive to minimize the impact of smoke on local communities. However, smoldering combustion can still occur, leading to complaints of smoke exposure and reduced visibility. It is clear that we need better understanding of prescribed fire emissions both for the sake of land managers who conduct these burns and for the communities affected by smoke. In October-November of 2011 we measured the trace gas emission factors from seven prescribed fires in South Carolina, U.S. using two Fourier transform infrared spectrometer (FTIR) systems and whole air sampling (WAS) into canisters followed by gas-chromatographic analyses. A total of 97 trace gas species are reported here from both airborne and ground-based platforms making this one of the most detailed field studies of fire emissions to date. The measurements included the first data for a suite of monoterpene compounds emitted via distillation of plant tissues during real fires. The known chemistry of the monoterpenes and their measured abundance suggests that they influenced post-emission formation of ozone, aerosol, and small organic trace gases such as methanol and formaldehyde in the sampled plumes. The variability in the terpene emissions in South Carolina (SC) fire plumes was high and, in general, the speciation of the emitted gas-phase non-methane organic compounds was surprisingly different from that observed in a similar study in nominally similar pine forests in North Carolina ~20 months earlier. On the other hand, the $\Delta HCN/\Delta CO$ emission ratio is fairly consistent at 0.9 ± 0.06 % for airborne fire measurements in coniferous-dominated ecosystems further confirming the value of HCN as a biomass burning indicator/tracer. The SC results also support an earlier finding that C_3-C_4 alkynes may be of use as biomass burning indicators on the time-scale of hours to a day. It was possible to measure the chemical evolution of the plume on four of the fires and significant ozone (O_3) formation ($\Delta O_3/\Delta CO$ from 10-90%) occurred in all of these plumes. Slower O_3 production was observed on a cloudy day with low co-emissions of NO_x and the fastest O_3 production was observed on a sunny day when the plume almost certainly incorporated significant additional NO_x by passing over the Columbia, SC metro area. Due to rapid plume dilution, it was only possible to acquire high quality downwind data for two other species (formaldehyde and methanol) on two of the fires. In all four cases significant increases were observed. This is likely the first direct observation of post-emission methanol production in biomass burning plumes and the precursors likely included terpenes.

ACKNOWLEDGEMENTS

Thanks to everyone who advised, helped, and encouraged me as I worked through my degree. The years I've spent in Missoula have been some of the most memorable years for me. I owe a great deal of thanks to my advisor Bob Yokelson, who has supported me in choosing a project that suited my strengths and challenged my weaknesses— thanks for encouraging me to come into my own. Thanks to my thesis committee, Ian Burling, and Ted Christian for their mentoring and guidance. I also need to acknowledge several scientists who I've thoroughly enjoyed working with over the last year: Ian Burling, Isobel Simpson, Donald R. Blake, Gavin McMeeking, Sonia Kreidenweis, Amy Sullivan, Taehyoung Lee, Shawn Urbanski, Jim Reardon, Melanie Cameron, David Griffith, Tim Johnson, David Weise, Brian Gullet, Holly Eissinger, and Hugh Coe: thank you for your contributions to this paper and for all your advise, contructive criticism, and guidance while working on this project. Thanks to my friends and the other graduate students who have been such a huge support over the years. And lastly, a big thanks to my family and Jesse, both of which whom I wouldn't have been able to do this without.

ABSTRACT…..……..…..II

ACKNOWLEDGEMENTS……..III

TABLE OF CONTENTS……...…….....IV

LIST OF FIGURES……...…….....VI

LIST OF TABLES……...…….....IX

TABLE OF CONTENTS

CHAPTER 1: INTRODUCTION **1**

1.1 GLOBAL IMPACT OF BIOMASS BURNING 1
1.2 REGIONAL IMPACT OF BIOMASS BURNING 2
1.3 MOTIVATION 3
1.3.1 Chapter 2 ..... *4*
1.3.2 Chapter 3 ..... *4*

CHAPTER 2: TERMINOLOGY AND DEFINITIONS **5**

2.1 EMISSION RATIOS, EMISSION FACTORS AND COMBUSTION EFFICIENCY 5
2.2 RESIDUAL SMOLDERING COMBUSTION (RSC) 8
2.3 NMOC, OVOC, AND NMHC 8
2.4 COMMON TERMINOLOGY USED IN COMPUTING REGIONAL/GLOBAL EMISSION ESTIMATES 9
2.5 SAMPLING CONSIDERATIONS 10
2.6 APPLICATION OF TERMINOLOGY TO A FIELD CAMPAIGN 11

CHAPTER 3: SOUTH CAROLINA REGIONAL EMISSIONS AND AGING MEASUREMENTS (SCREAM) CAMPAIGN **12**

3.1 INTRODUCTION 12
3.2 EXPERIMENTAL 15
3.2.1 Airborne Fourier transform infrared spectrometer (AFTIR) *15*
3.2.2 Land-based Fourier transform infrared spectrometer (LAFTIR) *18*
3.2.3 Whole Air Sampling (WAS) Canisters *24*
3.2.4 Other measurements on the Twin Otter *25*
3.2.5 Calculation of excess mixing ratios, normalized excess mixing ratios (NEMR), emission ratios (ER), and emission factors (EF) *28*
3.2.6 Site descriptions *30*
3.2.7 Airborne and ground-based sampling approach *33*
3.3 RESULTS AND DISCUSSION 39
3.3.1 Initial emissions *39*
3.3.2 Brief comparison to similar work *48*
3.3.3 Observation of large initial emissions of terpenes *51*
3.3.4 C_3-C_4 alkynes *62*
3.3.5 Initial emissions of nitrogen species *63*

3.3.6 Sulfur containing species *69*
3.3.7 Plume aging *70*

CHAPTER 4: CONCLUSIONS **83**

4.1 THE SOUTH CAROLINA REGIONAL EMISSIONS AND AGING MEASUREMENTS CAMPAIGN 83
4.2 FUTURE WORK 85

5 REFERENCES **86**

6 APPENDIX **110**

6.1 SCREAM ACKNOWLEDGEMENTS 110

LIST OF FIGURES

Figure 3.1. (a) A measured spectrum (red) overlaid with a limonene reference spectrum (blue). We see strong evidence of limonene in this sample, along with evidence of various other species. (b) A measured absorbance spectrum (red) and a fitted spectrum (blue) overlaid, with the residual shown above (aqua). MALT was used to generate concentrations of limonene, along with other absorbing species in this wavelength range as shown beneath.……..……17

Figure 3.2. The LAndbased Fourier Transform Infrared Spectrometer (LAFTIR) used during the South Carolina Regional Emissions and Aging Measurements Campaign…….…..19

Figure 3.3. (a) MIDAC Spectrometer, and (b) Adjusting the spot pattern for optimal pathlength and alignment of the IR beam into and out of the cell……...22

Figure 3.4. Two LAFTIR absorbance spectra acquired before (red) and after (blue) instrument upgrades. The 2450-2600 cm^{-1} noise region is shown, which is typically void of absorbing species. The spectrum shown in blue has lower noise by a factor of ~3. ……..……..….24

Figure 3.5. Photographs of some of the fuels sampled in this work that are major contributers to residual smoldering emissions including (a) a live tree base, and (b) dead/down debris……..**.....**34

Figure 3.6. Overview of all flight tracks in the South Carolina regional emissions and aging measurements (SCREAM) study. "RF" indicates research flight and the dates of each research flight are shown in Table 3.3 except for RF06, which sampled urban emissions only on 5 Nov. "Hotspots" are the MODIS thermal anomalies from 30 Oct to 10 Nov, 2011. Of the seven fires sampled in this study, only the pine plantation fire was detected as a hotspot. Due to a GPS malfunction, the 10 Nov flight track is at 2-min resolution retrieved from the USFS automated flight following system…….……..…..35

Figure 3.7. Detailed flight track and AFTIR downwind sample locations for the Twin Otter aircraft during RF03 (pink) and RF04 (black), which sampled the Block 9b fire at Fort Jackson on 1 Nov 2011. (The hotspot, which appears to intersect RF03 is actually from the pine plantation fire sampled on 2 Nov.)…….36

Figure 3.8. Detailed flight tracks and AFTIR downwind sample locations for the Twin Otter aircraft during RF07 (red) and RF08 (black) on 7 and 8 Nov, sampling the Georgetown and Francis Marion fires, respectively……..…...37

Figure 3.9. Emission ratio plots for ΔCH4/ΔCO from (a) the AFTIR cell and (b) independent RSC targets on the ground from burn blocks 6 and 9b, respectively. Black circles denote samples collected by FTIR and red circles denote samples that were collected by WAS on the indicated fires……...40

Figure 3.10. Comparison of this work (blue) with Burling et al. (2011) (orange) from (a) airborne and (b) ground-based platforms..…….....50

Figure 3.11. Absorption spectra of ground-based smoke samples normalized to the CO absorption band centered at 2143 cm^{-1} presented in Burling et al. (2011). The reference spectrum is a linear sum of the three equal parts of the monoterpene species, alpha-pinene, beta-pinene, and limonene spectra (Sharpe et al., 2004) and is shown only as a qualitative comparison…….……..……...53

Figure 3.12. Emission factors (g kg^{-1}) of monoterpenes and isoprene measured from this work. We compare with data from Simpson et al. (2011) who measured alpha/beta-pinene and isoprene from an airborne platform (orange), though EF(isoprene) is too small to be visible…...……...…..56

Figure 3.13. Alkyne emission factors (g kg^{-1}) as a function of MCE from the Block 6, 9, 22b, and plantation fires in this study measured from airborne and ground-based platforms. The positive correlation of EF vs. MCE suggests all alkynes are emitted chiefly by flaming combustion processes…….……..…...……63

Figure 3.14. EF(NH_3) (g kg^{-1}) as a function of MCE for the Fort Jackson pine burns of this study measured from both airborne (blue) and ground-based (red) platforms. We also show ground-based, airborne, and laboratory (green) measurements in similar fuels from Burling et al. (2011), airborne data from Mexican pineoak forests from Yokelson et al. (2011), and pine litter laboratory data from Fort Benning, GA (Burling et al., 2010). Anti-correlations of EF(NH_3) vs. MCE for ground-based (red line) and airborne (blue line) measurements are shown.…….……..64

Figure 3.15. Comparison of HCN/CO study-average emission ratios (mol/mol) measured from airborne (blue), ground-based (red), and laboratory (green) platforms from five North American studies in pine forest fuels. We also show four ER(HCN/CO) in other fuel types for comparison. The large variation shown for peat is due to a very large value for Indonesian peat that is included in the calculation…….…….…..66

Figure 3.16. HCN fire-average emission factors (g kg^{-1}) as a function of MCE for pine/conifer fuel types measured airborne, ground-based, and laboratory platforms. The data show a general anti-correlation with MCE, however, ground-based data alone have higher variability and less MCE dependence…….…..67

Figure 3.17. $\Delta O_3/\Delta CO$ NEMR ratios vs. time since emission (h). Airborne measurements were collected up to ~2.5 h downwind. Fires that we were able to collect downwind data on are shown: Block 9b (1 Nov, black), Georgetown (7 Nov, blue), Francis Marion (7 Nov, green), and Bamberg (10 Nov, red). The y-intercept of observed trendlines is forced to the average $\Delta O_3/\Delta CO$ NEMR at time t = 0 h for each given fire. Solid circles reflect data that was considered Lagrangian while open circles labeled "non-L" represent non-Lagrangian samples collected on that respective day……..……...……73

Figure 3.18. Downwind sample locations from both flights on 1 Nov (Block 9b) fire at Fort Jackson. Urban emission sources (airport and power plant, indicated as red and black squares, respectively) are also shown...……....…….75

Figure 3.19. $\Delta O_3/\Delta CO$ vs. time since emission from this study (black), Yokelson et al. (2009) (red), and Akagi et al. (2012) (green)…….……..77

Figure 3.20. $\Delta CH_3OH/\Delta CO$ NEMR ratios vs. time since emission (h). Airborne measurements were collected up to ~2.5 h downwind. Fires on which we were able to collect downwind data with good SNR are included here: Block 9b (1 Nov, black) and Francis Marion (8 Nov, green). The y-intercept of observed trendlines is forced to the average ER(CH_3OH) at time t=0 for each particular fire. Solid circles reflect data that was considered Lagrangian while open circles labeled "non-L" represent non-Lagrangian samples collected on that respective day……...…....80

Figure 3.21. $\Delta HCHO/\Delta CO$ NEMR ratios vs. time since emission (h). Airborne measurements were collected up to ~2.5 h downwind. Fires which we were able to collect downwind data, Block 9b (1 Nov, black) and Francis Marion (8 Nov, green), are included here. The y-intercept of observed trendlines is forced to the average ER(HCHO) at time t=0 for each particular fire. Solid circles reflect data that was considered Lagrangian while open circles labeled "non-L" represent non-Lagrangian samples collected on that respective day…….....82

LIST OF TABLES

Table 3.1. Fire name, location, date, fuels description, size, atmospheric conditions, and burn history of fires sampled in this work…….……..……32

Table 3.2. Unique ground-based fuels sampled by LAFTIR from Blocks 6, 9b, and 22b at Fort Jackson, SC……..…….……...34

Table 3.3. Emission factors (g kg^{-1}) measured using FTIR and WAS from ground-based and airborne platforms…….…..……42

Table 3.4. Statistics for the linear regression of EF as a function of MCE for combined ground-based and airborne fire-average measurements. Values in parentheses represent 1-σ standard deviation…….……...46

Table 3.5. Airborne and ground-based emission ratios of measured terpenes from SC fires, shown in order of abundance……...……54

CHAPTER 1: INTRODUCTION

1.1 *Global impact of biomass burning*

Biomass burning (BB) can be broadly defined as open or quasi-open combustion of any non-fossilized vegetative or organic fuel. Examples range from open fires in forests, savannas, crop residues, semi-fossilized peatlands, etc. to biofuel burning (e.g. cooking fires, dung burning, charcoal or brick making, etc.). Savanna fires, domestic and industrial biofuel use, tropical forest fires, extratropical (mostly boreal) forest fires, and crop residue burning are thought to account for the most global biomass consumption (in the order given). Overall, BB is the largest source of primary fine carbonaceous particles and the second largest source of trace gases in the global atmosphere (Bond et al., 2004; Andreae and Merlet, 2001; Forster et al., 2007; Guenther et al., 2006).

Although episodic in nature and highly variable, biomass burning emissions can contribute to local, regional, and global air quality and climate forcings (Wiedinmyer and Hurteau, 2010). Particles emitted and formed in BB plumes have major direct and indirect effects on climate (Hobbs et al., 1997; Rosenfeld, 1999) and contribute to dense continental-scale haze layers that occupy much of the tropical boundary layer (and sometimes large parts of the boreal boundary layer) during the dry season (Andreae et al., 1988; Reid et al., 1998; Wofsy et al., 1992; Eck et al., 2003). A multipart review by Reid et al. (2005a; b) focused on the physical and optical properties of biomass burning particles and their impacts. These topics have been the subject of much ongoing research (e.g. Andreae et al., 2004; Ramanathan and Carmichael, 2008; Grieshop et al., 2009).

The trace gases emitted by biomass burning have a significant influence on the atmosphere, which includes a major contribution to the formation of global tropospheric ozone (O_3), an important greenhouse gas (Sudo and Akimoto, 2007). The O_3 formed can also affect air quality: e.g. Pfister et al. (2007) show that BB emissions from California wildfires in 2007 increased downwind ozone concentrations in rural regions. Trace gases from BB can also contribute to the secondary formation of aerosol particles (Reid et al., 1998; Alvarado and Prinn, 2009; Yokelson et al., 2009). The effect of BB trace gases on the oxidizing power of the troposphere is an important, complex issue. The hydroxyl radical (OH) is a key oxidant in the global troposphere and is mostly produced in the tropics, which is also where ~70-80% of BB is thought to occur (Crutzen and Andreae, 1990; van der Werf et al., 2010). The carbon monoxide (CO) and NMOC produced by BB are continually removed via reaction with OH while photolysis of some of the oxygenated NMOC and the O_3 formed in BB plumes can be an OH source (Crutzen and Andreae, 1990; Singh et al., 1995). Coupled with this picture are large tropical biogenic emissions of isoprene, which has a complex oxidation scheme that is still under investigation, but results in some OH regeneration and significant CO production (Lelieveld et al. 2008; Paulot et al., 2009; Archibald et al., 2010; Peeters et al., 2009).

1.2 *Regional impact of biomass burning*

In the US, biomass burning in the form of prescribed and wildfires can greatly impact regional air quality. In particular, biomass burning that occurs year-round is a prominent domestic source of gas and particle emissions. These fires may be prescribed or ignited naturally. Prescribed burning is a significant fraction of US BB and it is used to restore or maintain the natural, beneficial role of fire in many terrestrial ecosystems; reduce fire risk by

consuming accumulated wildland fuels under preferred weather conditions; and accomplish other land management objectives (Biswell 1989; Hardy et al., 2001; Carter and Foster, 2004; Wiedinmyer and Hurteau, 2010). These burns are often recurrent, sometimes near populated areas, and despite being controlled may occasionally have negative air quality impacts. Together, wild and prescribed fires are thought to produce about one-third of the total $PM_{2.5}$ (particle mass with aerodynamic diameter <2.5 μm) in the US (Watson, 2002; Park et al., 2007). The particles can impact local to regional air quality, health, and visibility (McMeeking et al., 2006). In addition, fires can influence regional levels of ozone (O_3), which is an air toxic (Pfister et al., 2006). Large areas of the US commonly have O_3 mixing ratios not far below the US national ambient O_3 air quality standard (75 ppb 8-hour average). Thus, in these areas even modest production of O_3 in a smoke plume can potentially lead to O_3 levels that exceed air quality criteria. Because fire has both benefits and drawbacks, the optimum amount and timing of prescribed fire is an area of active research and better information on the initial chemistry and evolution of BB emissions is a major need (Haines and Cleaves, 1999; Sandberg et al., 2002; Yoder et al., 2003; Kauffman, 2004; Stephens et al., 2007; Akagi et al., 2011).

1.3 *Motivation*

This work is aimed towards improving our knowledge of the chemistry of biomass burning emissions; both near the source and in evolving downwind plumes. Accurate representation of biomass burning in the troposphere is a key element in our ability to model climate, chemistry, and air quality in global and regional atmospheric chemistry models (GACMs).

1.3.1 **Chapter 2**

We define several important terms in biomass burning, including emission ratio (ER), emission factor (EF), and modified combustion efficiency (MCE). We discuss the acronyms used to describe categories of species emitted from biomass burning, and briefly define common terms used in quantifying biomass for emission estimates.

1.3.2 **Chapter 3**

In Chapter 3 we report prescribed fire emissions from the South Carolina Regional Emissions and Aging Measurement (SCREAM) campaign. The major feature of this study was to expand the scope of measurements to include: (1) emissions data for fires with additional important fuel types as well as fires that burned in forest stands with a broader range of management histories, (2) post-emission plume evolution data on days with different solar insolation and on a day with significant mixing of urban and fire emissions, and (3) addressing all these topics with a significantly expanded suite of instrumentation. By comparing emission factors presented here with previous EFs in pine-forest understory fuels, we can better understand the natural variability that can be observed even for study-averaged values for ecosystems considered nominally similar in the atmospheric community.

CHAPTER 2: TERMINOLOGY AND DEFINITIONS

2.1 *Emission ratios, emission factors and combustion efficiency*

An excess mixing ratio (EMR) is defined as the mixing ratio of species X in smoke minus its mixing ratio in background air. The EMR of X is often denoted by "ΔX," where the measured value reflects the degree of plume dilution and the instrument response time (Andreae et al., 1988; Yokelson et al., 1999). As a standardization measure, ΔX is often divided by an EMR of a fairly non-reactive co-emitted smoke tracer (ΔY), such as CO or CO_2; this molar ratio is defined as the Normalized Excess Mixing Ratio (NEMR), which can be measured anywhere within a plume. A special case of the NEMR is the "emission ratio" (ER): the molar ratio between two emitted compounds (also written as ΔX/ΔY), which should be reserved for emission measurements taken at the source (fresh smoke). The NEMR is highly variable for reactive gases and some aerosol species downwind from fires and dependent on the details of the post-emission processing. Thus for a reactive compound, a NEMR measured downwind may not be equal to the emission ratio even though it is expressed in similar fashion. A simpler alternative term sometimes used to refer to downwind NEMR is the "enhancement ratio" (Lefer et al., 1994), but since it would have the same abbreviation as "emission ratio" and some species are "depleted" downwind we do not use this term in this work.

We use ER to derive emission factors (EF) in units of grams of X emitted per kilogram of dry biomass burned using the carbon mass balance method (Ward and Radke, 1993), as will be discussed in Sect. 3.2.5. The method assumes that all burned carbon is volatilized or contained

in the emitted aerosol and that all major carbon-containing species have been measured. The inability to detect all carbon species can inflate emission factors by 1-2% when using the carbon mass balance method (Andreae and Merlet, 2001). The carbon content in the fuel must also be measured or estimated EF scale linearly in proportion to the assumed fuel carbon fraction.

Combustion efficiency (CE) - the fraction of fuel carbon converted to carbon as CO_2- can be estimated from measured emission ratios with the detailed equation given elsewhere (e.g. Sinha et al. 2003). The CE at any point in time during a fire, or for the fire as a whole, depends strongly on the relative contribution of flaming and smoldering combustion, with a higher CE indicating more flaming and lower MCE indiciating more smoldering (Ward and Radke, 1993; Yokelson et al., 1996). Flaming combustion involves rapid reaction of O_2 with gases evolved from the solid biomass fuel and is common in foliage or dry, small diameter aboveground biomass. Flaming combustion converts the C, H, N, and S in the fuel into highly oxidized gases such as CO_2, H_2O, NO_x, and SO_2, respectively, and produces most of the black (or elemental) carbon particles. As a fire progresses, smoldering combustion tends to play a more dominant role via surface oxidation (or gasification, commonly known as "glowing") and pyrolysis (mostly the thermal breakdown of solid fuel into gases), often affecting large-diameter aboveground biomass and belowground biomass. Smoldering produces most of the CO, CH_4, NMOC, and primary organic aerosol. Smoldering and flaming frequently occur simultaneously during a fire, and distinct combustion phases may not occur. Flaming (~1400 K) and glowing (~800-1000 K) are the two heat sources driving pyrolysis and fuel temperatures can range from unheated to that of a nearby heat source. We also note that smoldering is not caused by a deficiency of O_2; rather chemisorption of O_2 on char is exothermic and helps drive glowing combustion (Yokelson et al., 1996). Large natural

variability in fuel geometry, growth stage, moisture, windspeed, etc. causes large natural variability in the relative amount of biomass consumption by flaming and smoldering combustion, even within a single fire type category. This, coupled with variation in fuel chemistry, leads to a large range in the naturally occurring EF for most species for any fire type as discussed further.

The combustion efficiency, as stated above, can be useful in indicating the relative abundance of flaming and smoldering combustion. Since CE is hard to measure, the modified combustion efficiency (MCE), which is defined as $\Delta CO_2/(\Delta CO_2+\Delta CO)$, is commonly reported as an estimate of CE accurate within a few percent (Ferek et al., 1998). Pure flaming has an MCE near 0.99 while the MCE of smoldering varies over a larger range (~0.65-0.85), but is most often near 0.8. Thus an overall fire-integrated MCE near 0.9 suggests roughly equal amounts of biomass consumption by flaming and smoldering. Since both CE and MCE indicate the relative amount of flaming and smoldering combustion, both parameters often correlate reasonably well with EF (Fig. 4.3 in Ward and Radke, 1993; Fig. 3 in Yokelson et al., 2003). For example, in Fig. 3 of Yokelson et al. (2003) airborne measurements of EF(CH_4) for individual fires range from ~0.5 g kg^{-1} to ~3.5 g kg^{-1} (a factor of 7) with decreasing MCE. Additional variation in EF and MCE would result from considering the unlofted emissions from residual smoldering combustion (RSC) (see, e.g., Bertschi et al., 2003b; Christian et al., 2007; Yokelson et al., 2008). In general, the MCE dependence of "EF(X)" for a fire type allows calculation of a specific EF(X) for any known MCE. However, we do not yet have good data on how regional average MCE may evolve with time over the course of the biomass burning season for the major types of

burning. Thus, in this work we report fire-averaged EF and (where possible) an estimate of the expected naturally occurring range in the average EF as the standard deviation.

2.2 *Residual Smoldering Combustion (RSC)*

Prolonged smoldering after local convection from the flame front has ceased is often termed "residual smoldering combustion" (RSC, Bertschi et al., 2003) and is responsible for many of the negative air quality impacts of prescribed burning on a local scale (e.g. smoke exposure complaints, visibility-limited highway accidents (Achtemeier, 2006)). Ground-based systems are usually required for measurements of RSC smoke emissions. The emissions from RSC burning are quite different from those of flaming combustion due to the lower combustion efficiency. The strategies adopted by land managers for prescribed burning typically minimize the amount of RSC and its impacts on local populations. In contrast, wildfires normally burn when "fire danger" is at high levels and forest floor moisture is at a minimum (Deeming et al., 1978), often resulting in significant amounts of RSC. There are usually few or no options for reducing smoke impacts on populated areas from wildfires. Although not a factor in this study, in some wildfires, organic soils (peat) may also burn contributing to RSC. Residual smoldering combustion can continue for weeks after initial ignition and can account for a large portion of the total biomass consumed in a fire (Bertschi et al., 2003; Rein et al. 2009). There are very few peer-reviewed field measurements of the emissions from RSC in the temperate regions of the US.

2.3 *NMOC, OVOC, and NMHC*

Non-methane hydrocarbons (NMHC) are defined as organic compounds excluding methane (CH_4) that contain only C and H; examples include alkanes, alkenes, alkynes, aromatics, and

terpenes. Oxygenated volatile organic compounds (OVOC) contain C, H, and O; examples include alcohols, aldehydes, ketones, and organic acids. NMHC and OVOC together account for nearly all the gas-phase non-methane organic compounds (NMOC) emitted by fires. The distinction is important when discussing the role of NMOCs in post-emission chemistry. All of the organic compounds are important in secondary processes such as ozone and aerosol formation, but the OVOC are more abundant (60-80% of NMOC), and the OVOC and NMHC tend to have different atmospheric chemistry (Singh et al., 1995; Finlayson-Pitts and Pitts, 2000). It is also important to note that only on the order of 50% (by mass) of the observed gas-phase NMOC can be assigned to specific compounds (Christian et al., 2003; Karl et al., 2007). The remaining unidentified species are mostly high molecular weight NMOC. The unidentified species evidently play a large role in plume chemistry (Trentmann et al., 2005; Alvarado and Prinn, 2009).

2.4 *Common terminology used in computing regional/global emission estimates*

We briefly define common terms used in quantifying biomass for emission estimates. Biomass is described as primarily live (phytomass) or dead (necromass) plant material and can be discussed as total aboveground biomass (TAGB)—referring to the litter layer and everything above—or total belowground biomass (TBGB), referring to duff, peat, organic soils, and roots (Seiler and Crutzen, 1980). Both terms are normally expressed on a dry weight basis. Fuel moisture can be calculated as (wet weight-dry weight)/dry weight, and along with fuel geometry affects what biomass is likely to burn. The term "fuel" in the forestry literature refers to only that portion of the total available biomass that normally burns under specified fire conditions (Neary et al., 2005). Thus, "fuel" and "biomass" are not equivalent terms in forestry, although

they are sometimes used interchangeably by atmospheric chemists. Both fuel and biomass loading are typically expressed as the mass of fuel or biomass per unit area on a dry weight basis. A combustion factor is the fraction of biomass exposed to a fire that was actually consumed or volatilized. The biomass loading is often multiplied by a combustion factor to derive an estimate of how much biomass was consumed, otherwise known as the biomass consumption (per unit area). An estimate of the total combusted biomass can be obtained given biomass consumption per unit area and an estimate of the area burned.

2.5 *Sampling considerations*

Smoke contains numerous species with atmospheric lifetimes ranging from micro-seconds to years. Other than a few continuously regenerated intermediates, current technology can only measure atmospheric species that are abundant and stable enough to have lifetimes of a few minutes or longer. In practice this means that measurements show the effects of aging for some detected species unless samples are taken within 10s of meters above lab fires or within 1-2 km of fires in the field. Under these conditions, smoke typically has CO concentrations in the range 5-1500 ppmv in the lab or on the ground, and 2-30 ppmv in airborne studies. Figure 3 in Christian et al. (2003) or Figures 2-4 in Yokelson et al. (2008) show that field samples meeting the above "freshness criteria" can often return similar emission factors for trace gases when compared to lab studies at the same MCE. Laboratory fires sometimes tend to burn with a different average MCE than fires in similar fuels burning in the natural environment, but this can be accounted for as described in Yokelson et al. (2008).

Another important consideration for field studies is that smoldering combustion can produce unlofted smoke with low MCE that is not amenable to airborne sampling. Ground-based

sampling can measure these sometimes substantial emissions, but realistic estimates of the biomass consumption contributing to the two different types of smoke are needed to properly weight the ground-based and airborne measurements (Christian et al., 2007).

2.6 *Application of terminology to a field campaign*

All of the aforementioned definitions and terminology are important when interpreting "real" data from the field. The upcoming chapter applies the methodologies and terms discussed here to assess prescribed fire emissions from the South Carolina Regional Emissions and Aging Measurements (SCREAM) campaign.

CHAPTER 3: SOUTH CAROLINA REGIONAL EMISSIONS AND AGING MEASUREMENTS (SCREAM) CAMPAIGN

3.1 *Introduction*

On a global scale, biomass burning is thought to be the largest source of primary fine carbonaceous particles in the atmosphere and the second largest source of total trace gases (Crutzen and Andreae, 2000; Bond et al., 2004; Akagi et al., 2011). In the southeastern U.S. and to a lesser extent in other parts of the U.S. and other countries, prescribed fires are ignited to restore or maintain the natural, beneficial role that fire plays in some desirable, fire-adapted ecosystems and to reduce wildfire risk and smoke impacts by consuming accumulated fuels under "safe" weather conditions where smoke dispersion can be at least partially controlled (Biswell 1989; Hardy et al., 2001; Carter and Foster, 2004; Keeley et al., 2009; Wiedinmyer and Hurteau, 2010; Cochrane et al., 2012). On many southeastern U.S. wildland sites, land managers will implement prescribed burning every 1-4 years under conditions where fuel consumption is expected only in understory fuels and the forecast transport is such that smoke impacts should be minimized. However, despite land managers best efforts, prescribed fires, along with wildfires, do impact local to regional O_3, air quality, health, and visibility in the southeastern U.S. and elsewhere (McMeeking et al., 2006; Pfister et al., 2006; Park et al., 2007). Thus, an important element of optimizing land-use strategies for ecosystem health, climate, and human health requires is a detailed knowledge of the chemistry, evolution, and health effects of smoke (Rappold et al., 2011; Roberts et al., 2011).

The work reported here is the last field deployment in a series of DoD funded measurements of the emissions from southeastern U.S. prescribed fires (Burling et al., 2010; 2011; Yokelson et al., 2012), otherwise known as the South Carolina Regional Emissions and Aging Measurements (SCREAM) campaign. The major feature of this last study was to expand the scope of measurements to include: (1) emissions data for fires in additional important fuel types as well as fires that burned in forest stands with a broader range of management histories, (2) post-emission plume evolution data on days with different solar insolation and on one day with significant mixing of urban and fire emissions, and (3) addressing all these topics with a significantly expanded suite of instrumentation. The expanded range of relevant prescribed fire conditions we sampled involved several aspects. The previous pine-forest understory-fire measurements in this overall study had been made in February and March of 2010 after a prolonged period of high rainfall and in loblolly pine stands with a history of frequent prescribed fire. Through collaboration with Fort Jackson, in this final phase of the study we were able to sample the emissions from pine-forest understory fires in longleaf pine stands that had not been previously subjected to frequent prescribed fires. The lower historical frequency of prescribed fire contributed to denser stands with a higher ratio of litter/shrubs in the understory fuels. Further, the fires reported here occurred during the Fall 2011 prescribed fire season before the region had fully recovered from a prolonged summer drought. Thus, we did not isolate the effect of any one variable, but did very significantly increase the range of germane conditions under which prescribed fire emissions were measured. Plume evolution data could not be acquired during the Spring 2010 prescribed fire measurements in pine-forest understory fires, due primarily to air-space restrictions. In this study we did have access to the downwind plume on 4 of the 7 fires and

we measured photochemical changes on one day with thick cloud cover and three days with high solar insolation that included one day that featured mixing of fire emissions with the urban plume from the Columbia, SC metro area. The suite of instruments was very significantly expanded for the final deployment reported here. The Spring 2010 emissions data were produced by airborne and ground-based FTIR (AFTIR and LAFTIR, respectively) and an airborne nephelometer to estimate $PM_{2.5}$ (Burling et al., 2011). In the work reported here, the trace gas measurements were supplemented by whole air sampling (WAS) on the ground and in the air and by a long-open-path, telescope based FTIR system (OPAG) deployed on the ground on the fire perimeter at selected locations. The airborne measurements were augmented by a suite of aerosol instrumentation including: a high-resolution time-of-flight aerosol mass spectrometer, a single particle soot photometer, and a particles into liquid sampler (PILS) interfaced to a total organic carbon analyzer. In addition, the U.S. Environmental Protection Agency (EPA) deployed a suite of trace gas and particle analyzers on mobile all-terrain vehicles and fuel consumption and fire-spread rates were documented at several locations.

In this work we report the measurements obtained by AFTIR, LAFTIR, and WAS, which sampled trace gases in either well-lofted or initially unlofted emissions. The airborne aerosol measurements will be reported separately along with recent, previously unpublished aerosol data obtained with similar instrumentation on simulated fires in a laboratory. Both the OPAG and EPA data were sensitive to a mix of unlofted emissions and emissions that were similar to the lofted emissions, but temporarily accessible to ground-based sampling when redirected by wind gusts. The OPAG and EPA data will also be reported and interpreted separately.

3.2 *Experimental*

3.2.1 **Airborne Fourier transform infrared spectrometer (AFTIR)**

The AFTIR on the Twin Otter was similar in concept to AFTIR instruments flown from 1997-2010 and described elsewhere (Yokelson et al., 1999; Burling et al., 2011). However, the 2011 version of AFTIR featured several hardware changes including the deployment of a Bruker Matrix-M IR Cube FTIR spectrometer. The FTIR was operated at a spectral resolution of 0.67 cm^{-1} (slightly lower than the previously used resolution of 0.5 cm^{-1}) and four spectra were acquired every 1.5 seconds with a duty cycle > 95%. The f-matched exit beam from the FTIR was directed by MgF_2-coated, silver, flat mirrors into a closed-path doubled White cell (IR Analysis) permanently aligned at 78 m. The exit beam from the cell was directed by similar optics back into the FTIR, which contained an internal, wide-band, LN_2-cooled, MCT detector. A forward-facing halocarbon wax coated inlet (25 mm i.d.) opening 30 cm above the top of the leading edge of the aircraft cabin ceiling directed ram air into a 25 mm diameter PFA (perfluoroalkoxy) tube that conducted the air to the White cell. The noise level for the four scans co-added every 1.5 seconds was ~0.0004 absorbance units, which allowed CO and CH_4 to be measured in near "real time" with about 3-5 ppb peak to peak noise. Peak to peak noise for CO_2 operating in this manner was about 1 ppm. The temporal resolution with the valves open was actually limited by the cell 1/*e* exchange time of about 5-10 s at typical Twin Otter sampling speeds of ~40-80 m s^{-1}. Fast-acting, electronically activated valves located at the cell inlet and outlet allowed flow through the cell to be temporarily halted so that more scans could be averaged of "grab samples" to increase sensitivity. Averaging ~100 scans (150 s) of a "grab sample" reduced peak to peak noise to ~0.00003 absorbance units providing e.g. a methanol

detection limit better than ~400 pptv (SNR = 1). At times we averaged scans obtained with the control valves open, which gave SNR dependent on the time to transect the plume. AFTIR sensitivity is also impacted by interference from water vapor, which is highly variable. In general the sensitivity has improved up to a factor of 30 depending on the spectral region since the first prototype AFTIR system was flown in 1997-2006 and detection limits for the compounds we report (see list below) other than CO_2 ranged from the hundreds of ppt to ten ppb for NO and NO_2 where the gain in SNR was partially canceled by the decreased resolution. Total weight and power requirements for the AFTIR system remained at 136 kg and 160 W, respectively.

The averaged sample spectra were analyzed either directly as single-beam spectra, or as transmission spectra referenced to an appropriate background spectrum, via multi-component fits to selected frequency regions with a synthetic calibration non-linear least-squares method (Burling et al., 2011; Griffith, 1996; Yokelson et al., 2007a). The fits utilized both the HITRAN (Rothman et al., 2009) and Pacific Northwest National Laboratory (PNNL) (Johnson et al., 2006; Johnson et al., 2010; Sharpe et al., 2004) spectral databases. As an example, a measured smoke absorbance spectrum (red) overlaid with a reference spectrum for limonene (blue) is shown in Fig. 3.1a, where we see strong evidence of limonene absorption in this sample. However, due to overlapping features from multiple compounds, traditional single-peak analysis techniques cannot be used to quantify the contributions of individual species. In Fig. 3.1b our multi-component fit analysis technique has been used to generate the mixing ratios of limonene and other species that absorb in this spectral window. Fig 3.1b shows a typical spectral fit (blue) overlaid the measured spectrum (red) from Fig 3.1a (note the unknown compound appearing at 882 cm^{-1}).

(a)

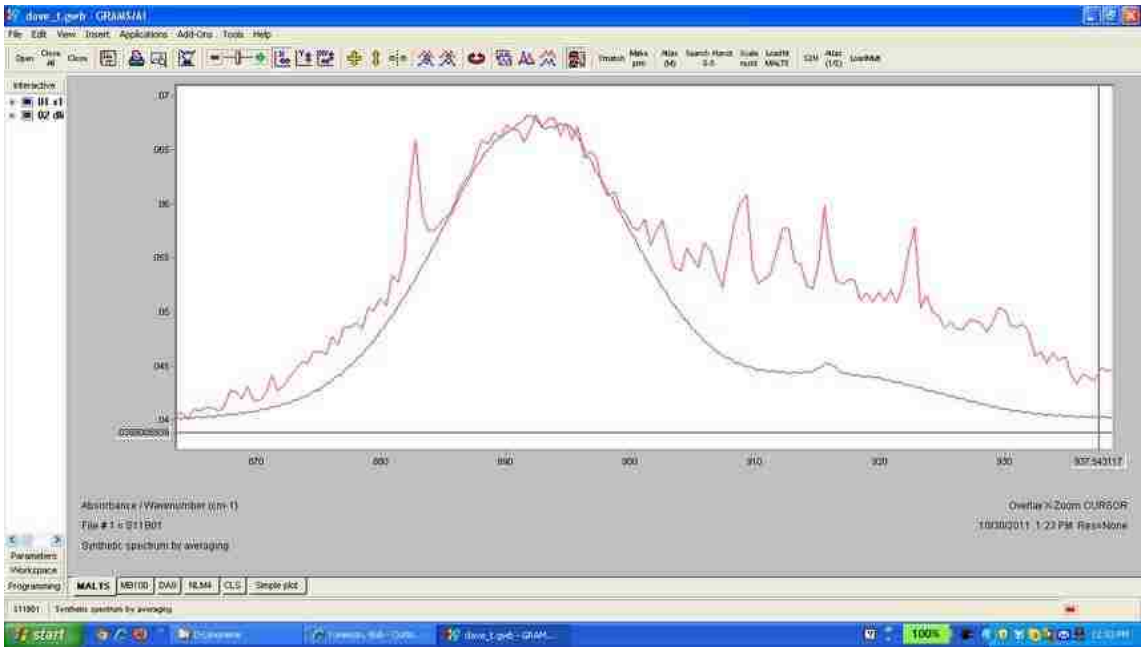

(b)

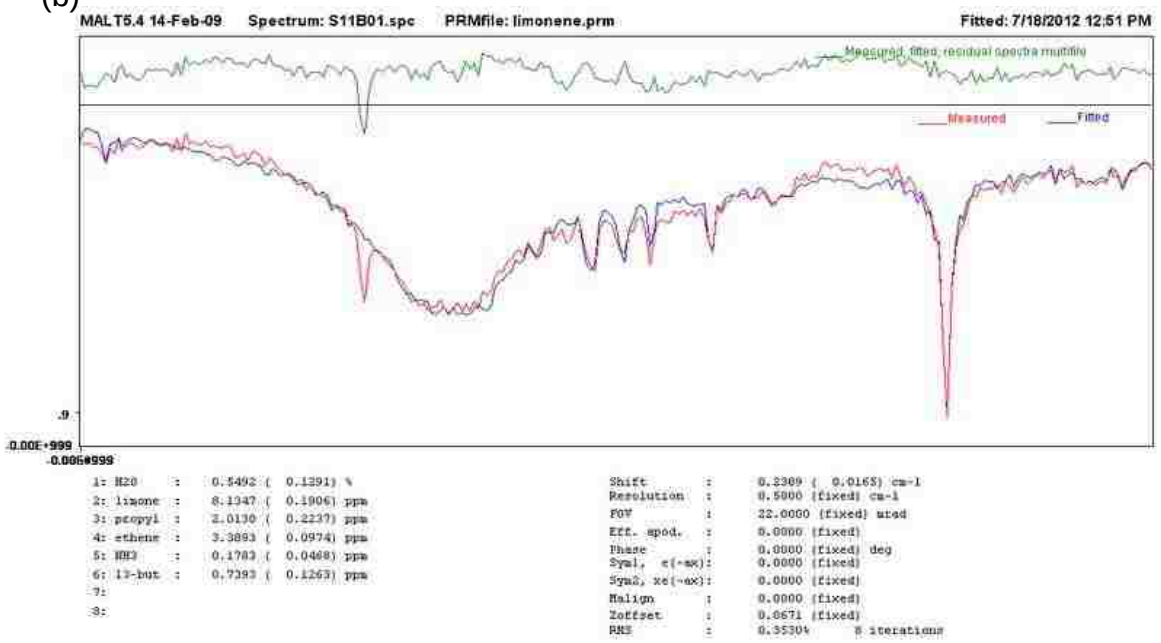

Figure 3.1. (a) A measured spectrum (red) overlaid with a limonene reference spectrum (blue). We see strong evidence of limonene in this sample, along with evidence of various other species. (b) A measured absorbance spectrum (red) and a fitted spectrum (blue) overlaid, with the residual shown above (aqua). MALT was used to generate concentrations of limonene, along with other absorbing species in this wavelength range as shown beneath.

As an exception to the fitting process, NO and NO_2 only were analyzed by integration of selected, isolated peaks in the absorbance spectra. In all, the following gases were quantified and accounted for most of the features observed in the smoke spectra: water vapor (H_2O), carbon dioxide (CO_2), carbon monoxide (CO), methane (CH_4), nitric oxide (NO), nitrogen dioxide (NO_2), ammonia (NH_3), hydrogen cyanide (HCN), nitrous acid (HONO), peroxy acetyl nitrate (PAN, $CH_3C(O)OONO_2$), ozone (O_3), glycolaldehyde ($HOCH_2CHO$), ethylene (C_2H_4), acetylene (C_2H_2), propylene (C_3H_6), limonene ($C_{10}H_{18}$), formaldehyde (HCHO), 1,3-butadiene (C_4H_6), methanol (CH_3OH), furan (C_4H_4O), phenol (C_6H_5OH), acetic acid (CH_3COOH), and formic acid (HCOOH). The spectral retrievals were almost always within 1% of the nominal values for a series of NIST-traceable standards of CO_2, CO, and CH_4 with accuracies between 1 and 2%. For NH_3 only, we corrected for losses on the cell walls as described in Yokelson et al. (2003). The excess mixing ratios for any species "X" in the plumes (denoted ΔX, the mixing ratio of species "X" in a plume minus its mixing ratio in background air) were obtained directly from the absorbance or transmission spectra retrievals or by difference between the appropriate single beam retrievals for H_2O, CO_2, CO, and CH_4.

3.2.2 **Land-based Fourier transform infrared spectrometer (LAFTIR)**

Ground-based FTIR measurements were made with our mobile, battery-powered Fourier transform infrared spectrometer (Christian et al., 2007; Figure 3.2). This easily transportable, self-powered system can be wheeled across varied terrain to access remote smoke sampling sites. The vibration-isolated LAFTIR optical bench holds a MIDAC 2500 spectrometer with an LN_2 external detector. IR radiation is directed in and out of a multipass White cell (Infrared Analysis,

Inc. 16-V; 11.35 m pathlength) via transfer and focusing optics (Janos Technology). Sample air is drawn into the cell by an onboard DC pump through several meters of 0.635 cm o.d. corrugated Teflon tubing. Two manual Teflon shutoff valves allow trapping of the sample in the cell while IR spectra are collected (for signal averaging).

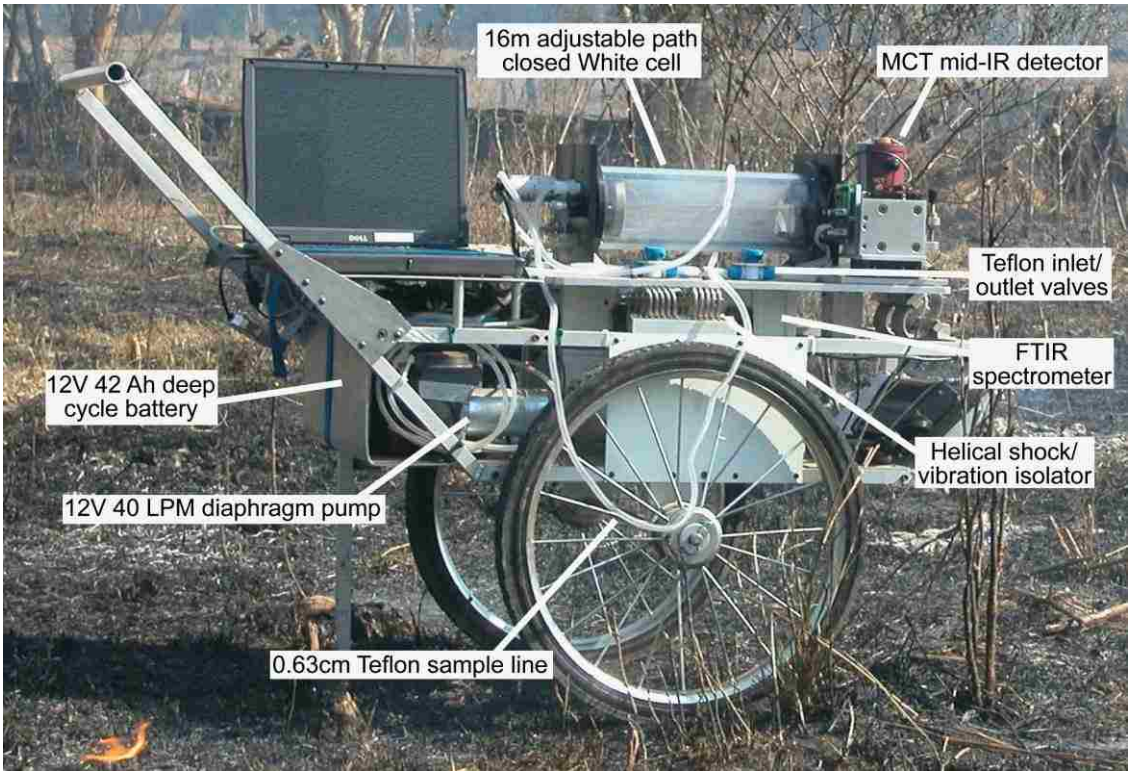

Figure 3.2. The LAndbased Fourier Transform Infrared Spectrometer (LAFTIR) used during the South Carolina Regional Emissions and Aging Measurements Campaign.

Temperature and pressure inside the White cell are monitored and logged in real time (Minco TT176 RTD, MKS Baratron 722A, respectively). Additional onboard features include a laptop computer, A/D and AC/DC converters, and a 73 amp hour 12V battery. The FTIR was operated at 0.50 cm^{-1} and three scans were co-added every 1.15 seconds (with a duty cycle of about 38%). Smoke or background samples were typically held in the cell for several minutes while ~100-200

spectra were collected at ~1 Hz that could later be signal averaged. The spectral quantification method was essentially the same as that used in the AFTIR analysis. Signal averaged, grab sample, single beam spectra were analyzed directly for H_2O, CO_2, CO, and CH_4 and referenced to appropriate background spectra to analyze for the following gases: NH_3, HCN, C_2H_2, C_2H_4, C_3H_6, HCHO, CH_3OH, CH_3COOH, C_6H_5OH, C_4H_4O, $C_{10}H_{16}$, and C_4H_6. The new software enabled us to correct for NH_3 losses on the pyrex cell walls during storage for the first time with the LAFTIR system, which increased the LAFTIR NH_3 retrievals in this study by about 40% on average (Yokelson et al., 2003). It is not clear if this increase should be applied to older NH_3 retrievals from LAFTIR since the cell previously had a Teflon coating, which was unfortunately unstable and removed for this mission. Due mostly to a relatively shorter pathlength (compared to the airborne FTIR system, see previous section), the LAFTIR detection limits ranged from ~50-200 ppb for most gases, which is sufficient for detection of many species as much higher concentrations are sampled on the ground than in lofted smoke (Burling et al., 2011). Comparisons to the NIST-traceable standards for CO, CO_2, and high levels of CH_4 were usually within 1-2%, and comparison to the low calibration for CH_4 (1.493 ppm) was within 6%. Several compounds observed by the AFTIR system (formic acid, glycolaldehyde, PAN, O_3, NO, NO_2, and HONO) were below the detection limits of the ground-based system. Finally, in several LAFTIR spectra a prominent peak was seen at 882.5 cm^{-1} that we could not assign.

3.2.2.1 *Instrument upgrades*

Several upgrades to the FTIR in the system originally described by Christian et al. (2007) were incorporated for this mission. Starting at the IR source, a current limiting resistor in series with the source was removed in order to produce a greater output of photons. This increases

signal levels because absorbing the same percentage of a greater number of photons results in larger peaks. Next, an adjustable spherical mirror was mounted behind the source in order to capture a large solid angle of the photons initially directed away from the interferometer. These photons would be lost without the spherical mirror to "redirect" them towards the interferometer optics, which would ultimately result in a reduced amount of photons reaching the detector, and thus, a reduction in signal. A custom designed aperture was made and mounted to increase spectral resolution. Because our collimated source output beam has some divergence, some light travels different distances through the interferometer. The different path lengths cause peak broadening. This aperture was placed in front of the source and at the focal point of the spherical mirror to block "off-axis" rays and reduce the beam divergence. Too small an aperture blocks too many photons and decreases signal levels. Too large an aperture allows unacceptable peak broadening, which results in overlap between adjacent peaks and more susceptibility to chemical interference. An ideal aperture hole size of about 2 mm increased resolution sufficient for various spectral retrievals with a small acceptable increase in spectral noise. Our experiments showed that placing the aperture at the focal point of the spherical mirror optimized the resolution/signal trade-off much better than placing the aperture at other system focal points (e.g. the entrance to the white cell). This is likely because the spherical mirror had a 2" focal length, whereas the off-axis parabolic mirror focusing into the white cell had a 8" focal length to avoid overfilling the first objective mirror. Shorter focal length optics have a better defined focal point. Further, a smaller aperture offers better control of scattered light. Additionally, we consulted with the manufacturer (MIDAC) regarding options for increasing the scan rate of the moving mirror. By removing the interferometer from the chassis and adjusting several jumpers we were

able to increase the mirror drive board speed from 59 kHz to 234 Hz, thus scanning the moving mirror four times as fast. We were the first customer to determine the fastest mirror speed compatible with the data acquisition electronics. The spectrometer now averages three scans in roughly 1 s instead of one scan in 1 s (there is not a direct relationship between scanning speed and the number of scans given system signal processing downtime requirements). Having three times as many scans per unit time increases the S:N per unit time by almost a factor of two (square root of 3). Other manufacturer upgrades were made including a dual ADC, providing improved vertical resolution of the interferogram peaks. The zero path difference (ZPD) peak sets the high end of the voltage range, and all smaller peaks cannot be as well defined with a single ADC. This is because the voltage increments are fixed as the total voltage range divided by 2^{16} (or 65536), which is the smallest voltage increment the ADC can resolve.

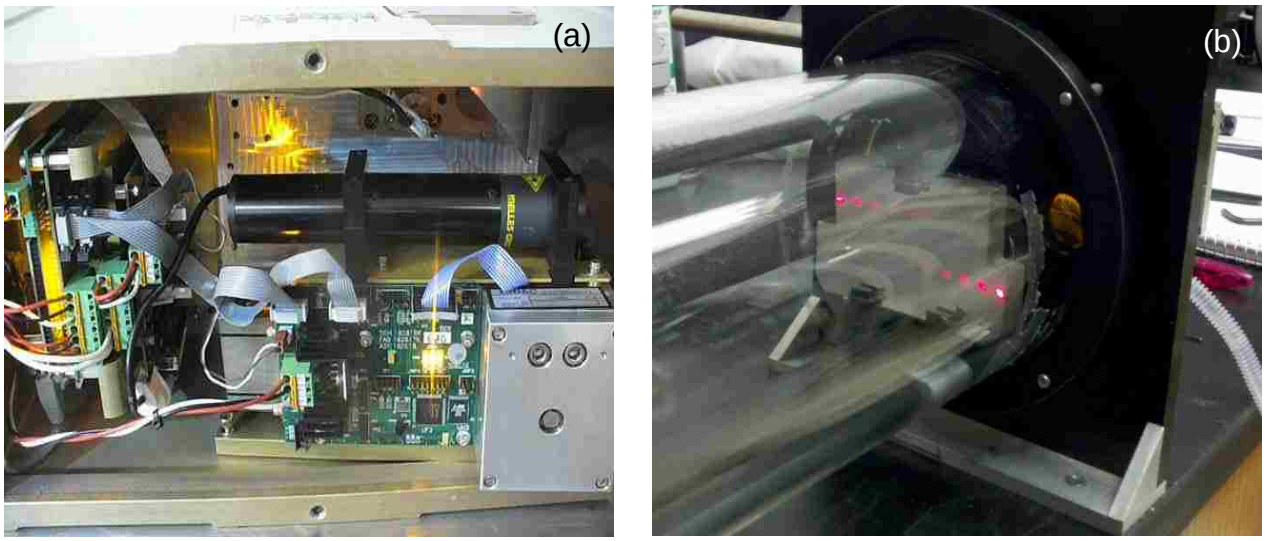

Figure 3.3. (a) MIDAC Spectrometer, and (b) Adjusting the spot pattern for optimal pathlength and alignment of the IR beam into and out of the cell.

With the additional ADC, we can "zoom in" on the portion of the interferogram where the structure is very small and we can we can now resolve that structure with smaller (and more appropriate) voltage increments. This means the amplitude of small peaks (near detection limits) in the spectra is more accurately measured, which results in more accurate measurements of the amount of substance. The LAFTIR cell badly needed repairs. It was completely dis-assembled and cleaned with soapy water and then solvents and distilled water to remove all the residual smoke that had adhered to the cell walls. The old Teflon coating had deteriorated and was starting to peel off and block the optical path. It was removed from the cell walls for this campaign. Next, the cell was reassembled and realigned using a laser to set the spot pattern (e.g align at the desired path length, See Fig 3.3b). Another step before the field campaign was to adjust the interferometer optics to maximize the signal (number of photons reaching the detector). Lastly, the new larger MIDAC chassis was remounted on the optical bench with the help of the machine shop at the US Forest Service Fire Sciences Laboratory. This required dis-assembling the system and remounting several other components. Example of S:N before and after our improvements can be seen in Fig 3.4, where the work described above reduced spectral noise by a factor of ~3.

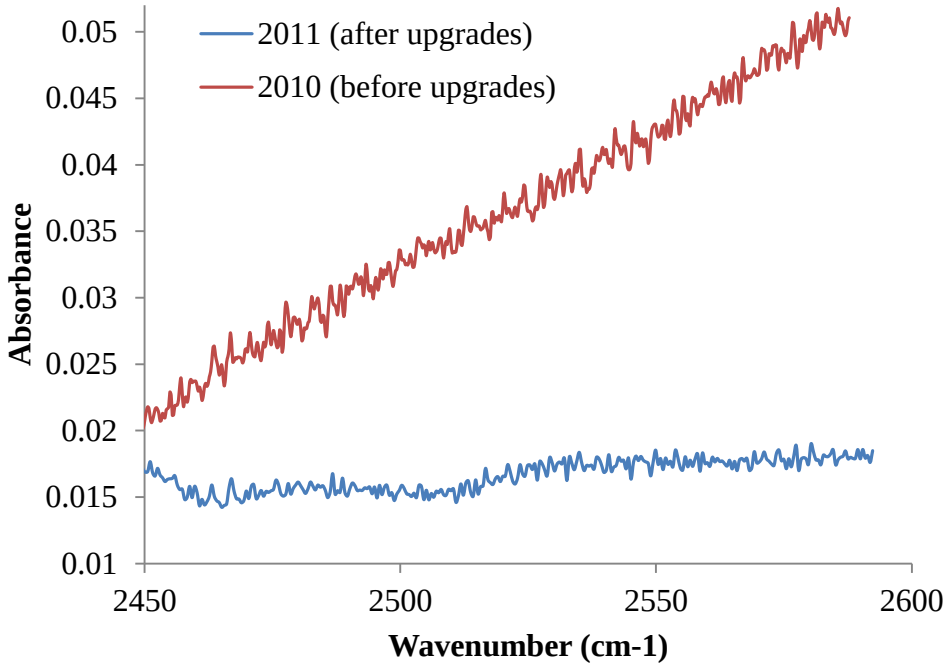

Figure 3.4. Two LAFTIR absorbance spectra acquired before (red) and after (blue) instrument upgrades. The 2450-2600 cm^{-1} noise region is shown, which is typically void of absorbing species. The spectrum shown in blue shows lower noise by a factor of ~3.

3.2.3 **Whole Air Sampling (WAS) Canisters**

WAS canisters were filled both on the ground and from the Twin Otter to measure an extensive suite of gases, mostly non-methane organic compounds (NMOCs). The electropolished, stainless steel canisters were conditioned for field use via a series of pump-and-flush procedures. Sampling was manually controlled and involved allowing the evacuated canisters to fill in ~10-20 s to ambient pressure in background air or various smoke plumes accessed on the ground. On the ground, the WAS samples were obtained in more dilute portions of the plumes than sampled by LAFTIR since the subsequent pre-concentration step could otherwise cause a non-linear detector response (Hanst et al., 1975; Simpson et al., 2011). In the

aircraft, the canisters were filled to ambient pressure directly from the AFTIR multipass cell via a dedicated Teflon valve and connecting tube after IR signal averaging was complete. During the SCREAM campaign we collected 4 WAS canisters from the ground and 4 from the air (1 background and 3 smoke samples per platform per fire) on each of the first three fires (Block 6, Block 9b, and Block 22b). All 24 canisters were sent to UC-Irvine for immediate analysis of 89 gases: CO_2, CH_4, CO, carbonyl sulfide (OCS), dimethyl sulfide (DMS), carbon disulfide (CS_2), and 83 NMOCs by gas chromatography (GC) coupled with flame ionization detection (FID), electron capture detection (ECD), and quadrupole mass spectrometer detection (MSD). Every peak of interest on every chromatogram was individually inspected and manually integrated. The GC run times were extended to target quantification of limonene, which was suspected to be an important smoke constituent based on previously incompletely assigned features in the IR spectrum of smoke (Yokelson et al., 1996) and the recent observation of high levels of other monoterpenes in smoke (Simpson et al., 2011). In addition, other prominent peaks in the chromatograms were observed, assigned, and quantified for species not in the suite of compounds usually analyzed by UC-Irvine. Additional details on WAS preparation, technical specifications, and analysis protocols can be found in Simpson et al. (2011).

3.2.4 **Other measurements on the Twin Otter**

The instruments below are discussed in full elsewhere (McMeeking et al., 2012). In this paper we present a short overview and we briefly compare to some of the organic aerosol data.

3.2.4.1 *Aerosol mass spectrometer (AMS)*

An Aerodyne high resolution time-of-flight (HR-ToF) aerosol mass spectrometer (AMS) was used to measure aerosol chemical composition. An isokinetic particle inlet sampling fine particles with a diameter cut-off of a few microns (followed directly by a PM_1 cyclone in line) supplied the AMS, a particles into liquid sampler (PILS), and a single particle soot photometer (SP2). The AMS data were processed with a ToF-AMS Analysis Toolkit in Igor Pro 6 (Wavemetrics, Lake Oswego, OR) to retrieve the mass concentration at STP ($\mu g\ sm^{-3}$, 273 K, 1 atm) for the major non-refractory particle species: organic aerosol (OA), non-sea salt chloride, nitrate, sulfate, and ammonium. The AMS has been described in full detail elsewhere (Drewnick et al., 2005; Canagaratna et al., 2007).

3.2.4.2 *Single particle soot photometer (SP2)*

Refractory black carbon (rBC, $\mu g\ sm^{-3}$) was measured using a single particle soot photometer (SP2) described in Stephens et al. (2003). The isokinetic particle inlet/cyclone that supplied the AMS was followed by a three-way splitter and also supplied the SP2 with carefully matched flow rates. Particles were drawn through a 1064 Nd:YAG laser cavity where scattered light was measured by two avalanche photodiode detectors. Sufficiently light –absorbing particles (at 1064 nm) were heated to vaporization and the emitted incandescent light was detected by two photomultiplier tubes with optical filters to measure light over two wavelength ranges. The incandescence signal was related linearly to rBC mass, regardless of the presence or type of rBC coating (Moteki and Kondo, 2007). The sample flow into the SP2 was diluted with filtered air at a ratio of 7:1 for smoke plume samples near the fire source, while a dilution of 0.35:1 was used for the less concentrated downwind samples. The SP2 data products were

collected at >1 Hz and later averaged as needed to match the sampling rates of the other instruments.

3.2.4.3 *Particle into liquid sampler- total organic carbon (PILS-TOC)*

A fraction of the particles that passed through the aerosol inlet, and the cyclone with a PM_1 cutoff, were then directed by a third branch of the splitter through an activated carbon denuder. Steam was then introduced and aerosol was captured in water droplets, and liquid samples were obtained via syringe pumps, providing 2-s integrated measurement of water-soluble organic carbon (WSOC) present in ambient aerosol. A fraction collector was integrated into the PILS-TOC system and automatically collected separate, 2-min samples from the PILS. Vials were later analyzed in the CSU laboratory for smoke markers, (levoglucosan and other carbohydrates) by high-performance anion-exchange chromatography- pulsed amperometric detection, or HPAEC-PAD). This method has a low detection limit of < ~0.1 ng m^{-3} for carbohydrate analysis. Samples were also analyzed for anions and cations by anion/cation-exchange chromatography.

3.2.4.4 *Other airborne measurements*

Measurements of the aircraft position, ambient three-dimensional wind velocity, temperature, relative humidity, and barometric pressure at 1-Hz were obtained with a wing-mounted Aircraft Integrated Meteorological Measuring System probe (AIMMS-20, Aventech Research, Inc.) (Beswick et al., 2008). This data allowed calculation of the time since smoke samples were emitted.

3.2.5 **Calculation of excess mixing ratios, normalized excess mixing ratios (NEMR), emission ratios (ER), and emission factors (EF)**

Excess mixing ratios for FTIR species were calculated following the procedure in Sect. 3.2.1. Excess mixing ratios for WAS species were obtained by subtracting WAS background values from WAS plume values. The normalized excess mixing ratio (NEMR) is calculated for all instruments by dividing ΔX by the excess mixing ratio of a long lived plume "tracer" ΔY measured in the same sample as "X." The normalizing species is usually ΔCO or ΔCO_2, and a NEMR can be measured anywhere in the plume. NEMRs collected at the source of a fire are equivalent to an initial molar emission ratio (ER) at the time of measurement. The ER has two important uses: (1) Since the CO or CO_2 tracers dilute at the same rate as the other species, differences between the ERs and the NEMRs measured downwind can sometimes allow us to quantify post-emission chemical changes. (2) The ER can be used to calculate emission factors (EF). Details of these two uses are described below.

In this study, downwind data was only collected in the aircraft and the ER obtained while the aircraft was sampling the source did not follow clear, time-dependent trends. Thus we combined all the source samples collected from each fire to compute a single fire-average initial emission ratio (and 1-σ standard deviation) for each fire. The fire-average ER was subsequently used both to calculate EF and as our best estimate of the starting conditions in the plumes. We computed the fire-average ERs from the slope of the linear least-squares line with the intercept forced to zero when plotting ΔX against ΔY (Yokelson et al., 1999) for all X/Y pairs from the fire. The intercept is forced to zero since the background concentration is typically well known and variability in the plume can affect the slope and intercept if the intercept is not forced. This

method heavily weights the large excess mixing ratios that may reflect more intense combustion (relative to other source samples) and that were collected with higher signal-to-noise. FTIR and WAS excess mixing ratios were combined in the calculation of ER if a species was measured by both techniques.

For any carbonaceous fuel, source ERs can be used to calculate emission factors (EF) expressed in grams of compound emitted per kilogram of biomass burned (on a dry weight basis). A set of ER obtained at any point during the fire could be used to calculate a set of EFs relevant to the time of the sample. In this study though we use the fire-average ER, obtained as described above, to calculate a single set of fire-average EFs for each fire using the carbon mass-balance method (Yokelson et al., 1996; 1999), shown below (Equation 1).

$$EF\left(\frac{g}{kg}\right) = F_c \times \frac{MM_x}{MM_C} \times \frac{C_x}{C_T} \qquad \text{Eq. 1}$$

Where F_c is the mass fraction of carbon in the fuel (in this study we assume a 50% carbon content by mass (dry weight) when a measured value is not available, except for organic soils and dung, where the carbon content of biomass normally ranges between 45 and 55%; Susott et al., 1996; Yokelson et al., 1997; McMeeking et al., 2009; Ebeling and Jenkins, 1985), MM_x is the molecular mass of compound *X*, MM_C is the molecular mass of carbon (12.011 g/mol), and C_X/C_T is the number of emitted moles of compound *X* divided by the total number of moles of carbon emitted. The carbon mass balance method is most accurate when the fraction of carbon in the fuel is precisely known and all the burnt carbon is volatilized and detected. Based on literature values for similar fuels (Susott et al., 1996; Burling et al., 2010) we assumed a carbon fraction of 0.50 by mass on a dry weight basis for the fuels that burned in SCREAM. The actual

fuel carbon fraction likely varied from this by less than 5-10% of this value. EF scale linearly with the assumed fuel carbon fraction. Total emitted C in this study was determined from the sum of the C from AFTIR species and WAS species. This sum could underestimate the total carbon by 1-2% due to unmeasured C. That would lead to a slight, across the board overestimate of our calculated EF by a factor of 1-2% (Akagi et al., 2011).

The emissions from flaming and smoldering processes differ and we use the modified combustion efficiency (MCE, $\Delta CO_2/\Delta CO+\Delta CO_2$) to describe the relative contribution of each of these combustion processes, where higher MCE's indicate more flaming combustion (Ward and Radke, 1993; Yokelson et al., 1996). Pure flaming has an MCE near 0.99 while the MCE of smoldering varies over a larger range (~0.65-0.85). Since MCE is an indicator of the relative amount of flaming and smoldering combustion, it often correlates reasonably well with EF (Fig. 4.3 in Ward and Radke, 1993; Fig. 3 in Yokelson et al., 2008). Generally, the MCE dependence of "EF(X)" for a fire type allows calculation of a specific EF(X) for any measured or assumed MCE (Akagi et al., 2011).

3.2.6 **Site descriptions**

For each of the seven prescribed fires sampled in this study, Table 3.1 shows some available details regarding the fuels, weather, size, location, etc. The three prescribed fires of 30 Oct, 1 Nov, and 2 Nov 2011 (referred to as Blocks 6, 9b, and 22b, respectively) were located on the Fort Jackson (FJ) Army Base northeast of Columbia, South Carolina (SC). The overstory vegetation consisted primarily of mature southern pines, including longleaf pine (*Pinus palustris*)

and loblolly pine (*Pinus taeda*), both of which are native to the southeastern U.S. High density pine areas had high canopy closure and limited understory vegetation with a thick litter layer (mostly pine needles). Lower density pine areas had scrub oak and other deciduous and herbaceous vegetation (i.e. grasses) as significant components of the understory. Sparkleberry (*Vaccinium arboretum*) was particularly significant intermixed with mature pine in Block 9b. Some additional information on the fuels for the Fort Jackson fires is available from one author (J. Reardon). For the other fires we had to rely on observations from the air and the limited information available is shown in Table 3.1.

Table 3.1. Fire name, location, date, fuels description, size, atmospheric conditions, and burn history of fires sampled in this work.

Fire Name	Location	Date	Veg Description	Area Burned (ha)	Temperature (°C)	Relative Humidity (%RH)	Windspeed ($m\ s^{-1}$)	Atmospheric conditions	Burn history?	Latitude (°N)	Longitude (°W)
Block 6	Fort Jackson, SC	30 Oct 2011	Block 6, mature long leaf pine	61.9	8-16	64	3-5	0.14" rain previous morning	Last burned 1957	34°1'29"	80°52'16"
Block 9b	Fort Jackson, SC	1 Nov 2011	Block 9b, mature long leaf, sparkleberry	36.0	9-18	58-69	3-4	Mixing height 5400 ft. Clear skies	Last burned 1956	34°0'15"	80°52'37"
Block 22b	Fort Jackson, SC	2 Nov 2011	Block 22b, mature long leaf, loblolly and heartwood	28.7	13-18	~70 (avg)	2-3	Clear, Mixing height 3800 ft.	Last burned 2003	34°5'4"	80°46'23"
Pine Plantation	Near North AFB, SC	2 Nov 2011	Plantation fire, loblolly pine debris	nd	~19	~71 (avg)	2-3	Sunny/clear	nd	33°34'46"	81°9'55"
Georgetown	Georgetown, SC	7 Nov 2011	SC coastal grass understory fire	63.9	20-22	~74 (avg)	4-4.5	Sunny/clear	nd	33°12'9"	79°24'6"
Francis Marion	Georgetown, SC	8 Nov 2011	Loblolly pine understory (Francis Marion)	141.6	19-21	~83 (avg)	0.5-3	Sunny/clear	nd	33°12'55"	79°28'34"
Bamberg	Bamberg, SC	10 Nov 2011	longleaf/loblolly pine understory	36.4	16-21	~71 (avg)	2-3	Cloudy with rain at end of flight	nd	33°14'5"	80°56'41"

nd = no data

3.2.7 **Airborne and ground-based sampling approach**

The first three prescribed burns (Blocks 6, 9b, and 22b) were part of a collaboration with the forestry staff at Fort Jackson Army Base. Advance notice was provided on all of the fires. The LAFTIR ground-based sampling protocol was similar to that described in Burling et al. (2011). Backgrounds were acquired before the fire and burns were ignited in the late morning. Ground-based sampling access was sometimes precluded during ignition, but sampling access then continued through late afternoon until the fire was effectively out. During post-ignition access, numerous point sources of residual smoldering combustion (RSC) smoke were sampled by the mobile LAFTIR system minutes to hours after passage of a flame front. The spot sources of white smoke included smoldering stumps, fallen logs, litter layers, etc., and they contributed to a dense smoke layer usually confined below the canopy. Point sources were usually sampled repeatedly to quantify their variability. Four WAS canisters were collected on the ground at each Fort Jackson fire (one WAS canister was always collected prior to ignition as a background and three were of RSC point sources also sampled by the LAFTIR system). Table 3.2 shows the RSC fuel types sampled on the ground on the Fort Jackson fires and Figure 3.5 illustrates two of these fuels. The OPAG and EPA sampling protocols had some differences with the LAFTIR. The OPAG was set up before the fire with an approximately 30 m optical path on a pre-selected portion of the fire perimeter. Spectra collected before ignition served as backgrounds and after ignition the OPAG sampled both unlofted RSC emissions and lofted emissions that were fortuitously directed through the path by wind gusts. The EPA ground-based mobile samplers actively sought the most intense combustion they could safely sample with the benefit of respiratory protection.

Table 3.2. Unique ground-based fuels sampled by LAFTIR from Blocks 6, 9b, and 22b at Fort Jackson, SC.

Fuel type	# of Samples
Dead/down debris	9
Stump	3
Live tree base	2
Litter	4
Fatwood	2
Slash pile	1

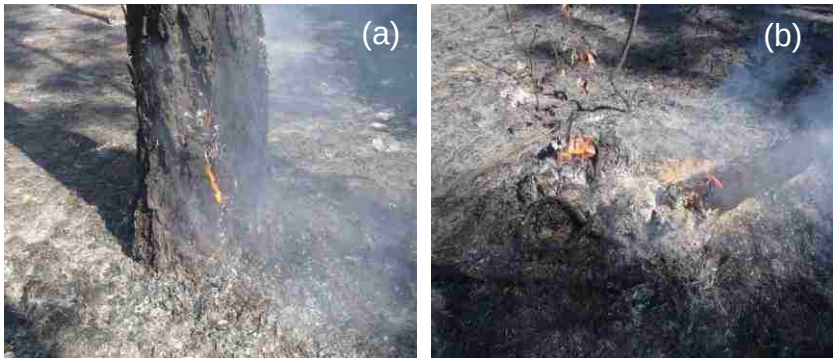

Figure 3.5. Photographs of some of the fuels sampled in this work that are major contributers to residual smoldering emissions including (a) a live tree base, and (b) dead/down debris.

The airborne sampling of the Fort Jackson fires proceeded as follows. In general, mid-morning take-offs enabled us to sample pre-fire backgrounds and initial emissions for as long as the fire produced a convection column that exceeded several hundred meters in height. Afternoon flights were conducted to complete sampling the initial emissions if necessary and to search for and sample the fire emissions downwind (Fig 3.6, 3.7, and 3.8). The plumes diluted rapidly near the top of a somewhat hazy mixed boundary layer due to variable winds. Thus, of the Fort Jackson fires, it was only possible to locate the downwind plume and obtain much quality downwind data on the Block 9b fire (1 Nov, research flights number 3 and 4 (RF03 & RF04 in Fig. 3.7)). The prevailing winds on 1 Nov directed the plume over the Columbia metro area, an airport and a powerplant, thus mixing of smoke with fossil fuel emissions was unavoidable. The plume from the Block 22b fire directly entered a large restricted area and could not be subsequently re-located. However, while searching for the downwind plume we located an active fire on a pine plantation about 40 km south of Columbia (Table 3.1). The Pine

Plantation fire generated a GOES hotspot from 13:02:00-17:15:00 LT and thus our samples at ~16:42 LT may have been collected towards the end of the fire.

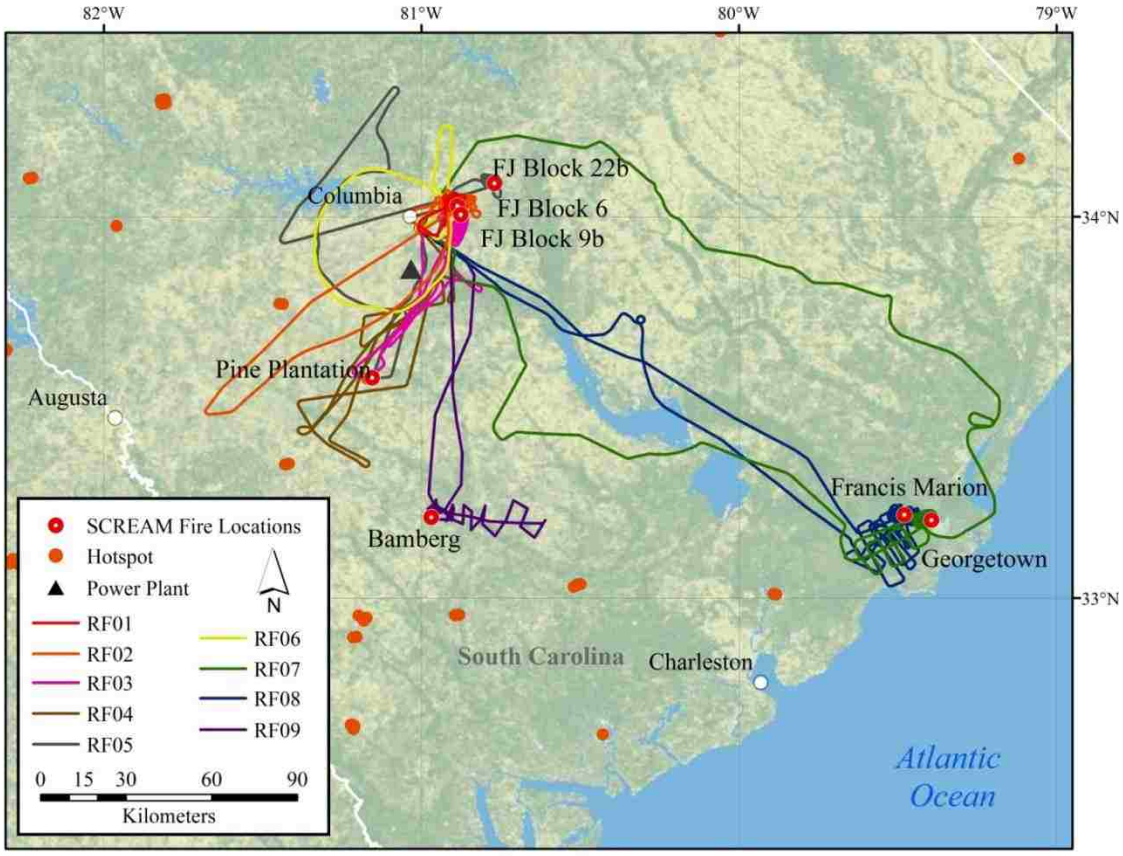

Figure 3.6. Overview of all flight tracks in the South Carolina regional emissions and aging measurements (SCREAM) study. "RF" indicates research flight and the dates of each research flight are shown in Table 3.3 except for RF06, which sampled urban emissions only on 5 Nov. "Hotspots" are the MODIS thermal anomalies from 30 Oct to 10 Nov, 2011. Of the seven fires sampled in this study, only the pine plantation fire was detected as a hotspot. Due to a GPS malfunction, the 10 Nov flight track is at 2-min resolution retrieved from the USFS automated flight following system.

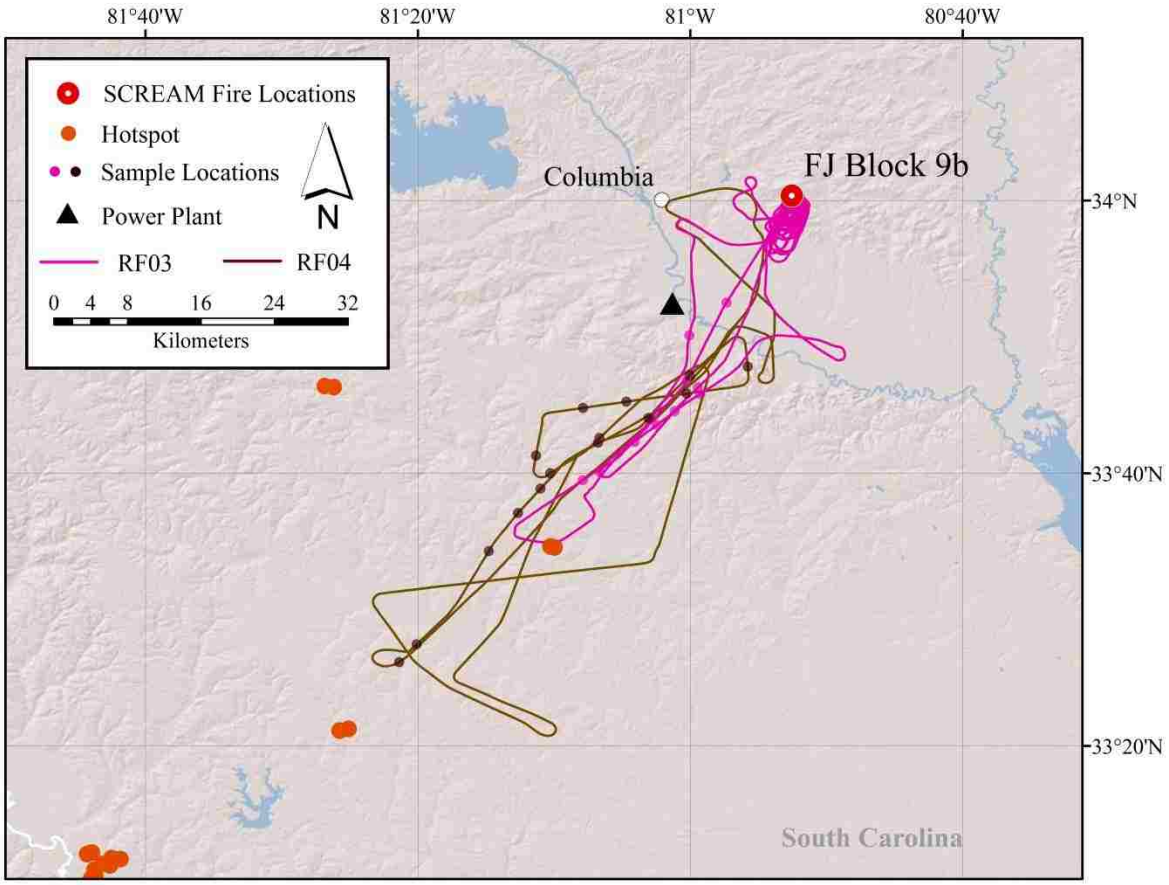

Figure 3.7. Detailed flight track and AFTIR downwind sample locations for the Twin Otter aircraft during RF03 (pink) and RF04 (black), which sampled the Block 9b fire at Fort Jackson on 1 Nov 2011. (The hotspot, which appears to intersect RF03 is actually from the pine plantation fire sampled on 2 Nov.)

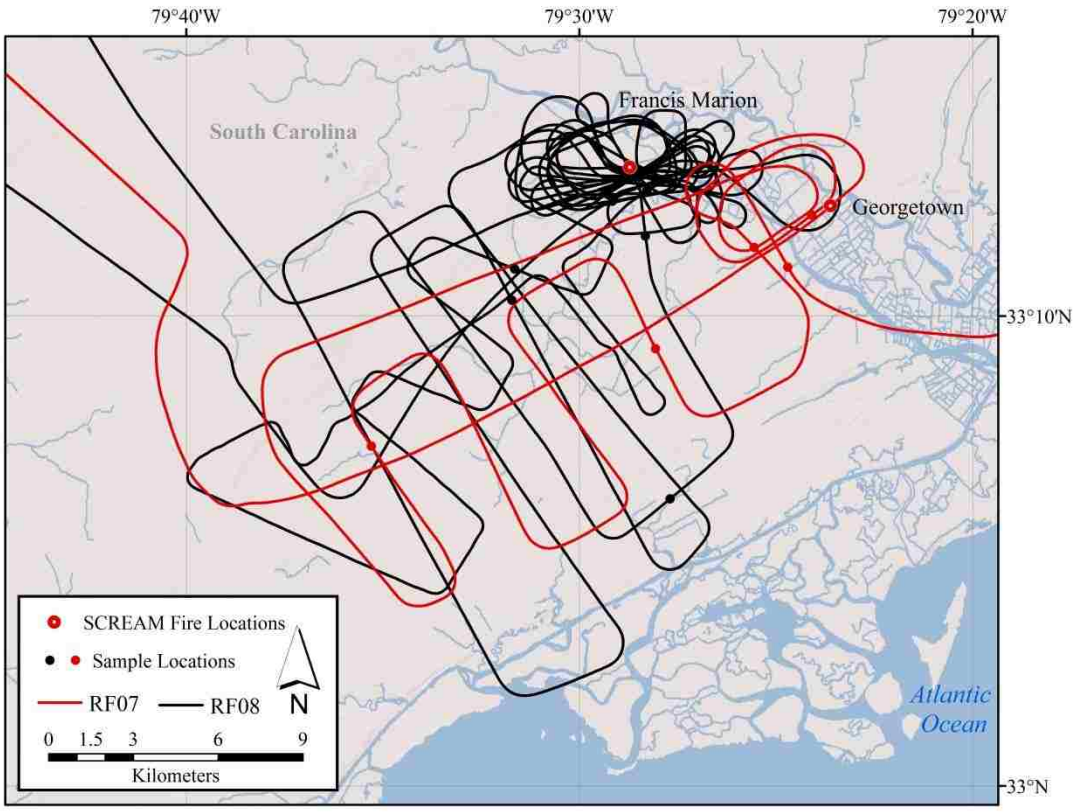

Figure 3.8. Detailed flight tracks and AFTIR downwind sample locations for the Twin Otter aircraft during RF07 (red) and RF08 (black) on 7 and 8 Nov, sampling the Georgetown and Francis Marion fires, respectively.

After completing the collaboration with Fort Jackson on 2 Nov we were able to conduct airborne sampling of additional fires on 7, 8, and 10 Nov (Georgetown, Francis Marion, and Bamberg Fires, respectively), via notification by the South Carolina Forestry Commission dispatch office. These fires were further from our base in Columbia and the Twin Otter typically arrived after the fire had been in progress for 0.5 to 1.0 hours (ground-based sampling was not feasible due to long travel times and short notice). The airborne sampling of these fires initially focused on the source emissions. After ~1-1.5 hours of repeatedly sampling the source, we would then cross the plume at increasing large downwind distances until it could not be

differentiated from background with our instruments. We then repeated the crossing pattern in reverse or returned directly to the source approximately along the plume center-line depending on conditions (see Figure 3.8). The plumes from these three fires also diluted rapidly in the boundary layer to form broad "fan-shaped" plumes under the influence of light and variable winds. We obtained quality downwind data on all three of these fires.

On all the fires during SCREAM, the AFTIR excess mixing ratios in the smoke plume grab samples were obtained from subtraction of background grab samples taken just outside the plume at a similar pressure and time. To measure the initial emissions from the fires, we sampled smoke less than several minutes old by penetrating the smoke column 150 to several thousand meters from the flame front. The goal was to sample smoke that had already cooled to the ambient temperature since the chemical changes associated with smoke cooling are not explicitly included in most atmospheric models. This approach also sampled smoke before most of the photochemical processing, which is explicitly included in most models. More than a few kilometers downwind from the source, smoke samples have usually already undergone noticeable photochemical aging (e.g. O_3 and PAN formation). Thus, this smoke is better for probing post-emission chemistry than estimating initial emissions (Akagi et al., 2012; Trentmann et al., 2005). We attempted to acquire downwind plume samples near the plume centerline by monitoring the AFTIR CO lines in real time, but due to the broad dilute plumes we sometimes acquired downwind samples near the plume edges (Fig. 3.8). Thus, as an experiment, for most of the downwind sampling on 10 Nov (Bamberg fire) we ran the AFTIR continuously with the valves open while maintaining a constant flight altitude. The idea was that the relatively long downwind plume transects orthogonal to the plume would have similar temperature, pressure,

and age and could be averaged together to create a "sample" without the need to identify a plume maximum. The averaged sample spectra obtained this way typically had about half the SNR of averaged sample spectra collected with the valves closed. Estimated times since emission, or smoke "ages", were calculated for all the downwind samples by first calculating the average windspeed for incremental altitude bins of 100 m above mean sea level (a.m.s.l.). The smoke sample distance from the plume source was then divided by the average windspeed at the sample altitude.

3.3 *Results and Discussion*

3.3.1 **Initial emissions**

As mentioned above, FTIR and WAS samples were combined in the calculation of fire-average emission ratios for species measured by both techniques from airborne and ground-based platforms. Good agreement (within 20%) was observed when ER were instead calculated by each technique independently as shown in Figures 3.9a and 3.9b.

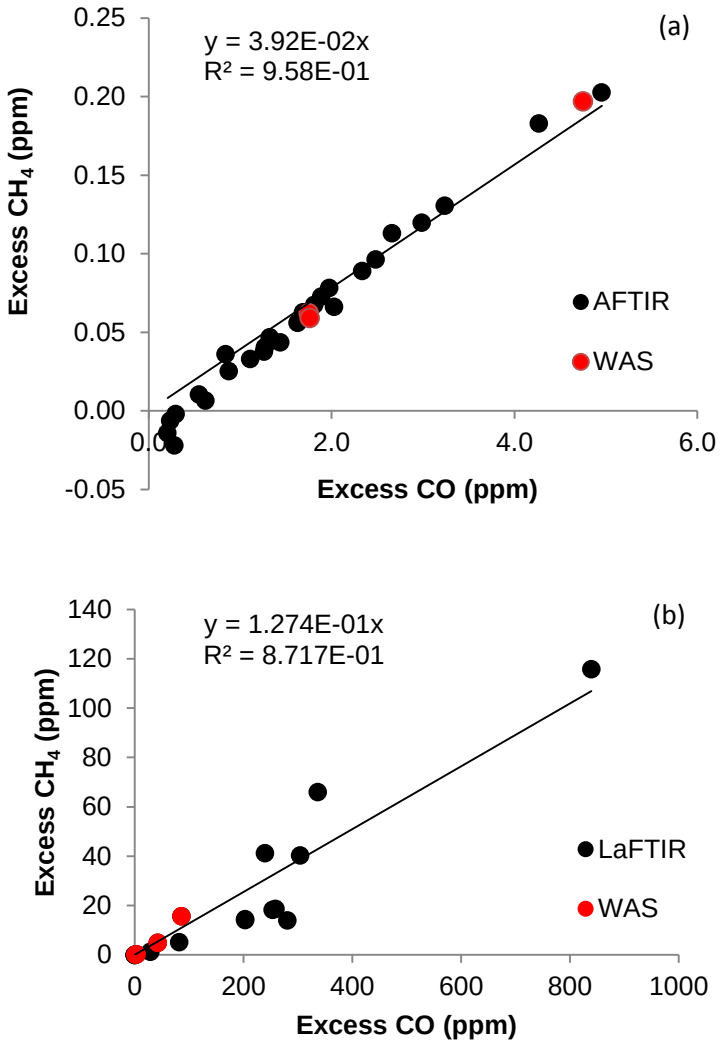

Figure 3.9. Emission ratio plots for $\Delta CH_4/\Delta CO$ from (a) the AFTIR cell and (b) independent RSC targets on the ground from burn blocks 6 and 9b, respectively. Black circles denote samples collected by FTIR and red circles denote samples that were collected by WAS on the indicated fires.

The majority of ER plots show good correlation with CO as the reference species. However, the LAFTIR ground-based measurements showed greater scatter compared to airborne measurements, as the individual contributions from fuel types are measured rather than a blended sample in a convection column (Bertschi et al., 2003). However, this increased scatter simply

reflects real variability and not a decreased quality of the measurement of ER. The fire-average and platform-based study average emission factors for all species measured in SCREAM are shown in Table 3.3. Measurements were obtained from both airborne and ground platforms for all Fort Jackson fires (Blocks 6, 9b, and 22b). Only airborne data was collected for the remaining four fires, where we did not have timely ground-based access to the fire site. WAS cans were only collected for the Fort Jackson burns and the 2 Nov Pine Plantation burn. Organic aerosol (OA) was measured by the AMS on 5 of the 7 fires and detailed AMS results can be found in a complementary work (McMeeking et al., in preparation). A total of 97 trace gas species was quantified by FTIR and WAS from both airborne and ground-based platforms; possibly the most comprehensive suite of trace gas species measured in the field for biomass burning fires to date.

Table 3.3. Emission factors (g kg^{-1}) measured using FTIR and WAS from ground-based and airborne platforms.

	Ground-based					Airborne								
Fire Name	**Block 6**	**Block 9b**	**Block 22b**	Average Ground EF	± 1σ	**Block 6, RF01/02**	**Block 9b, RF03/04**	**Block 22b, RF05**	**Pine Plantation, RF05**	**George-town, RF07**	**Francis Marion, RF08**	**Bamberg, RF09**	Average Airborne EF	± 1σ
Date	30 Oct 2011	1 Nov 2011	2 Nov 2011			30 Oct 2011	1 Nov 2011	2 Nov 2011	2 Nov 2011	7 Nov 2011	8 Nov 2011	10 Nov 2011		
MCE	0.876	0.858	0.789	0.841	0.046	0.932	0.919	0.935	0.904	0.938	0.933	0.957	0.931	0.016
FTIR Species														
CO2	1554	1496	1305	1452	130	1674	1643	1679	1606	1696	1686	1739	1675	42
CO	140	158	222	173	43	78	92	74	109	72	78	49	79	19
CH4	5.20	11.50	10.34	9.01	3.35	1.74	2.08	2.01	6.66	2.22	1.88	2.02	2.66	1.77
C2H2	0.25	0.22	0.14	0.20	0.06	0.35	0.24	0.20	0.28	0.73	0.43	0.45	0.38	0.18
C2H4	0.89	1.53	1.25	1.22	0.32	1.21	1.23	0.94	1.34	1.62	1.27	0.60	1.17	0.32
C3H6	0.40	1.02	1.00	0.81	0.35	0.55	0.70	0.51	0.84	0.29	0.54	0.23	0.52	0.21
HCHO	1.79	2.42	2.51	2.24	0.39	1.87	2.11	1.70	1.98	2.13	1.97	1.36	1.87	0.27
CH3OH	2.35	6.42	3.60	4.12	2.09	1.18	1.45	1.16	2.09	0.53	1.08	0.90	1.20	0.49
CH3COOH	1.03	3.84	2.42	2.43	1.41	1.24	0.75	1.25	1.85	2.33	1.60	2.82	1.69	0.71
C6H5OH	0.11	0.18	0.16	0.15	0.04	0.23	0.21	0.12	0.53	bdl	bdl	bdl	0.27	0.18
C4H4O	0.44	1.60	0.86	0.97	0.59	0.20	0.20	0.11	0.54	bdl	bdl	bdl	0.27	0.19
HCN	0.95	0.85	1.12	0.98	0.14	0.74	0.82	0.84	0.18	0.94	0.68	0.42	0.66	0.27
NH3	0.05	0.23	0.33	0.20	0.15	0.11	0.13	0.14	0.13	bdl	0.06	bdl	0.11	0.03
C4H6	0.10	0.15	0.09	0.11	0.03	0.26	0.32	0.26	0.24	0.19	0.28	bdl	0.26	0.04
C5H8[a]	0.08	0.02	0.15	0.08	0.06	0.18	0.14	0.14	0.11	-	-	-	0.14	0.03
C10H16	2.58	bdl	5.36	3.97	1.97	1.62	2.84	1.65	0.09	bdl	1.20	bdl	1.48	0.99
HCOOH	bdl	bdl	bdl	-	-	0.08	0.09	0.11	0.03	bdl	0.08	bdl	0.08	0.03
C2H4O2	bdl	bdl	bdl	-	-	0.41	0.10	0.31	0.60	0.69	0.24	bdl	0.39	0.22
HONO	bdl	bdl	bdl	-	-	0.40	bdl	0.38	bdl	0.34	0.60	bdl	0.43	0.12
NO	bdl	bdl	bdl	-	-	0.37	0.28	0.28	bdl	bdl	0.23	0.41	0.32	0.07
NO2	bdl	bdl	bdl	-	-	2.21	1.30	1.58	1.89	bdl	1.52	1.83	1.72	0.32
NOx	bdl	bdl	bdl	-	-	1.63	1.03	1.25	1.23	bdl	1.17	1.53	1.31	0.23
WAS species														
OCS	0.011	0.017	0.338	0.122	0.187	0.010	0.011	0.014	0.006	-	-	-	0.010	0.003
DMS	0.007	0.011	0.078	0.032	0.040	0.011	0.004	0.010	0.008	-	-	-	0.008	0.003
Ethane	0.503	2.033	5.632	2.723	2.633	0.261	0.347	0.324	1.026	-	-	-	0.489	0.359
Propyne	0.018	0.009	0.031	0.019	0.011	0.057	0.059	0.048	0.061	-	-	-	0.056	0.006

1-Butyne	0.001	0.001	0.002	0.001	0.001	0.005	0.005	0.005	0.008	-	-	-	0.006	0.002
2-Butyne	0.001	0.001	0.003	0.002	0.001	0.003	0.003	0.003	0.007	-	-	-	0.004	0.002
1,2-Propadiene	0.005	0.002	0.008	0.005	0.003	0.016	0.015	0.013	0.017	-	-	-	0.015	0.002
Propane	0.171	0.544	1.692	0.802	0.793	0.081	0.115	0.116	0.299	-	-	-	0.153	0.099
i-Butane	0.012	0.026	0.169	0.069	0.087	0.007	0.007	0.011	0.016	-	-	-	0.010	0.005
n-Butane	0.032	0.122	0.431	0.195	0.209	0.020	0.033	0.033	0.058	-	-	-	0.036	0.016
1-Butene	0.066	0.200	0.478	0.248	0.210	0.105	0.118	0.122	0.182	-	-	-	0.131	0.034
i-Butene	0.063	0.150	0.603	0.272	0.290	0.073	0.079	0.090	0.111	-	-	-	0.088	0.017
trans-2-Butene	0.026	0.099	0.212	0.112	0.093	0.021	0.028	0.029	0.061	-	-	-	0.035	0.018
cis-2-Butene	0.020	0.081	0.166	0.089	0.073	0.017	0.021	0.022	0.052	-	-	-	0.028	0.016
i-Pentane	0.005	0.011	0.074	0.030	0.039	0.005	0.009	0.008	0.007	-	-	-	0.007	0.002
n-Pentane	0.014	0.054	0.218	0.095	0.108	0.014	0.019	0.021	0.022	-	-	-	0.019	0.003
1-Pentene	0.013	0.060	0.123	0.065	0.055	0.028	0.032	0.035	0.024	-	-	-	0.030	0.005
trans-2-Pentene	0.009	0.034	0.078	0.040	0.035	0.011	0.012	0.013	0.026	-	-	-	0.016	0.007
cis-2-Pentene	0.005	0.018	0.039	0.021	0.017	0.006	0.008	0.007	0.016	-	-	-	0.009	0.004
3-Methyl-1-butene	0.009	0.011	0.055	0.025	0.026	0.012	0.014	0.013	0.016	-	-	-	0.014	0.002
2-Methyl-1-butene	0.013	0.029	0.096	0.046	0.044	0.015	0.018	0.018	0.027	-	-	-	0.019	0.005
Methyl acetate	0.017	0.062	0.128	0.069	0.056	bdl	bdl	0.003	0.026	-	-	-	0.015	0.016
2-Methyl-2-butene	0.010	0.036	0.169	0.071	0.085	0.022	0.022	0.025	0.025	-	-	-	0.024	0.002
1,3-Pentadiene	0.007	0.022	0.046	0.025	0.020	0.022	0.016	0.023	0.031	-	-	-	0.023	0.006
1-Heptene	0.011	0.061	0.100	0.057	0.045	0.026	0.022	0.036	0.015	-	-	-	0.025	0.009
1-Octene	0.012	0.064	0.122	0.066	0.055	0.021	0.022	0.026	0.018	-	-	-	0.022	0.003
Cyclopentene	0.021	0.043	0.145	0.070	0.066	0.043	0.043	0.051	0.042	-	-	-	0.045	0.004
n-Hexane	0.010	0.046	0.128	0.062	0.060	0.008	0.015	0.013	0.012	-	-	-	0.012	0.003
n-Heptane	0.005	0.042	0.082	0.043	0.039	0.006	0.015	0.009	0.005	-	-	-	0.008	0.005
n-Octane	0.004	0.032	0.071	0.036	0.034	0.004	0.022	0.006	0.000	-	-	-	0.008	0.010
n-Nonane	0.004	0.025	0.073	0.034	0.035	0.003	0.063	0.008	bdl	-	-	-	0.025	0.033
n-Decane	0.007	0.021	0.053	0.027	0.024	bdl	0.077	bdl	bdl	-	-	-	0.077	-
2,3-Dimethylbutane	0.001	0.002	0.011	0.005	0.005	bdl	bdl	bdl	bdl	-	-	-	-	-
2-Methylpentane	0.006	0.010	0.071	0.029	0.036	0.004	0.010	0.006	0.006	-	-	-	0.007	0.002
3-Methylpentane	0.001	0.003	0.012	0.005	0.006	0.002	0.005	0.002	0.003	-	-	-	0.003	0.001
Benzene	0.268	0.429	1.712	0.803	0.791	0.251	0.254	0.284	0.345	-	-	-	0.283	0.043
Toluene	0.515	0.283	0.938	0.579	0.332	0.164	0.204	0.190	0.237	-	-	-	0.199	0.031
Ethylbenzene	0.064	0.039	0.112	0.072	0.037	0.035	0.061	0.026	0.032	-	-	-	0.039	0.016
p-Xylene	0.017	0.034	0.092	0.048	0.039	0.027	0.050	0.022	0.024	-	-	-	0.031	0.013
m-Xylene	0.112	0.074	0.555	0.247	0.267	0.054	0.009	0.070	0.062	-	-	-	0.049	0.027
o-Xylene	0.026	0.043	0.146	0.071	0.065	0.021	0.042	0.022	0.016	-	-	-	0.025	0.011
Styrene	0.059	0.031	0.101	0.064	0.035	0.043	0.035	0.042	0.040	-	-	-	0.040	0.003
i-Propylbenzene	0.006	0.013	bdl	0.009	0.005	bdl	bdl	bdl	0.002	-	-	-	0.002	-

n-Propylbenzene	0.012	0.010	0.072	0.031	0.035	0.004	0.008	0.004	0.003	-	-	-	0.005	0.002
3-Ethyltoluene	0.157	0.016	0.293	0.155	0.139	0.028	0.046	0.023	0.018	-	-	-	0.029	0.012
4-Ethyltoluene	0.122	0.010	0.121	0.084	0.064	0.008	0.021	0.014	0.009	-	-	-	0.013	0.006
2-Ethyltoluene	0.010	0.015	0.027	0.017	0.009	0.017	0.015	0.008	0.001	-	-	-	0.010	0.007
1,3,5-Trimethylbenzene	0.016	0.010	0.048	0.024	0.020	0.025	0.046	0.009	bdl	-	-	-	0.027	0.019
1,2,4-Trimethylbenzene	0.053	0.040	0.280	0.124	0.135	0.072	0.109	0.055	0.049	-	-	-	0.071	0.027
1,2,3-Trimethylbenzene	0.052	0.019	0.429	0.167	0.228	0.037	0.090	0.042	0.019	-	-	-	0.047	0.030
methylisopropylbenzene	0.288	bdl	0.977	0.632	0.487	bdl	bdl	bdl	0.002	-	-	-	0.002	-
alpha-Pinene	1.677	0.026	6.248	2.650	3.223	0.086	0.103	0.069	0.117	-	-	-	0.094	0.021
beta-Pinene	0.200	0.091	0.657	0.316	0.301	0.062	0.061	0.052	0.033	-	-	-	0.052	0.013
4-Carene	0.101	bdl	0.174	0.137	0.052	0.014	0.010	0.006	0.008	-	-	-	0.009	0.004
Camphene	0.427	bdl	0.657	0.542	0.163	0.023	bdl	bdl	0.007	-	-	-	0.015	0.011
Myrcene	0.068	bdl	0.105	0.086	0.026	bdl	bdl	bdl	0.008	-	-	-	0.008	-
Acetonitrile	0.032	0.060	1.127	0.406	0.624	bdl	bdl	0.032	bdl	-	-	-	0.032	-
Acrylonitrile	0.011	0.022	0.049	0.027	0.020	0.045	0.029	0.092	0.049	-	-	-	0.054	0.027
2-Methylfuran	0.172	0.515	1.251	0.646	0.551	0.094	0.109	0.126	0.286	-	-	-	0.153	0.089
2-Ethylfuran	0.008	0.029	0.072	0.036	0.033	0.007	0.006	0.005	0.017	-	-	-	0.009	0.006
2,5-Dimethylfuran	0.045	0.125	0.413	0.194	0.194	0.020	0.019	0.036	0.049	-	-	-	0.031	0.014
Acetaldehyde	0.531	0.987	3.120	1.546	1.382	0.602	0.506	0.803	0.651	-	-	-	0.641	0.124
Butanal	0.015	0.037	0.092	0.048	0.040	0.015	0.030	0.045	0.041	-	-	-	0.032	0.013
2-Methylpropanal	0.015	0.039	0.289	0.115	0.152	0.011	0.018	0.040	0.017	-	-	-	0.021	0.013
3-Methylbutanal	0.028	0.050	0.309	0.129	0.156	0.016	0.031	0.037	0.019	-	-	-	0.026	0.010
2-Propenal	0.144	0.296	0.977	0.472	0.443	0.185	0.287	0.410	0.409	-	-	-	0.323	0.108
Methacrolein (MAC)	0.036	0.034	0.172	0.081	0.079	0.041	0.033	0.038	0.042	-	-	-	0.039	0.004
Furfural	0.012	0.028	0.161	0.067	0.082	0.067	0.032	0.135	0.035	-	-	-	0.067	0.048
Acetone	0.409	1.052	3.182	1.548	1.451	0.545	0.344	0.740	0.974	-	-	-	0.651	0.269
Butanone	0.083	0.293	0.592	0.323	0.256	0.068	0.085	0.108	0.133	-	-	-	0.098	0.028
MVK	0.062	0.146	0.374	0.194	0.161	0.024	0.050	0.109	0.047	-	-	-	0.058	0.036
3-Methyl-2-butanone	0.014	0.048	0.124	0.062	0.056	0.013	0.016	0.005	0.010	-	-	-	0.011	0.005
3-Methyl-3-buten-2-one	0.079	0.129	0.511	0.240	0.236	0.017	0.039	0.050	0.030	-	-	-	0.034	0.014
Ethanol	0.006	0.016	0.036	0.019	0.016	0.013	bdl	0.022	0.012	-	-	-	0.016	0.006
Nitromethane	0.028	0.060	0.132	0.073	0.053	0.128	0.081	0.151	0.139	-	-	-	0.125	0.031
Organic Aerosol (OA)[b]	-	-	-	-	-	-	8.28	10.32	-	6.45	7.76	5.40	7.64	1.87
ΣMonoterpenes	5.05	0.12	13.20	6.12	6.61	1.81	3.01	1.77	0.27	-	1.20	-	1.61	1.00
ΣTerpenes	5.12	0.14	13.35	6.21	6.67	1.98	3.15	1.91	0.37	-	1.20	-	1.72	1.03
ΣNMOC	18.06	27.37	57.12	34.18	20.40	13.94	15.35	14.38	16.93	9.44	9.37	6.78	12.31	3.76

[a] EF(C5H8) from airborne data collected 30 Oct – 2 Nov provided by WAS.

[b] OA measurements provided by AMS.

Given that EF are dependent on the flaming to smoldering ratio or "MCE," some variation in EF between studies (and between fires within a study) occurs because fires naturally burn with a range of flaming to smoldering ratios (F/S). Thus, comparing the correlation of EF vs. MCE between studies provides more insight than simply comparing emission factors, as the latter does not factor in fire-to-fire variability in F/S. Given that fires do not produce "ideal" plumes, there is some temporal and spatial fluctuation about the EF and MCE. We fit EF vs. MCE plots to linear functions to assist in discerning any differences or trends in EF between "smoldering" and "flaming" compounds. Linear functions are selected empirically based on how well they fit the data and cannot necessarily be rigorously derived from the complex, sometimes unknown, underlying chemistry. In the case of poorly correlated data, this may simply suggest a compound's emission from both flaming and smoldering combustion, and does not reflect the quality of the data itself. Additionally, we do not assume that these fits describe the behavior beyond the MCE's measured here.

Table 3.4 shows linear regression statistics of EF as a function of MCE for all fires sampled in this study. A negative slope denotes higher EF at lower MCE, meaning that the compound is likely emitted by smoldering combustion (ie. CH_3OH). Conversely, a positive slope suggesting higher EF with increasing MCE is normally observed for a flaming compound (ie. alkynes, NO_x). Some species show poor correlation with MCE with very low R^2 values: this does not suggest that the data are of poor quality or too variable to draw any valuable conclusions. Differences in fuel composition (e.g. %N) can affect EF for a given MCE (Bertschi et al., 2003; Christian et al., 2007). Also, some compounds may be emitted to some extent from both flaming and smoldering combustion, such as C_2H_2. Ethyne has a strong positive correlation with MCE in Yokelson et al. (2008), a weak positive correlation with MCE in this work and Burling et al. (2011), while others (Yokelson et al., 2011; Burling et al., 2010) report a weak anti-correlation

with MCE. This is not surprising, since numerous variables affect emissions and the predictive power of any one variable or small group of variables is limited.

Table 3.4. Statistics for the linear regression of EF as a function of MCE for combined ground-based and airborne fire-average measurements. Values in parentheses represent 1-σ standard deviation.

	Slope	Y-Intercept	R^2	n
FTIR Species				
CH4	-65.01 (12.65)	63.34 (11.45)	0.77	10
C2H2	2.07 (0.96)	-1.54 (0.87)	0.37	10
C2H4	-1.50 (2.06)	2.55 (1.87)	0.06	10
C3H6	-4.12 (1.28)	4.34 (1.16)	0.57	10
HCHO	-4.97 (1.58)	6.48 (1.43)	0.55	10
CH3OH	-25.72 (8.39)	25.33 (7.60)	0.54	10
CH3COOH	-5.49 (6.36)	6.88 (5.76)	0.09	10
C6H5OH	0.53 (1.20)	-0.26 (1.07)	0.04	7
C4H4O	-6.65 (3.40)	6.47 (3.02)	0.43	7
HCN	-2.75 (1.67)	3.24 (1.51)	0.25	10
NH3	-1.48 (0.45)	1.47 (0.41)	0.64	8
C4H6	1.32 (0.38)	-0.97 (0.35)	0.63	9
C5H8	0.26 (0.43)	-0.11 (0.38)	0.07	7
C10H16	-25.8 (8.23)	25.3 (7.41)	0.66	7
HCOOH	-1.78 (0.67)	-1.57 (0.62)	0.70	5
C2H4O2	-0.84 (8.63)	1.17 (8.00)	0.00	6
HONO	-25.7 (25.7)	24.5 (24.0)	0.33	4
NO	3.56 (2.31)	-3.02 (2.16)	0.44	5
NO2	1.90 (9.02)	-0.05 (8.39)	0.01	6
NOx	6.99 (5.42)	-5.19 (5.04)	0.29	6
WAS species				
OCS	-2.00 (0.57)	1.83 (0.51)	0.71	7
DMS	-0.43 (0.12)	0.40 (0.11)	0.70	7
Ethane	-34.95 (6.09)	32.47 (5.42)	0.87	7
Propyne	0.25 (0.14)	-0.18 (0.13)	0.39	7
1-Butyne	0.032 (0.017)	-0.025 (0.015)	0.42	7
2-Butyne	0.012 (0.016)	-0.007 (0.014)	0.09	7
1,2-Propadiene	0.071 (0.038)	-0.052 (0.034)	0.41	7
Propane	-10.32 (1.784)	9.59 (1.67)	0.86	7
i-Butane	-1.00 (0.24)	0.93 (0.22)	0.78	7
n-Butane	-2.59 (0.53)	2.40 (0.47)	0.83	7
1-Butene	-2.26 (0.63)	2.19 (0.56)	0.72	7
i-Butene	-3.26 (0.82)	3.06 (0.73)	0.76	7
trans-2-Butene	-1.23 (0.23)	1.16 (0.21)	0.85	7

cis-2-Butene	-0.97 (0.18)	0.91 (0.16)	0.85	7
i-Pentane	-0.42 (0.12)	0.39 (0.10)	0.72	7
n-Pentane	1.28 (0.30)	1.18 (0.26)	0.79	7
1-Pentene	-0.60 (0.17)	0.58 (0.15)	0.71	7
trans-2-Pentene	-0.43 (0.09)	0.40 (0.08)	0.80	7
cis-2-Pentene	-0.20 (0.05)	0.19 (0.04)	0.78	7
3-Methyl-1-butene	-0.248 (0.085)	0.238 (0.076)	0.63	7
2-Methyl-1-butene	-0.49 (0.12)	0.47 (0.11)	0.76	7
Methyl acetate	-0.87 (0.16)	0.80 (0.14)	0.90	5
2-Methyl-2-butene	-0.90 (0.26)	0.84 (0.23)	0.70	7
1,3-Pentadiene	-0.14 (0.09)	0.15 (0.08)	0.34	7
1-Heptene	-0.49 (0.16)	0.47 (0.14)	0.65	7
1-Octene	-0.67 (0.16)	0.64 (0.14)	0.78	7
Cyclopentene	-0.58 (0.23)	0.57 (0.21)	0.55	7
n-Hexane	-0.77 (0.16)	0.72 (0.14)	0.83	7
n-Heptane	-0.50 (0.11)	0.47 (0.10)	0.81	7
n-Octane	-0.42 (0.11)	0.39 (0.10)	0.75	7
n-Nonane	-0.32 (0.22)	0.31 (0.20)	0.34	6
n-Decane	0.09 (0.41)	-0.04 (0.35)	0.02	4
2,3-Dimethylbutane	-0.12 (0.01)	0.10 (0.01)	0.99	3
2-Methylpentane	-0.40 (0.11)	0.37 (0.10)	0.74	7
3-Methylpentane	-0.055 (0.020)	0.053 (0.018)	0.59	7
Benzene	-9.03 (2.22)	8.52 (1.98)	0.77	7
Toluene	-4.95 (0.96)	4.75 (0.85)	0.84	7
Ethylbenzene	-0.48 (0.15)	0.47 (0.13)	0.68	7
p-Xylene	-0.38 (0.15)	0.37 (0.13)	0.56	7
m-Xylene	-3.16 (0.79)	2.93 (0.70)	0.76	7
o-Xylene	-0.76 (0.19)	0.72 (0.17)	0.76	7
Styrene	-0.36 (0.13)	0.37 (0.11)	0.62	7
i-Propylbenzene	-0.23 (0.07)	0.21 (0.06)	0.92	3
n-Propylbenzene	-0.42 (0.10)	0.39 (0.09)	0.78	7
3-Ethyltoluene	-1.67 (0.51)	1.57 (0.45)	0.68	7
4-Ethyltoluene	-0.73 (0.32)	0.69 (0.29)	0.50	7
2-Ethyltoluene	-0.10 (0.05)	0.10 (0.05)	0.41	7
1,3,5-Trimethylbenzene	-0.11 (0.15)	0.12 (0.13)	0.12	6
1,2,4-Trimethylbenzene	-1.20 (0.50)	1.16 (0.45)	0.53	7
1,2,3-Trimethylbenzene	-2.26 (0.77)	2.11 (0.69)	0.63	7
methylisopropylbenzene	-8.34 (0.44)	7.57 (0.38)	1.00	3
alpha-Pinene	-38.49 (9.92)	35.35 (8.82)	0.75	7
beta-Pinene	-3.84 (0.88)	3.57 (0.78)	0.79	7
4-Carene	-1.22 (0.18)	1.14 (0.16)	0.92	6
Camphene	-4.78 (1.36)	4.46 (1.19)	0.86	4
Myrcene	-0.74 (0.34)	0.69 (0.29)	0.83	3
Acetonitrile	-7.64 (3.41)	6.92 (2.95)	0.72	4
Acrylonitrile	0.15 (0.22)	-0.09 (0.19)	0.09	7
2-Methylfuran	-7.55 (1.24)	7.06 (1.10)	0.88	7
2-Ethylfuran	-0.43 (0.08)	0.40 (0.07)	0.86	7
2,5-Dimethylfuran	-2.53 (0.47)	2.35 (0.42)	0.85	7
Acetaldehyde	-15.52 (4.11)	14.80 (3.65)	0.74	7

Butanal	-0.37 (0.15)	0.37 (0.14)	0.54	7
2-Methylpropanal	-1.65 (0.47)	1.52 (0.41)	0.71	7
3-Methylbutanal	-1.77 (0.46)	1.64 (0.41)	0.75	7
2-Propenal	-3.91 (1.65)	3.86 (1.46)	0.53	7
Methacrolein (MAC)	-0.80 (0.25)	0.77 (0.22)	0.67	7
Furfural	-0.36 (0.47)	0.39 (0.42)	0.10	7
Acetone	-16.26 (4.34)	15.46 (3.86)	0.74	7
Butanone	-3.39 (0.64)	3.21 (0.57)	0.85	7
MVK	-2.06 (0.49)	1.94 (0.44)	0.78	7
3-Methyl-2-butanone	-0.76 (0.13)	0.71 (0.12)	0.86	7
3-Methyl-3-buten-2-one	-3.10 (0.60)	2.87 (0.53)	0.84	7
Ethanol	-0.11 (0.08)	0.12 (0.07)	0.34	6
Nitromethane	0.16 (0.39)	-0.04 (0.35)	0.03	7

3.3.2 **Brief comparison to similar work**

It is of interest to compare both the airborne and ground-based emission factors in this work to those from Burling et al. (2011) (Fig. 3.10). In the minimally-detailed global vegetation schemes in common use, both studies measured EF in temperate forest; more specifically, both studies measured EF in pine forest understory fires. However, there are some differences in the vegetation communities probed in this study and those primarily in North Carolina probed by Burling et al. (2011). Fuels from the latter study were comprised mostly of fine woody material and foliage, whereas the present study included at least three fires where the fuels were mostly litter. In addition, the Burling et al. measurements were during an exceptionally wet Spring, while the present study was conducted in the Fall after a prolonged drought. Thus, multiple factors contribute to differences between these two studies and this provides us with an idea of the natural variability that can occur in study-average values between prescribed fires within a fairly narrowly defined ecosystem classification. Our study-average MCE from airborne sampling is 0.931±0.016 which is almost within 1σ standard deviation of the average airborne MCE for North Carolina conifer forest understory burns (0.948±0.006) of Burling et al. (2011).

Of the 17 species (besides CO_2 and CO) measured from the aircraft in both studies, only six compounds have EF that agree within 35%. We observe significantly less NO_x in this work, along with 22 and 33% lower EF(HONO) and EF(NH_3) (respectively) compared to Burling et al. (2011) (Fig. 3.10a). The fuels burned in the NC fires likely included more foliage which typically has a high N content. Airborne EF for all hydrocarbons and oxygenated VOCs are higher in this work. Ground-based sampling of Fort Jackson fires resulted in an MCE of 0.841±0.046 and Burling et al. (2011) measured a very similar MCE of 0.838±0.055. EF(CO) and EF(CO_2) agree within 4%, and EF(CH_4) agrees within 30%. However, less agreement was observed for all other 11 compounds measured in both studies: We report 73-97% lower EF for all non-methane hydrocarbons (NMHC) that were measured in both studies (C_2H_2, C_2H_4, C_3H_6, 1,3-butadiene, and isoprene), which is the opposite of the higher EF(NMHC) seen in the air. We also observe 13-78% higher EF for all oxygenated VOC (OVOC) measured in both studies (HCHO, CH_3OH, CH_3COOH, and C_4H_4O), which mimics the airborne comparison (Fig. 3.10b). The ground-based EF(NMHC) from this work, despite being lower than the field EF(NMHC) of Burling et al. (2011), are higher than all EF(NMHC) measured in laboratory burns of southeast pine litter (Burling et al. 2010). Differences in observed EF(HCN) and EF(NH_3) are discussed in more detail in Sect. 3.3.5. However, this brief overview makes it clear that high variability can be observed even for study average values for ecosystems considered nominally similar in the atmospheric community.

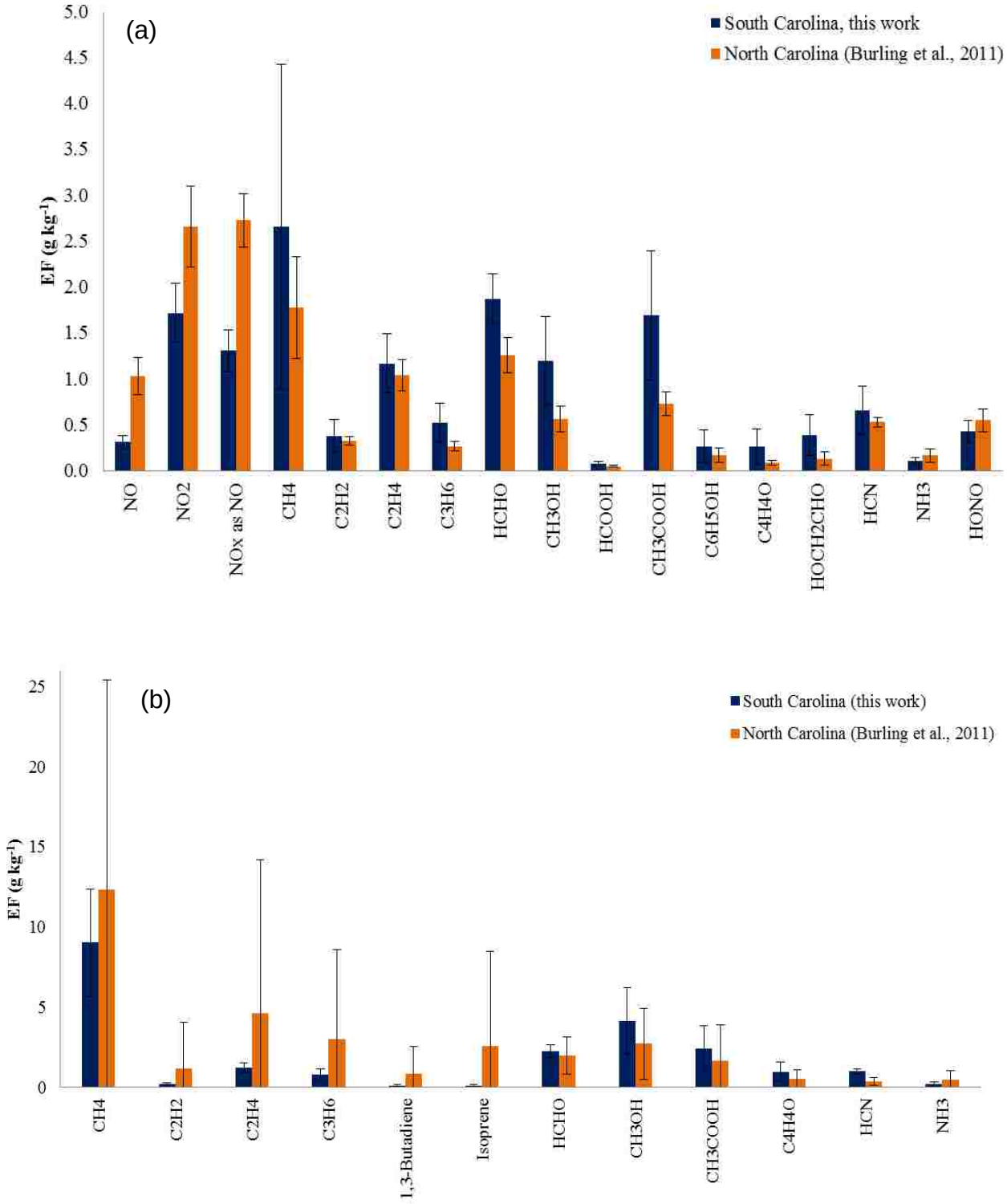

Figure 3.10. Comparison of this work (blue) with Burling et al. (2011) (orange) from (a) airborne and (b) ground-based platforms.

3.3.3 **Observation of large initial emissions of terpenes**

3.3.3.1 ***Background levels, atmospheric chemistry, and possible effects in smoke plumes***

Terpenes— hemiterpenes (isoprene), monoterpenes ($C_{10}H_{16}$), and sesquiterpenes ($C_{15}H_{24}$)— are emitted from most coniferous trees as part of a complex response mechanism to injury and disease (Paine et al., 1987; Guenther et al., 2006). Isoprene comprises nearly 50% of global biogenic trace gas emissions and roughly 11% are monoterpenes, with alpha-pinene and limonene making up the highest fractions of monoterpenes at about 25 and 16%, respectively (Kanakidou et al., 2005). These compounds are known to play an important role in atmospheric oxidation and secondary organic aerosol (SOA) formation (Holzinger et al., 2010).

Isoprene is synthesized by plants and then immediately emitted, but it is also a combustion product that is for instance emitted in high quantities by smoldering peat (Christian et al., 2003). In contrast, monoterpenes, once synthesized, can be stored for months in plant tissue. A fraction of the synthesized monoterpenes are emitted immediately following synthesis, but the highest concentration of these emissions immediately adjacent to the plant is only a few ppb under normal conditions. However, very large concentrations of terpenes may be emitted into the gas phase (or "boiled off" via distillation) due to exposure to heat from fires. Thus, the absolute mixing ratios of terpenes in relatively undiluted fire emissions can exceed several ppm and is much greater than the mixing ratios of these compounds in natural vegetative emissions. Once emitted into the atmosphere, rapid atmospheric oxidation of terpenes by OH, O_3, and NO_3 produces both VOC (Pan et al., 2009) and byproducts typically less volatile than their parent

compounds, resulting in condensation into secondary organic aerosol (SOA) (Capouet et al., 2004) on a timescale of minutes to hours (Atkinson and Arey, 2003). Terpene oxidation can occur via OH and O_3 during daylight hours and by O_3 and NO_3 at night (Fry et al., 2011). Limonene and alpha-pinene oxidation have been shown in chamber experiments to yield substantial amounts of SOA (Fry et al., 2011) and C_1-C_3 OVOC (Pan et al., 2009) dependent on the oxidant, concentration regime, temperature, water, and type of seed particle (if any) (Hamilton et al., 2011; Saathoff et al., 2009; Lee et al., 2006). Limonene is particularly of interest, because the two double bonds (a.k.a. reactive sites) provide limonene with a quick, direct route to forming low-vapor pressure oxidation products that are likely to form SOA (Fry et al., 2011). Consequentially this compound may be responsible for a disproportionate amount of total SOA relative to other monoterpenes (Lane et al., 2008; Maksymuik et al., 2009).

3.3.3.2 ***High levels of terpenes in fresh smoke***

We note that several measurements of the initial emissions of terpenes from biomass burning have been made previously. Isoprene is well-known to be emitted by fires and the isoprene EF has already been measured for many biomass fuels (Christian et al., 2003; Yokelson et al., 2007b; Burling et al., 2011; Simpson et al., 2011). Additionally, Yokelson et al. (1996) and Burling et al. (2011) noted large, IR spectral features in smoke similar to monoterpene absorption, suggesting possible large emissions of monoterpenes (Fig. 3.11). Simpson et al. (2011) reported large EF for two monoterpenes, alpha- and beta-pinene, as measured by WAS from Canadian boreal forest fires. In this work we present the first quantitative FTIR observations of a monoterpene (limonene) in smoke along with an expanded suite of monoterpenes measured by WAS including alpha-/beta-pinene, limonene, camphene, 4-carene,

and myrcene. Our measured fire-average ERs of these monoterpenes (and isoprene) from ground-based and airborne platforms are shown in order of abundance in Table 3.5.

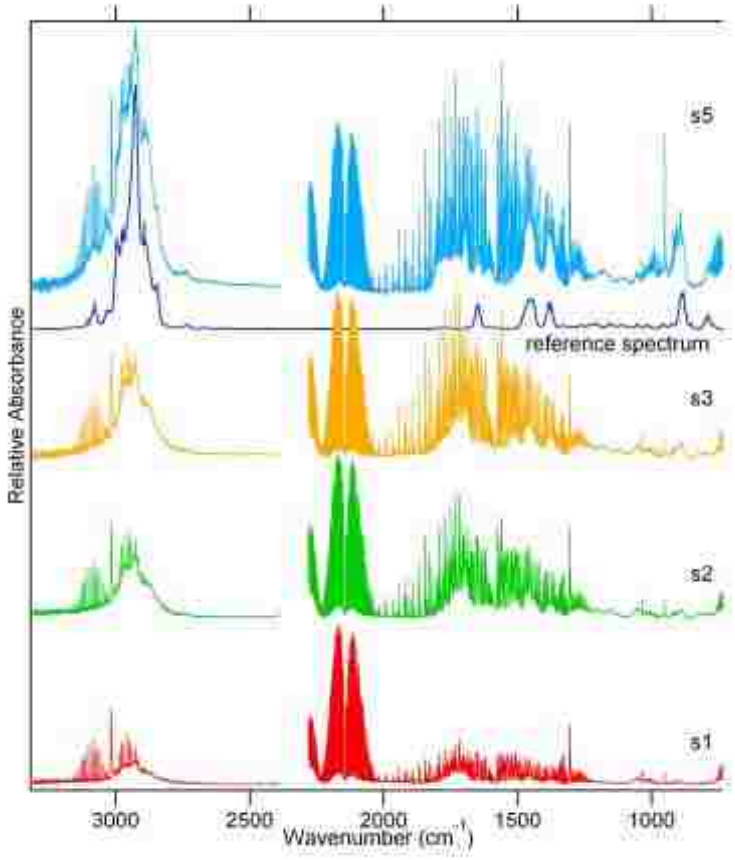

Figure 3.11. Absorption spectra of ground-based smoke samples normalized to the CO absorption band centered at 2143 cm^{-1} presented in Burling et al. (2011). The reference spectrum is a linear sum of the three equal parts of the monoterpene species, alpha-pinene, beta-pinene, and limonene spectra (Sharpe et al., 2004) and is shown only as a qualitative comparison.

Table 3.5. Airborne and ground-based emission ratios of measured terpenes from SC fires, shown in order of abundance.

Airborne

Fire Name	**Block 6**	**Block 9b**	**Block 22b**	**Pine Plantation**	**Georgetown**	**Francis Marion**	**Bamberg**	Average	
Date	30 Oct 2011	1 Nov 2011	2 Nov 2011	2 Nov 2011	7 Nov 2011	8 Nov 2011	10 Nov 2011	Airborne ER	± 1σ
Limonene	4.30E-03	6.38E-03	4.60E-03	1.78E-04	bdl	3.19E-03	bdl	3.73E-03	2.29E-03
Isoprene	9.44E-04	6.20E-04	7.83E-04	3.96E-04				6.86E-04	2.34E-04
alpha-Pinene	2.27E-04	2.30E-04	1.92E-04	2.20E-04				2.17E-04	1.73E-05
beta-Pinene	1.63E-04	1.37E-04	1.44E-04	6.14E-05				1.26E-04	4.47E-05
Camphene	6.05E-05	bdl	bdl	1.26E-05				3.66E-05	3.39E-05
4-Carene	3.68E-05	2.32E-05	1.56E-05	1.51E-05				2.27E-05	1.01E-05
Myrcene	bdl	bdl	bdl	1.46E-05				1.46E-05	
Σmonoterpenes	4.79E-03	6.77E-03	4.95E-03	5.01E-04		3.19E-03		4.04E-03	2.35E-03
Σterpenes	5.73E-03	7.39E-03	5.73E-03	8.97E-04		3.19E-03		4.59E-03	2.55E-03
ΣNMOC	1.14E-01	1.02E-01	1.20E-01	1.02E-01	1.05E-01	8.85E-02	1.02E-01	1.05E-01	9.94E-03

Ground-based

Fire Name	**Block 6**	**Block 9b**	**Block 22b**	Average Ground ER	
Date	30 Oct 2011	1 Nov 2011	2 Nov 2011		± 1σ
Limonene	3.78E-03	bdl	4.97E-03	4.37E-03	8.41E-04
alpha-Pinene	2.46E-03	3.37E-05	5.78E-03	2.76E-03	2.89E-03
Camphene	6.26E-04	bdl	6.09E-04	6.18E-04	1.25E-05
beta-Pinene	2.93E-04	1.19E-04	6.09E-04	3.40E-04	2.48E-04
Isoprene	2.23E-04	6.52E-05	2.79E-04	1.89E-04	1.11E-04
4-Carene	1.47E-04	bdl	1.61E-04	1.54E-04	9.83E-06
Myrcene	9.89E-05	bdl	9.68E-05	9.78E-05	1.48E-06
Σmonoterpenes	7.40E-03	1.52E-04	1.22E-02	6.59E-03	6.08E-03
Σterpenes	7.62E-03	2.18E-04	1.25E-02	6.78E-03	6.19E-03
ΣNMOC	7.17E-02	1.20E-01	1.32E-01	1.08E-01	3.19E-02

Our study-average ER (Δα-pinene/ΔCO) was over a factor of 12 times lower in our aircraft measurements than on the ground (the Block 9b fire was an exception, where ER(Δα-pinene/ΔCO) on the ground was a factor of 7 times lower than airborne). In contrast, the study-average ER(Δlimonene/ΔCO) was only lower by a factor of 1.2 in the air (Table 3.5). The alpha-pinene rate constants with respect to OH, O_3, and NO_3 are slower than those of limonene with

these oxidants, suggesting that the much lower alpha-pinene/limonene ratio in lofted smoke that reached the aircraft is not mostly due to atmospheric oxidation. We suggest that alpha-pinene may be preferentially released from fuels that burn largely by RSC (duff, dead-down woody fuels etc.) and thus is relatively more abundant in smoke that was poorly lofted in this study. We observe ~3.6 times greater Δisoprene/ΔCO ER in the lofted emissions sampled from the air in this work suggesting that RSC fuels may produce lower isoprene to CO ratios than the fuels that typically produce the bulk of lofted smoke (fine fuels, Akagi et al., 2011).

Figure 3.12 compares emission factors (g kg^{-1}) of monoterpenes and isoprene measured in this work. In light of the above fuel-specific observations, it is of interest to further compare our terpene EFs with the alpha-/beta-pinene and isoprene EFs for boreal forest fires in Alberta, Canada, measured by Simpson et al. (2011) during the ARCTAS campaign. Simpson et al. (2011) did not include limonene or other monoterpenes in the ARCTAS analysis due to the long GC run-times required for the additional compounds.

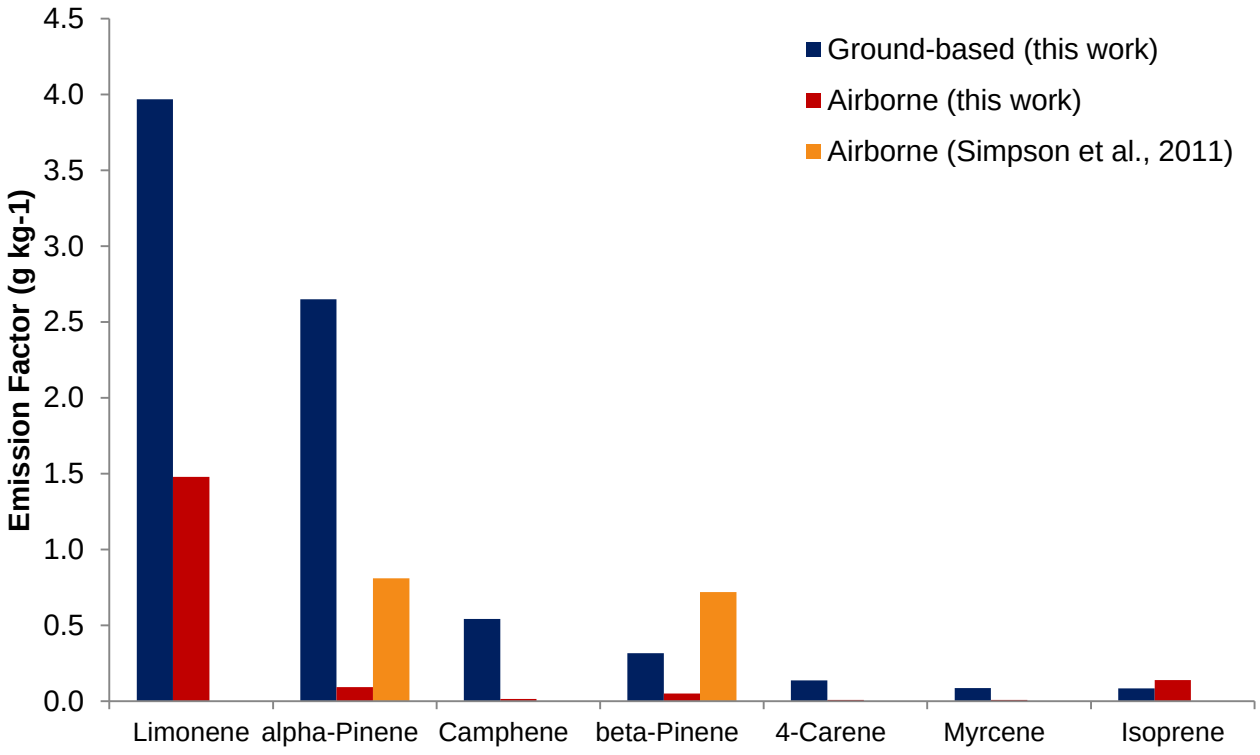

Figure 3.12. Emission factors (g kg^{-1}) of monoterpenes and isoprene measured from this work. We compare with data from Simpson et al. (2011) who measured alpha/beta-pinene and isoprene from an airborne platform (orange), though EF(isoprene) is too small to be visible.

The sum of our study-average alpha- and beta-pinene emission factors was 2.97 g kg^{-1} for the ground-based measurements and 0.146 g kg^{-1} for the airborne measurements, respectively. The sum of the alpha- and beta-pinene EF obtained from an aircraft by Simpson et al. (2011) had an intermediate value of 1.53 g kg^{-1} and was obtained at an intermediate MCE of 0.90. The boreal forest often has much greater loading of dead-down woody fuels (due in part to slower decomposition), and so relatively more of the emissions from these fuels may have been entrained in the lofted emissions sampled by Simpson et al. (2011). A higher contribution from the dead down woody fuels would also be consistent with lower isoprene EF of Simpson et al. (2011) shown in Figure 3.12 (too small to be visible). It should not be assumed, however, that

unlofted smoke will always have lower abundance of isoprene than lofted smoke since a very high isoprene EF was observed by Christian et al. (2003) for smoldering peat. Finally, given that high EF for both alpha- and beta-pinene were observed in the ARCTAS campaign, it is likely there were also high levels of additional terpenes present in the ARCTAS samples that went unmeasured.

In the SC smoke plumes, limonene and alpha-pinene dominate as the most abundant monoterpenes measured from both the airborne and ground-based platforms. Most prevalent from both the air and the ground, we observed limonene concentrations as high as 8.4 ppm. Limonene is highly susceptible to oxidation with high reaction rate constants with OH, O_3, and NO_3 (compared with other measured monoterpenes). In assessing the daytime downwind VOC production in our biomass burning plumes, O_3 was depleted in the freshest smoke via rapid reaction of background O_3 (~50–80 ppb) with NO emitted by the fire (Akagi et al., 2011; 2012; Yokelson et al., 2003). Thus, the reaction of limonene with OH would initially be the main daytime oxidation pathway forming small molecular weight byproducts including methanol, formaldehyde, and acetone (Muller et al., 2005; Holzinger et al., 2005). Alpha-pinene was the second most abundant monoterpene measured in this work, due mainly to high emissions measured by the ground-based platform. While toting slower reaction rates compared with limonene, oxidation pathways of alpha-pinene via OH and O_3 are important and under depleted O_3 conditions, alpha-pinene + OH is expected to produce low molecular weight products such as acetone, formaldehyde, formic acid, and acetic acid (Capouet et al., 2004). Oxidation of terpenes via OH will be the main oxidation pathway for terpenes until O_3 levels rebound in the plume, which can happen in as little as 0.5 h, at which time oxidation by both O_3 and OH become

important channels for the reaction of remaining terpenes. For the case of the two main monoterpenes, limonene and alpha-pinene, we can estimate how long these species would remain in the atmosphere given elevated OH concentrations typically found in biomass burning plumes ($5\times10^{6} – 1\times10^{7}$ molec cm^{-3}; Hobbs et al., 2003; Yokelson et al., 2009; Akagi et al., 2012). Assuming a pseudo first-order decay of limonene and alpha-pinene with respect to OH ($k_{OH+limonene} = 1.7\times10^{-10}$ cm^3 $molec^{-1}$ s^{-1}, $k_{OH+alpha\text{-}pinene} = 5.3\times10^{-11}$ cm^3 $molec^{-1}$ s^{-1}; Bouvier-Brown et al., 2009) we predict 99% of limonene and alpha-pinene will have reacted within 0.8–1.6 h and 2.5–4.9 h following emission, respectively, with the higher [OH] estimate corresponding to faster monoterpene loss. As will be later discussed in Sect. 3.3.7, O_3 can rebound to 80–100 ppb in as little as 1 h following emission (e.g. O_3 levels can be well above background despite dilution of the plume). This suggests that there will typically be some unreacted limonene and alpha-pinene remaining in the plume once O_3 recovers to significant levels. At an estimated O_3 mixing ratio of 80–100 ppb, 1 h after emission 19–32% and 9–16% of remaining limonene and alpha-pinene (respectively) would be due to oxidation via the O_3 channel ($k_{O3+limonene} = 2.0\times10^{-16}$ cm^3 $molec^{-1}$ s^{-1}, $k_{O3+alpha\text{-}pinene} = 8.4\times10^{-17}$ cm^3 $molec^{-1}$ s^{-1}; Bouvier-Brown et al., 2009), making reaction with O_3 (and its byproducts) important though likely secondary to the OH reaction. Recent work suggests the oxidation of alpha-pinene with ozone produces small byproducts including formaldehyde, acetaldehyde, formic acid, acetone, and acetic acid (Lee et al., 2006). Limonene with O_3 has been known to produce secondary photoproducts such as formic and acetic acid, acetaldehyde, methanol, formaldehyde, and acetone (Pan et al., 2009; Walser et al., 2007; Lee et al., 2006) dependent on limonene and ozone levels. Monoterpene ozonolysis also produces OH with OH molar yields of 0.86, 0.7-0.85, and

1.15 for limonene, alpha-pinene, and myrcene, respectively (Finlayson-Pitts and Pitts, 2000). Thus, reaction via the O_3 channel would generate OH, increasing the oxidative capacity of the plume and encouraging further plume evolution. High levels of OH lead to increased O_3 formation which may help explain the high O_3 formation rates observed during this campaign. The OH and ozone small molecule oxidation products of the other monoterpenes such as beta-pinene and myrcene are similar to those already listed and include formaldehyde, formic and acetic acid, acetaldehyde, and acetone (Lee et al., 2006). Evidence of downwind growth in several of these VOCs has been previously observed in biomass burning plumes (Holzinger et al., 2005; Jost et al., 2003; Karl et al., 2007). In addition to secondary produced VOC, lower vapor pressure products of terpene oxidation likely contribute to SOA as well. While much effort has gone into understanding and identifying these monoterpene byproducts, there is still considerable carbon mass tied up in unidentified species that goes unaccounted for (Lee et al., 2006). In summary, since both the oxidant levels and the initial emissions of terpenes are highly variable in biomass burning plumes, we expect this to contribute to high variability in post-emission VOC production as discussed in later sections and more generally in Akagi et al. (2011).

Thus far we have only looked into the VOC products of the most important daytime oxidation pathways. We now briefly explore the important oxidizing agents of terpenes at night when reaction via ozone and NO_3 become more favorable. Most commonly in wildfires, especially boreal forest fires, it is sometime the case that much of the fuel is consumed at night by smoldering or even flaming that is perhaps promoted by nighttime frontal passage (Vermote et al., 2009). In this circumstance, much of the NO_x may be tied up as NO_3 (Tereszchuk et al.,

2011) promoting the reactions of terpenes and NO_3, which produce formaldehyde, HNO_3, and large organic nitrates and aldehydes, where the latter two products have oxidation products that are not well studied (Fry et al., 2011). Assuming generic O_3 and NO_3 nighttime mixing ratios of 35 ppb and 5 ppt, respectively (Finlayson-Pitts and Pitts, 2000; Vrekoussis et al., 2004), about 90-91% of the monoterpenes would react with NO_3 and the remainder mostly with O_3. The high terpene reaction rates with NO_3 compared with OH and O_3 more than compensate for low nighttime concentrations of NO_3. Thus, at night, ~90% of the terpenes will generate the NO_3 reaction products listed above and the remaining ~10% of monoterpenes will likely react via ozonolysis, forming byproducts mentioned earlier. We note that production of alkyl nitrates from NO_3 oxidation of fire-generated monoterpenes may tie up NO_x for long-distance transport and may also change the composition of secondary aerosol. In summary, most prescribed fires are started during the day and most of the smoke will undergo daytime oxidation schemes, but is not uncommon for some fires to burn at night when emitted smoke is likely different and also subject to very different chemical oxidation pathways.

Considerable work has been done to investigate SOA yields from monoterpene oxidation (Saathoff et al., 2009; Griffin et al., 1999; Spittler et al., 2006; Fry et al., 2011). While SOA formation via nucleation processes has been observed, the more common path for SOA formation occurs via condensation of gas-phase oxidation products onto pre-existing aerosol, given the ubiquitous presence of condensation surfaces in the atmosphere (Hamilton et al., 2011). In a biomass burning plume, extremely high amounts of NMOCs, and organic and inorganic aerosol are simultaneously released creating numerous surface sites for condensation in a highly oxidizing plume environment (OH concentration reaching magnitudes of 10^7 cm^3

molec^{-1} s^{-1}; Hobbs et al., 2003; Yokelson et al., 2009). Most research regarding SOA from terpenes has been performed in controlled laboratories and/or photochemical chambers where variables such as "seed" aerosol or oxidant concentration can be varied. However, extrapolating chamber results to atmospheric conditions is not simplistic (Holzinger et al., 2010), but our confirmation of high levels of limonene and other terpenes in smoke plumes could help explain some of the variability in SOA production observed in BB plumes to date (Saathoff et al., 2009; Hennigan et al., 2011; Akagi et al., 2012). It was possible to measure both the sum of monoterpenes by FTIR and/or WAS and the initial OA by AMS on three fires, which yielded mass ratios (Σterpenes/OA g g^{-1}) of 0.17, 0.15, and 0.36 (Table 3.3). On average, monoterpenes measured in this work comprise 21% of measured OA on a mass basis. Monoterpenes will not convert 100% to SOA and OA aging in BB plumes has been observed to lead to small decreases in OA or increases up to a factor of ~3 (Hennigan et al., 2011). Thus, unless terpenes are emitted in much greater quantities from other fuel types they likely contribute to most of the total variability observed in SOA. Because each monoterpene has 10 carbon atoms, variability in monoterpenes and their subsequent oxidation could potentially contribute to a larger share of the variability observed in production of smaller OVOC downwind (Yokelson et al., 2008; 2009; Pan et al., 2009; Holzinger et al., 2010; Akagi et al., 2012; Jacob et al., 2002; Jost et al., 2003; Holzinger et al., 2005; Sect. 3.3.7). In this work monoterpenes comprise only 3.9% of NMOC on a molar basis, and NMOC other than monoterpenes are abundant and likely account for most of the SOA and OVOC variability as explored elsewhere (Yokelson et al., 2012).

3.3.4 C_3-C_4 alkynes

A recent study was able to assign CO and other air-quality-relevant species observed in the Mexico City area to either biomass burning or urban emissions by assuming that the great majority of HCN was emitted by biomass burning, while C_2H_2 was associated with both urban emissions and biomass burning, but with different ratios to CO (Crounse et al., 2009). C_2H_2 is emitted in higher proportion to CO in urban emissions than in biomass burning emissions and the C_2H_2 from biomass burning is usually produced mostly by flaming combustion of biomass (Lobert et al., 1991; Yokelson et al., 2008). C_2H_2 has a relatively slow reaction rate with OH resulting in an atmospheric lifetime of ~10 days to two weeks (Crounse et al., 2009), which is longer than most other hydrocarbons. Because of its emission from multiple sources, acetylene is not an ideal tracer for any one source. In the work of Simpson et al. (2011) it was observed that other alkynes, such as propyne and 1+2-butynes were emitted by biomass burning alone, making them of interest as possible BB indicators, despite having a relatively shorter lifetime of ~2 days. We report a study-average ER(Δpropyne/ΔCO) of $4.51 \pm 0.50 \times 10^{-4}$ from the airborne-based platform, which is 2.5 times greater than ER(Δpropyne/ΔCO) reported in Simpson et al. (2011) ($1.8 \pm 0.8 \times 10^{-4}$). We observed the emission of the higher alkynes from all the fires with WAS samples, which further suggests their potential use as biomass burning tracers. In addition, Figure 3.13 shows that the three C_3-C_4 alkynes detected in this work are positively correlated with MCE, however, the strength of this correlation is variable for the different alkynes. We use linear functions to fit MCE plots, however we do not suggest that we fully understand nor can explain this complex relationship between EF and MCE in such a simplistic manner. All sample points are shown in Figure 3.13 to emphasize the natural variability that can occur between

samples. This data suggest that, like C_2H_2, these C_3-C_4 alkynes are mostly produced by flaming combustion.

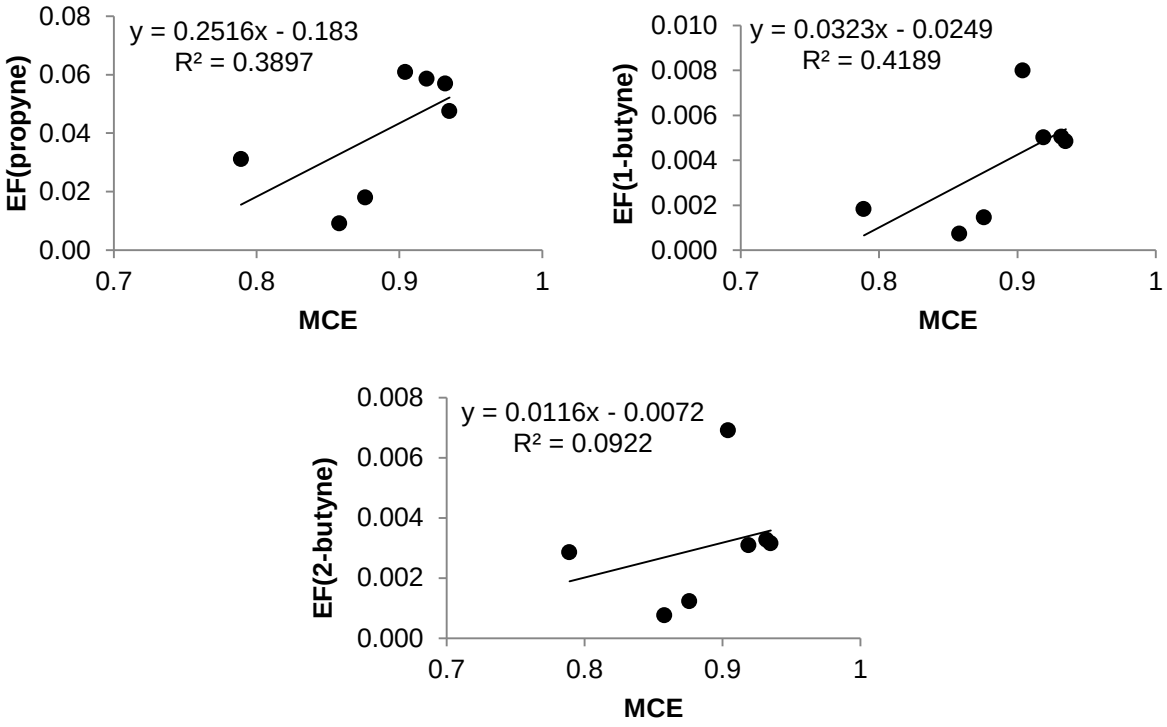

Figure 3.13. Alkyne emission factors (g kg^{-1}) as a function of MCE from the Block 6, 9, 22b, and plantation fires in this study measured from airborne and ground-based platforms. The positive correlation of EF vs. MCE suggests all alkynes are emitted chiefly by flaming combustion processes.

3.3.5 **Initial emissions of nitrogen species**

3.3.5.1 ***NH_3***

NH_3 is the most abundant alkaline gas in the atmosphere and is important in neutralizing acidic species in PM (Seinfeld and Pandis, 1998). Biomass burning is an important NH_3 source

(Crutzen and Andreae, 1990) and biomass burning emissions of NH_3 are typically strongly anti-correlated with MCE, meaning it is primarily emitted from smoldering combustion. We compare our EF(NH_3) from both the air and ground with other EF(NH_3) from biomass burning studies of similar fuel types (Fig. 3.14). The red, blue, and green points represent smoke sampled from the ground, air, and laboratory, respectively.

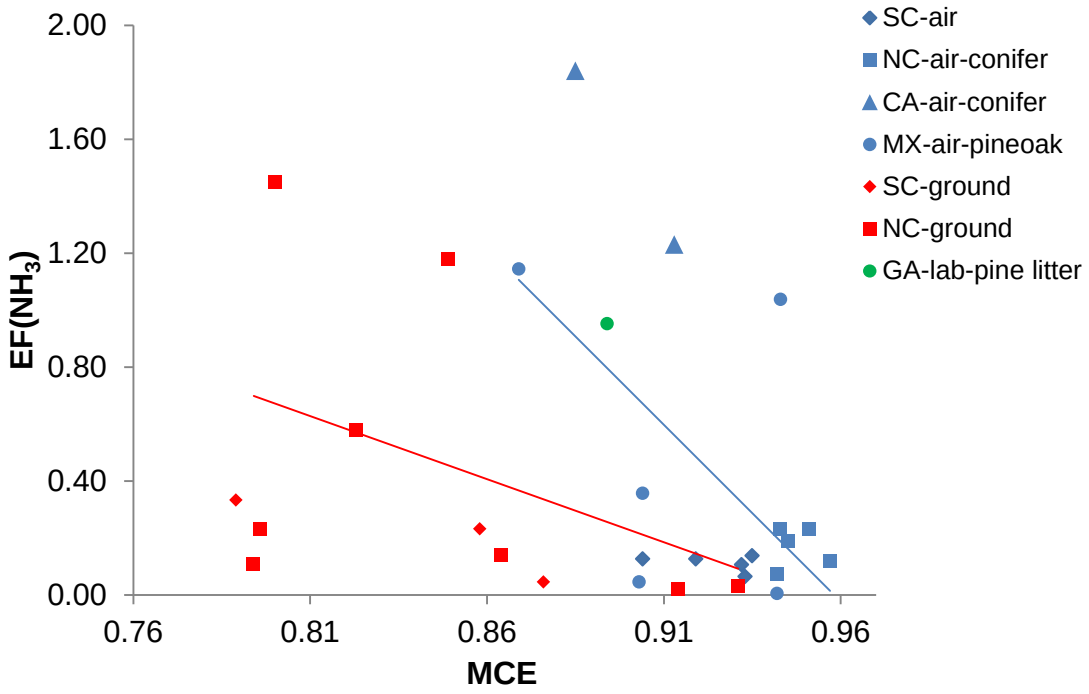

Figure 3.14. EF(NH_3) (g kg^{-1}) as a function of MCE for the Fort Jackson pine burns of this study measured from both airborne (blue) and ground-based (red) platforms. We also show ground-based, airborne, and laboratory (green) measurements in similar fuels from Burling et al. (2011), airborne data from Mexican pineoak forests from Yokelson et al. (2011), and pine litter laboratory data from Fort Benning, GA (Burling et al., 2010). Anti-correlations of EF(NH_3) vs. MCE for ground-based (red line) and airborne (blue line) measurements are shown.

A general pattern emerges that the airborne EF(NH_3) decrease going from California to Mexico to NC to SC and the ground-based EF(NH_3) decrease from NC to SC. Thus the SC

EF(NH_3) are systematically lower than observed in other studies of understory fires in pine-dominated forests. Other factors besides MCE can affect ammonia emissions, the most notable being the nitrogen content of vegetation. The nitrogen content tends to be lower in woody biomass (e.g. logs) compared to foliage (Susott et al., 1996; Burling et al., 2011). While the N content of fuels sampled in this work is unknown, this could explain why the ground-based samples (often of smoldering logs/stumps) had EF(NH_3) that were generally lower than the airborne data regression relationship (blue line)would predict.

3.3.5.2 ***HCN***

HCN is produced from the pyrolysis of amino acids and is now widely recognized as a useful biomass burning tracer or indicator (Li et al., 2003; Crounse et al., 2009). Here we compare the ER(ΔHCN/ΔCO) from this work to other works in similar fuels, including Burling et al. (2011), Yokelson et al. (2011), Simpson et al. (2011), and Burling et al. (2010), who report ER from US conifer forest understory burns, Mexican rural pine-oak forests, Canadian boreal fires, and pine litter from Fort Benning, Georgia, respectively (Fig. 3.15). We also include ERs from some very different, but globally important fuel types, including savanna fires from Africa (Yokelson et al., 2003), tropical evergreen deforestation fires from Brazil (Yokelson et al., 2007a), peat (Akagi et al., 2011), and fires in tropical dry forest (Yokelson et al., 2009).

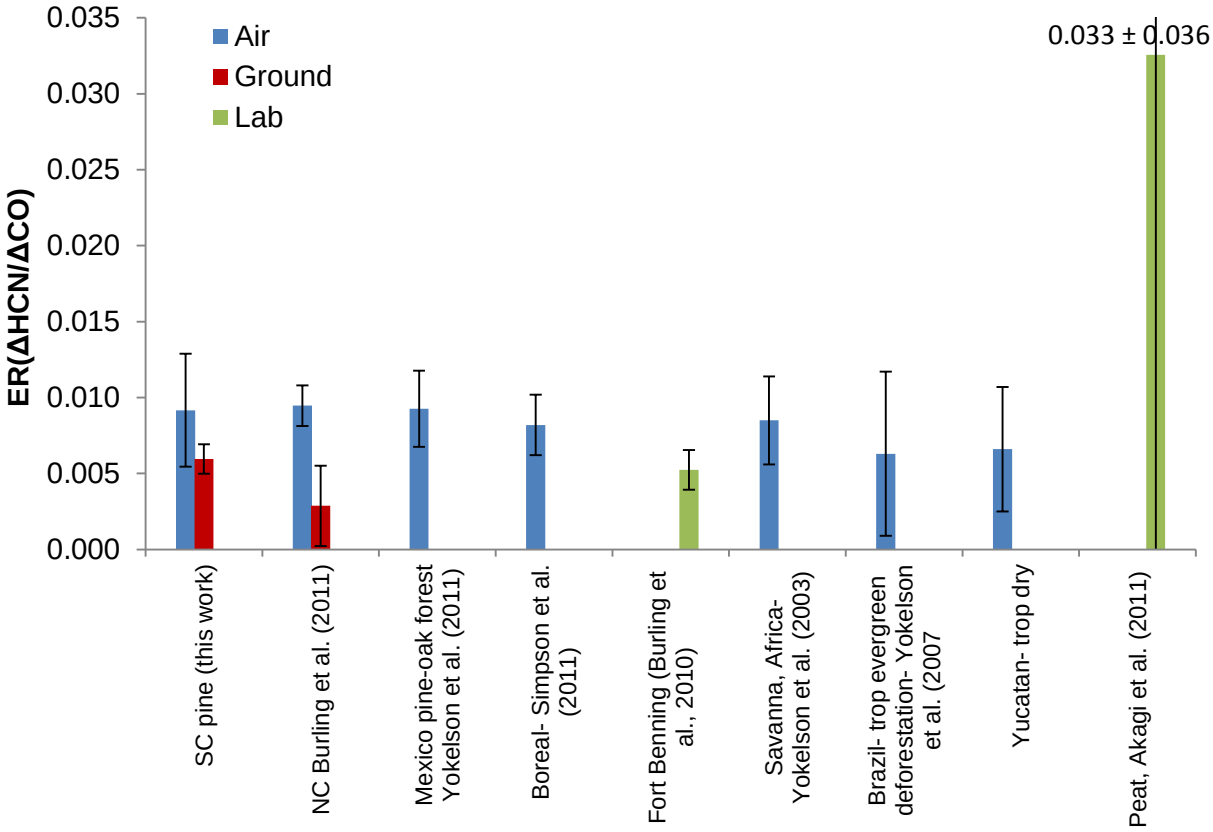

Figure 3.15. Comparison of HCN/CO study-average emission ratios (mol/mol) measured from airborne (blue), ground-based (red), and laboratory (green) platforms from five North American studies in pine forest fuels. We also show four ER(HCN/CO) in other fuel types for comparison. The large variation shown for peat is due to a very large value for Indonesian peat that is included in the calculation.

The airborne measurements of ER(ΔHCN/ΔCO) shown in Figure 3.15 are from fires in a variety of forest or savanna types and the study means all fall within the range 0.0063 to 0.0095. The ground-based and lab measurements shown are lower than this range with the exception of the ER(ΔHCN/ΔCO) from peat fires, which is more than three times larger than the other values at 0.035 (Akagi et al., 2011). In both this work and Burling et al. (2011) lower HCN emission ratios are observed from a ground-based platform compared to an airborne platform when

sampling the same fires. These Burling et al. (2011) NC ground-based measurements were made mostly right after high rainfall and a rare snow and much of the burn units were flooded with standing water. The SC ground-based measurements were made towards the end of a significant drought, and it is possible that more of the surface RSC fuels that emit HCN were able to burn in the SC fires. Fuel N was not measured in this work nor in Burling et al. (2011).

Overall, the airborne and ground-based data shown exhibit a strong EF(HCN) anti-correlation with MCE suggesting HCN release from smoldering combustion (Fig. 3.16) over a wide range of MCE's (0.85-0.96), despite airborne EF(HCN) being more or less independent of MCE in some studies of "non-pine" ecosystems (Yokelson et al., 2003). Also note in Figure 3.16 that the four or five outliers are all ground-based data, which may be probing emissions from a different mix of the overall fuel complex.

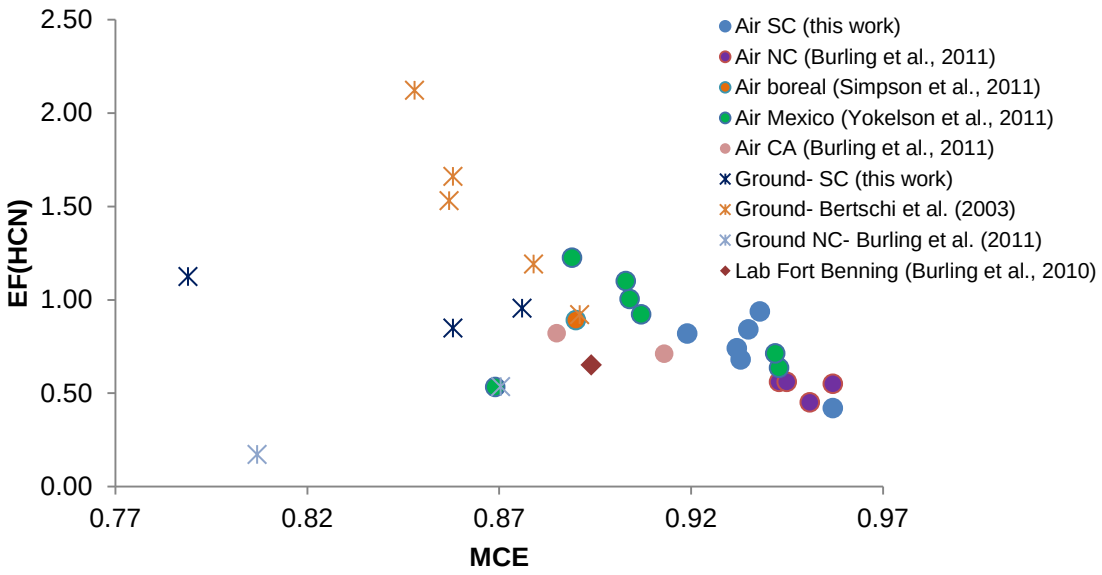

Figure 3.16. HCN fire-average emission factors (g kg^{-1}) as a function of MCE for pine/conifer fuel types measured airborne, ground-based, and laboratory platforms. The data show a general anti-correlation with MCE, however, ground-based data alone have higher variability and less MCE dependence.

The similarity of study averages shown in Figure 3.15 and noting that fire average MCE usually fall in the range of 0.90 – 0.94 (Figure 3.16) confirms that HCN is a useful tracer for the lofted emissions that account for much of the smoke generated by many global fires. However, more emissions measurements from other coniferous ecosystems in different regions (ex. boreal Russia) are needed before we can suggest that the anti-correlation in Figure 3.16 holds for all coniferous fuels globally. Additionally, the larger scatter at low MCE in Figure 3.16 suggests that HCN may be a better tracer for smoke that is lofted and transported as opposed to smoke that drifts at ground level. While EF(HCN) data from pine-forest organic soils collected from Montana, US and Northwest Territories, CA has high anti-correlation with MCE ($R^2 = 0.916$) (Bertschi et al., 2003), overall ground-level EF(HCN) from RSC are variable. As mentioned earlier, it is common for RSC data to have high scatter since the individual contributions from fuel types are measured rather than a blended sample in a convection column. Finally, the variability in HCN emissions is magnified when considering a broader range of fuel types. For instance, there are very high EF(HCN) emissions from peat, while Christian et al. (2010) report HCN levels below FTIR detection limits when sampling cooking fire emissions in both Mexico and Africa.

3.3.5.3 *Nitrous Acid (HONO)*

HONO is an important precursor for OH radicals in the atmosphere (Broske et al., 2003). Photolysis is the primary daytime fate of HONO and it forms OH and NO within 10-20 min (Sander et al., 2006). Given the importance of OH as a key atmospheric oxidant, photolysis of HONO could significantly affect the photochemistry of some aging plumes (Alvarado and Prinn,

2009). Originally believed to be formed by secondary reactions, HONO is now recognized as a substantial direct emission from fires that has been measured in both the lab and the field (Trentmann et al., 2005; Keene et al., 2006; Burling et al., 2010; 2011; Yokelson et al., 2007a). In this work, HONO was detected on four out of seven research flights and was below detection limit in all ground-based samples. The $\Delta HONO/\Delta NO_x$ molar ratios in this work ranged from 0.158 to 0.329 with an average of 0.226 ± 0.091, which is higher than ratios obtained from laboratory and airborne measurements of fires in pine forest understory fuels in both Burling et al. (2010) (0.109 ± 0.039) and Burling et al. (2011) (0.130 ± 0.045), respectively. The high $\Delta HONO/\Delta NO_x$ ratios in this work confirm that HONO can be a significant part of the total NO_y.

3.3.6 **Sulfur containing species**

Carbonyl sulfide (OCS) is a known emission from biomass burning and its long tropospheric lifetime of 2–7 years (Xu et al., 2002) makes it a major non-volcanic source of sulfur to the upper atmosphere (Blake et al., 2004). OCS is ultimately oxidized to SO_2 which is usually the main S-containing emission of fires (Akagi et al., 2011), but SO_2 was not measured in this work. We report an OCS ground-based emission factor of 0.122 ± 0.187 (Table 3.3). The large standard deviation is primarily due to the very high EF measured from the Block 22b fire, which was approximately 20 times greater than EF measured from Block 6 or Block 9b. We report an average airborne OCS emission factor of 0.010 ± 0.003. Simpson et al. (2011) report EF(OCS) of 0.029 ± 0.007 from Canadian boreal forest fires, which is almost three times higher than our airborne EF(OCS). Yokelson et al. (1997) measured a high EF(OCS) of 1.63 ± 3.01 from boreal peat in the lab. OCS is anti-correlated with MCE (Table 3.4) making it primarily a smoldering emission. Analogous to nitrogen, sulfur emissions are highly dependent on fuel S content so the

variable EF reported in literature are not unreasonable. We also observed dimethyl sulfide emissions and report EF(DMS) of 0.032 ± 0.040 (ground-based) and 0.008 ± 0.003 (airborne). Unlike OCS, dimethyl sulfide has a much shorter lifetime (~1 day, Lenschow et al., 1999) and is quickly oxidized to compounds like SO_2 during daylight hours. Simpson et al. (2011) report EF(DMS) of 0.0023 ± 0.0012, which is significantly lower than what was observed in this work. Like OCS we note good anti-correlation with MCE (Table 3.4), confirming emission of DMS from smoldering and RSC.

3.3.7 **Plume aging**

Complex, highly variable photochemistry can cause large changes in smoke composition within minutes after its initial emission. There are numerous other chemical and physical processes that can affect fresh smoke as it begins to mix with ambient air, such as mixing with biogenic and/or anthropogenic pollutants, cloud processing, coagulation, and gas-to-particle conversion (Reid et al., 1998). The complexity of the aging scenario is strongly influenced by variable factors such as temperature, time of day, humidity, cloud cover, windspeed, and potential changes in concentration and speciation of the initial emissions at the fire source (Akagi et al., 2012). In this work we present downwind smoke measurements that help assess how photochemical processes and a few other factors affect plume chemistry.

Plume aging data was collected from the aircraft on four flights: Block 9b (1 Nov), Georgetown (7 Nov), Francis Marion (8 Nov), and Bamberg (10 Nov) fires. However, the "useable" data from this study was strongly limited by the extremely fast dilution rate of the plumes. For context, in plume aging measurements from a California chaparral fire named the Williams Fire, ΔCO values of ~350-937 ppb were observed after 4.5 h of plume aging (Akagi et

al., 2012). In plume aging measurements in South Africa (the Timbavati Fire), ΔCO values of 549-644 ppb were observed after almost an hour of aging (Hobbs et al., 2003). Jost et al. (2003) measured CO levels averaging 417 ppb after approximately 2 h of aging of a Namibian BB plume and defined the extent of the measured plume as the region with the CO mixing ratio exceeding 400 ppb. In contrast, in the SC plumes we typically observed an excess CO of ~25 ppb after just 1-1.5 h of aging, except on the Block 9b and Francis Marion fires, which had a few downwind ΔCO near 100 ppb, which is still relatively low. In fact, ΔCO from the Bamberg fire was often less than 50 ppb in the source smoke and only one source sample had ΔCO > 239 ppb, which shows the effect of rapid dilution even at the source. A consequence of this rapid dilution is a downwind SNR often ~100 times lower in SC than at the Williams Fire or Timbavati Fire. Low ΔCO of 25 ppb in downwind samples approaches the uncertainty (natural variability) in background CO (5-6 ppb), and most NMOC species are only present at ~2 ± 1% of CO so they are near or below our detection limit of ~1 ppb for most species. In summary, we obtained good downwind CO and O_3 data for all flights, but with the exception of methanol and formaldehyde on the Block 9b and Francis Marion fires, downwind AFTIR NMOC mixing ratios were near or below our limit of detection and prevent us from presenting well-supported conclusions. Additionally, we only had enough WAS canisters to obtain one downwind WAS sample. Also worth noting is the high background CO during this study. The Williams Fire and Timbavati Fire had background CO of ~100 ppb, along with isolated locations far from urban emission sources. The SC fires show average background CO mixing ratios of 170-250 ppb and were sometimes located near major urban centers, suggesting the ubiquitous presence of urban emissions and the inevitability of biomass burning/fossil fuel (BB/FF) mixing scenarios.

Another concern was identifying which downwind samples were pseudo-Lagrangian. We estimated the emission time of each downwind sample by subtracting the calculated smoke "age" (time since emission based on windspeed and distance downwind) from the time the downwind sample was collected. If the aircraft was sampling the source of the fire at the estimated emission time of the downwind sample and the plume was well-mixed at the source, we then have initial ERs that represent the starting chemistry of the downwind sample and it was classified as pseudo-Lagrangian. Further, for each fire in SC, the ER did not exhibit significant increasing or decreasing trends during our source sampling period so we took the fire-average ER as our best guess of the starting ER for all pseudo-Lagrangian downwind samples. When a sample was emitted before or after we were at the source, the fire-average ER is still our best guess at the appropriate ER to compare the downwind NEMR too, but that guess is less strongly supported, because the possibility is higher that the initial smoke chemistry was different when we were not sampling the source. To make this distinction in confidence clear, all downwind samples from all flights that were pseudo-Lagrangian are shown as solid circles and those samples that were emitted when we were not sampling at the fire source are considered non-Lagrangian and shown as open circles in Figs. 3.17, 3.20, and 3.21. Stated differently, since initial emission ratios showed minimal variability over the several hours that initial emissions were sampled, this suggests that the fire source emissions remained fairly constant. If this was the case, these non-Lagrangian downwind samples are still showing changes in the downwind plume mostly due to photochemistry, but we uniquely identify these samples to properly qualify our discussion.

Ozone formation downwind has been measured in various fuel types from BB (Andreae et al., 1994; Yokelson et al., 2009; Akagi et al., 2012; Goode et al., 2000; Jost et al., 2003). Here

we show downwind ozone data acquired from Block 9b, Georgetown, Francis Marion, and Bamberg fires (on 1 Nov, 7 Nov, 8 Nov, and 10 Nov, respectively, Fig. 3.17).

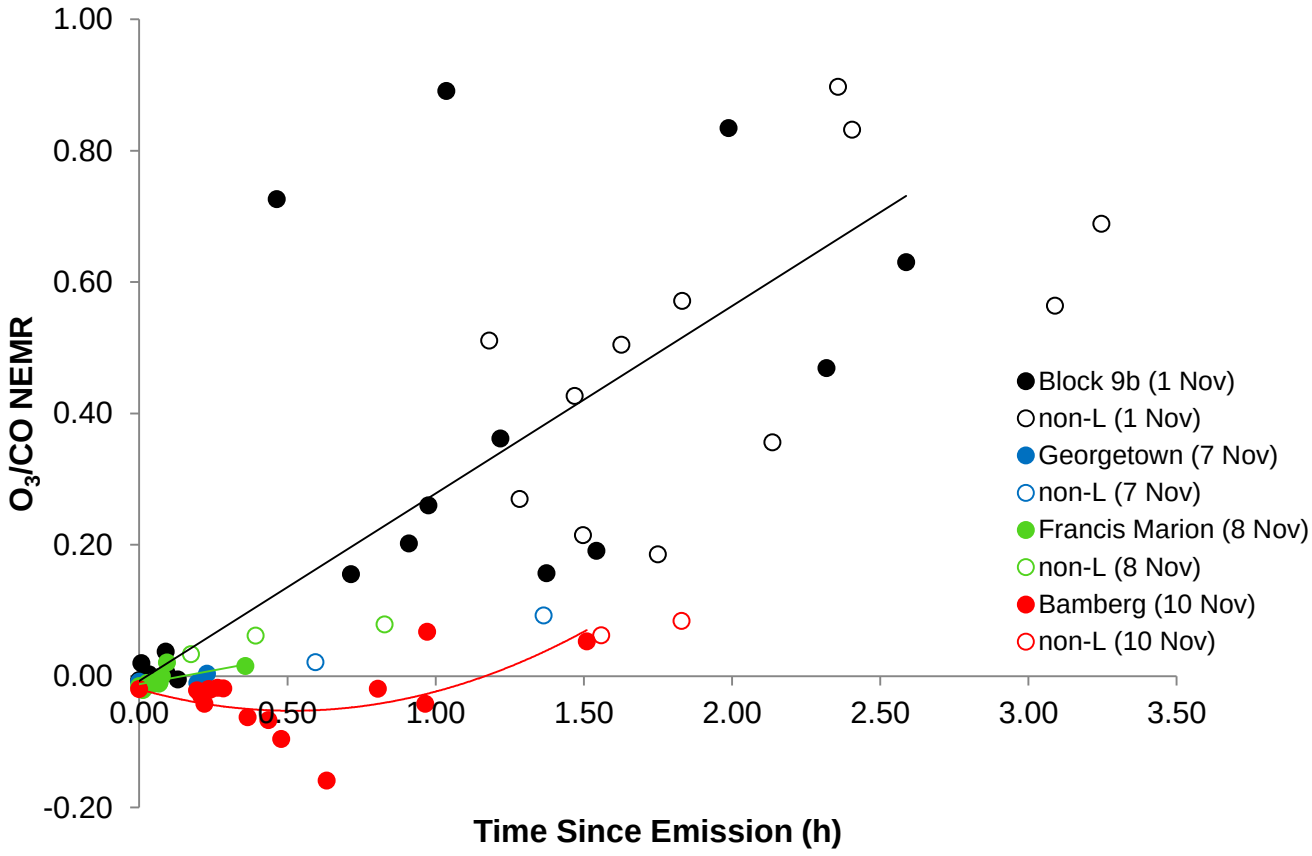

Figure 3.17. $\Delta O_3/\Delta CO$ NEMR ratios vs. time since emission (h). Airborne measurements were collected up to ~2.5 h downwind. Fires that we were able to collect downwind data on are shown: Block 9b (1 Nov, black), Georgetown (7 Nov, blue), Francis Marion (7 Nov, green), and Bamberg (10 Nov, red). The y-intercept of observed trendlines is forced to the average $\Delta O_3/\Delta CO$ NEMR at time t = 0 h for each given fire. Solid circles reflect data that was considered Lagrangian while open circles labeled "non-L" represent non-Lagrangian samples collected on that respective day.

Our most aged plume samples were collected from the Block 9b fire and are shown as black circles. Conditions were favorable for ozone formation with clear skies. Although variability in

the $\Delta O_3/\Delta CO$ NEMR is high on this day (e.g. a 15-90% range at 1.5 h), pseudo-Lagrangian and non-Lagrangian points basically follow the same trend suggesting about 70% $\Delta O_3/\Delta CO$ after 2.5 h, which is the fastest ozone formation that has been measured in a biomass burning plume to our knowledge. An additional feature of interest from the Block 9b fire is the low initial NO_x ER to CO (~0.01). Ozone production in BB plumes is normally NO_x limited downwind and so low initial NO_x would suggest minimal O_3 formation downwind. However, the Block 9b plume, though clearly composed primarily of BB smoke, was sampled downwind after transport over a region including part of the metropolitan Columbia area (population ~748,000), a large power plant and an airport (Fig. 3.18). We believe the plume mixed with background air that likely contained fresh NO_x from fossil fuel sources and we do not suggest that the rapid ozone formation observed is from an isolated biomass burning plume. Lee et al. (2008) and Jacob et al. (2010) have also reported an increase in ozone formation when biomass burning emissions are mixed with urban emissions.

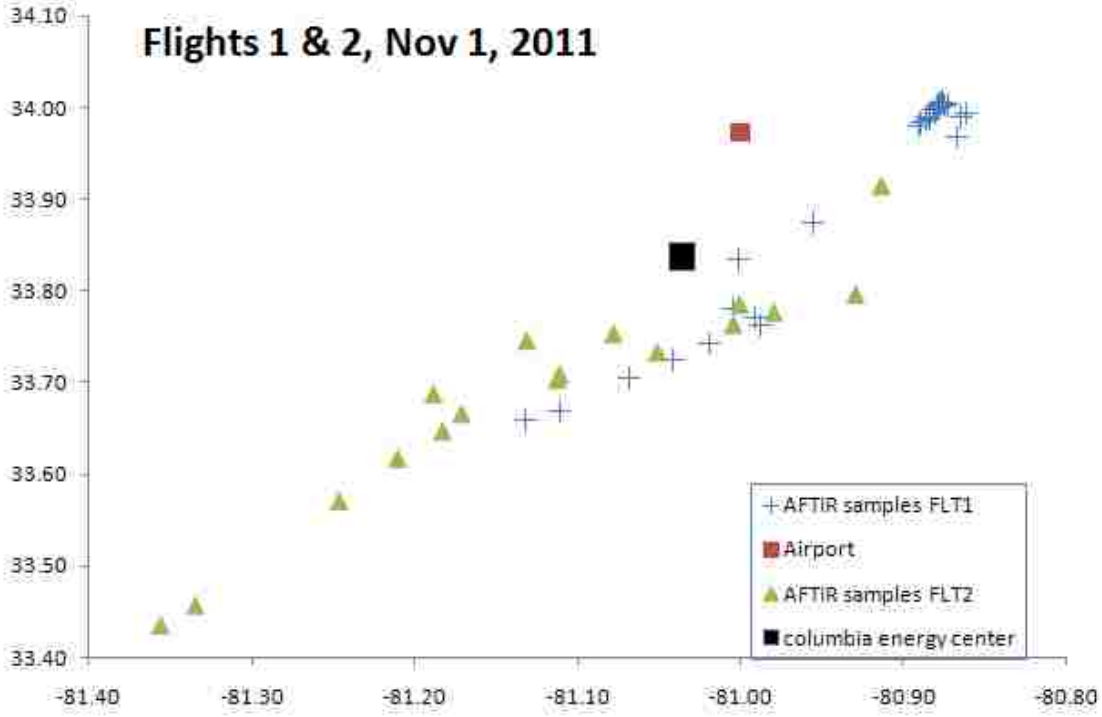

Figure 3.18. Downwind sample locations from both flights on 1 Nov (Block 9b) fire at Fort Jackson. Urban emission sources (airport and power plant, shown as red and black squares, respectively) are also shown.

The Georgetown and Francis Marion fires were on sunny days and in rural areas with no obvious sources of fossil fuel emissions to mix with. Downwind data were difficult to obtain because the fast dilution meant the plume could not be seen visually and had to be located by trial and error using the particle instruments. However variability at the source was minimal and we show quick ozone formation up to ~1.5% $\Delta O_3/\Delta CO$ in less than 30 min. This increase jumps to 8% in 50 min if non-Lagrangian samples are considered. This formation rate is considerably slower than that observed from Block 9b fire, but similar to the O_3 formation rate observed in tropical plumes in Africa and Mexico (Yokelson et al., 2003; Yokelson et al., 2009) and is over 4 times faster than the ~10% $\Delta O_3/\Delta CO$ observed in 4.5 h in the Williams Fire (Akagi et al., 2012).

The Bamberg fire shows the lowest/slowest formation of ozone from SC of less than 10% $\Delta O_3/\Delta CO$ after 2 h. This fire took place on a cloudy day with no notable FF/BB plume mixing, two factors which likely slowed down plume photochemistry. Ozone destruction appears to dominate over ozone formation resulting in a net loss of ozone during the first 30-45 min of plume aging. This is likely due in part to reaction with NO, but could be enhanced by the rapid reaction of ozone with VOCs such as terpenes within the first hour of plume aging. While this is the slowest O_3 formation in SCREAM, we note that overall O_3 formation calculated at the end of the aging measurements available was still as fast as ozone formation observed in the Williams Fire.

Figure 3.19 directly compares the SC ozone formation with two other studies discussed above: Akagi et al. (2012) who measured photochemical changes in the Williams Fire, and Yokelson et al. (2009) who observed ozone formation in a plume in the Yucatan, Mexico.

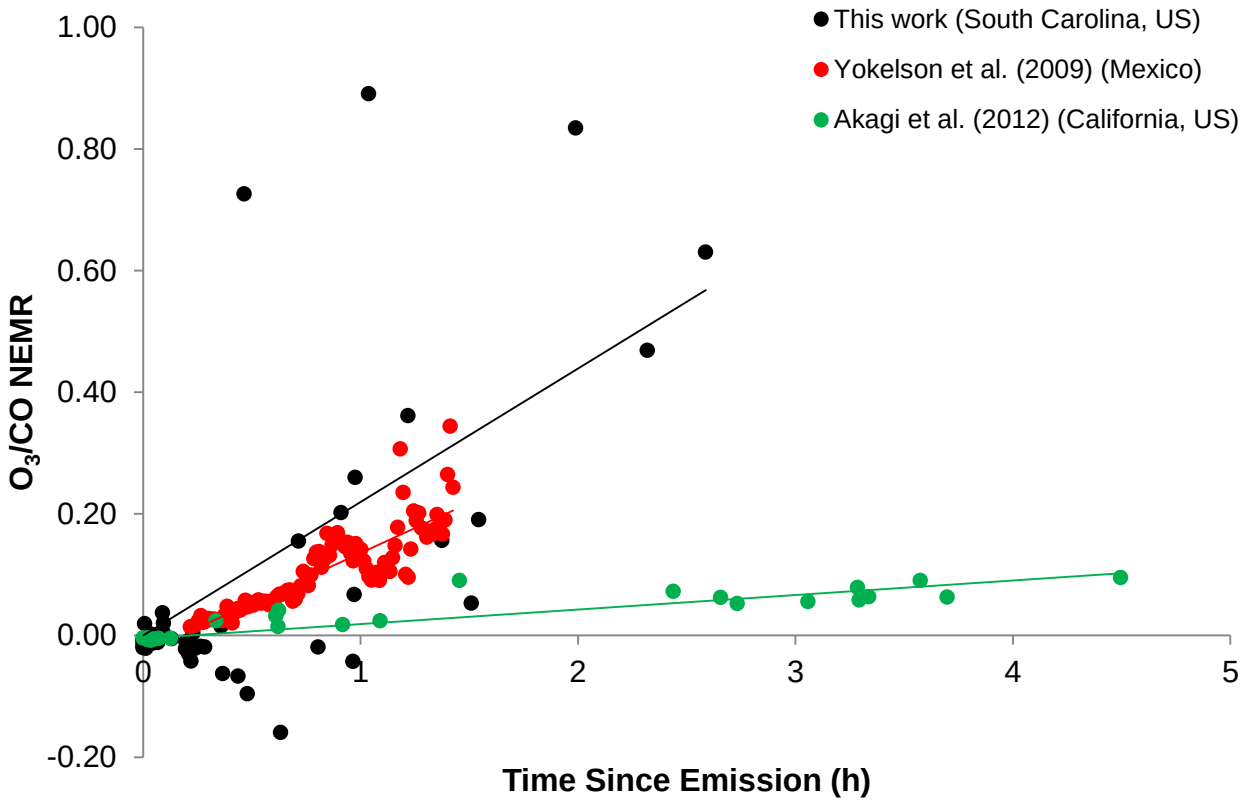

Figure 3.19. $\Delta O_3/\Delta CO$ vs. time since emission from this study (black), Yokelson et al. (2009) (red), and Akagi et al. (2012) (green).

As mentioned above, Akagi et al. (2012) observed a $\Delta O_3/\Delta CO$ NEMR increase up to ~10% of CO over the course of 4.5 h. Yokelson et al. (2009) measured a rapid increase in $\Delta O_3/\Delta CO$ to ~15% in less than 1 h from a plume in the Yucatan, similar to the fast ozone production (9% rise observed in just 0.7 h) measured from three isolated African BB plumes (Yokelson et al., 2003). In more general terms, O_3 formation is probably ubiquitous in tropical BB plumes, but O_3 destruction, as well as formation at many different rates can occur in extratropical plumes. For example, Goode et al. (2000) observed an ozone rise to 9% in ~2 h in an Alaskan plume and ozone formation in temperate BB fuels was noted previously by Hobbs et al. (1996) who report

1.5% $\Delta O_3/\Delta CO$ in 30 min in a BB plume in the Pacific Northwest. Nine plumes from boreal wildfires that were 6-15 days old were sampled in 2004 and 8 of the plumes had $\Delta O_3/\Delta CO$ ranging from 9% to 89% (Van Martin et al., 2006; Lapina et al., 2006). These levels are similar to what was observed in this work, however, we observed these high ozone levels in ~2.5 h compared with 6-15 days. We report a SC study average $\Delta O_3/\Delta CO$ of ~60% in 2.5 h. The highest ozone formation rates reported in this work are, as we mentioned above, the fastest we have seen reported in biomass burning plumes to date and we suggest they are linked to mixing with urban emissions, a plume mixing scenario that is expected to be widespread globally. Data on O_3 production in biomass burning plumes from ground stations, aircraft, and remote sensing are all important for validating global models, which consistently conclude that BB is a major global source of tropospheric O_3 (Fishman et al., 2003; Sudo and Akimoto, 2007).

3.3.7.1 ***Methanol***

In previous pseudo-Lagrangian measurements of aging biomass burning plumes the methanol to CO ratio was stable or slowly decreased (e.g. Goode et al., 2000). In non-Lagrangian measurements methanol/CO decreased rapidly in one biomass burning plume that was cloud-processed (Yokelson et al., 2003; Tabazadeh et al., 2004). Holzinger et al. (2005) measured NEMR for $\Delta CH_3OH/\Delta CO$ and $\Delta CH_3COOH/\Delta CO$ in biomass burning plumes several days old that were enhanced by factors of 2-6 and 2-14, respectively, above their estimate of the literature average ERs for these species. They attributed this to "pre-measurement" secondary formation of acetone and methanol in the plumes. In this study, in both fires with sufficient downwind SNR (Block 9b and Francis Marion burns), we observe a post-emission increase in CH_3OH, which confirms that methanol may sometimes be the oxidation product of co-emitted NMOC. The rates

of methanol formation downwind are variable (Figure 3.20). The Block 9b fire shows a $\Delta CH_3OH/\Delta CO$ increase from 0.013 to ~0.024 over 2 h following emission, an increase of a factor of 1.7. As was the case for ozone data from this fire, we see Lagrangian and non-Lagrangian data support the same general linear trend (though with high scatter) which further suggests that the source ER were relatively stable over most of the fire lifetime. From the Francis Marion burn we observe an even larger increase in $\Delta CH_3OH/\Delta CO$ from 0.012 up to ~0.03 within the first half hour, or an increase by a factor of 2.4. The results probably demonstrate how variability in the initial emissions can lead to differences in downwind evolution. Specifically, in this study, the oxidation of monoterpenes, which may have been at higher than average levels, probably contributed to the observed methanol increase. If all the initial monoterpenes (excluding isoprene) measured from the Francis Marion fire reacted to form methanol, we would observe a per carbon increase in $\Delta CH_3OH/\Delta CO$ of ~0.032, while the observed molar increase in $\Delta CH_3OH/\Delta CO$ on this day was ~0.018. While it is highly unlikely that ~50% of monoterpene photo-oxidation products end up as methanol, we simply show that there are sufficient monoterpene emissions to cause a large part of the increase in $\Delta CH_3OH/\Delta CO$. Furthermore, the initial "total" amount of monoterpenes from Francis Marion quoted above was due solely to limonene, as other monoterpenes were not measured on this fire, but were likely present (AFTIR could only specifically retrieve limonene). Thus, we'd expect the actual ER(Σmonoterpenes/CO) to be significantly higher. In summary, while the mechanism for CH_3OH formation remains speculation, this work confirms that secondary production can sometimes be significant compared with primary emission. Secondary production of methanol, if common, would suggest

a larger biomass burning contribution to the global methanol budget, but clearly vegetation would still be the dominant source (Jacob et al., 2005).

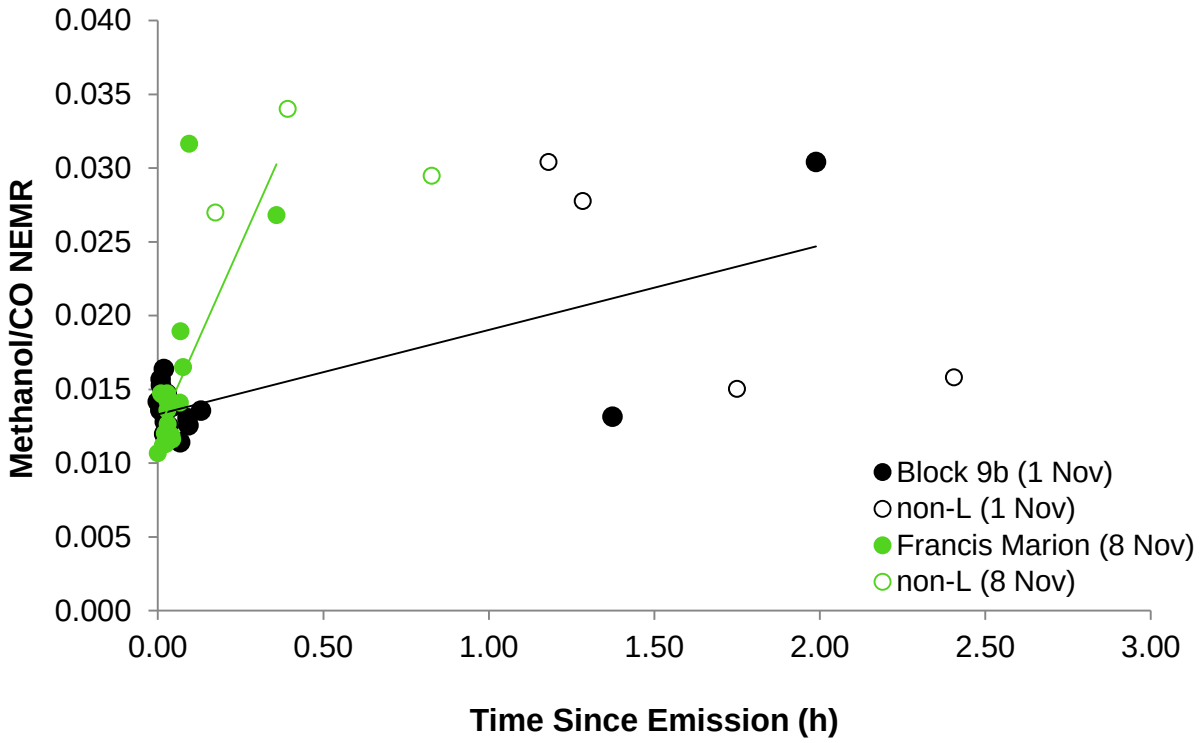

Figure 3.20. $\Delta CH_3OH/\Delta CO$ NEMR ratios vs. time since emission (h). Airborne measurements were collected up to ~2.5 h downwind. Fires on which we were able to collect downwind data with good SNR, Block 9b (1 Nov, black) and Francis Marion (8 Nov, green), are included here. The y-intercept of observed trendlines is forced to the average ER(CH_3OH) at time *t*=0 for each particular fire. Solid circles reflect data that was considered Lagrangian while open circles labeled "non-L" represent non-Lagrangian samples collected on that respective day.

3.3.7.2 ***Formaldehyde***

Increases in ΔHCHO/ΔCO were observed over the course of ~2 h following emission (Fig. 3.21). Data from Block 9b show an increase in ΔHCHO/ΔCO from 0.022 to 0.075, or by a factor of 3.5, in just under 2.5 h. On the Francis Marion burn we observed an immediate, sharp increase in ΔHCHO/ΔCO by a factor of ~3.7 from 0.024 to 0.089 in under 30 min. These increases are

larger than previously reported in pseudo-Lagrangian measurements (e.g. Akagi et al., 2012) although a similar increase was measured by the NCAR HCHO instrument, but not reported in Yokelson et al. (2009). The downwind ΔCO from the Francis Marion fire were all above ~120 ppb and the samples shown all have ΔHCHO well above the 1 ppb HCHO detection limit, suggesting that these dramatic increases are significant. Formaldehyde is an important source of OH in biomass burning plumes (Mason et al., 2001) and secondary production has previously been observed in biomass burning plumes (Akagi et al., 2012). Formaldehyde can be formed via oxidation of many reactive NMOC. For instance, it is a known product of monoterpene oxidation and has been the observed from alpha-pinene ozonolysis and limonene oxidation via OH (Capouet et al. 2004; Muller et al., 2005). On the other hand, HCHO is also lost by photolysis and reaction with OH or HO_2. Clearly NMOC in addition to the terpenes invoked as examples above also need to contribute to explain HCHO increases as large as we observe. Thus, HCHO, and by extension OH, will be at levels heavily influenced by the particular mix of many co-emitted NMOC.

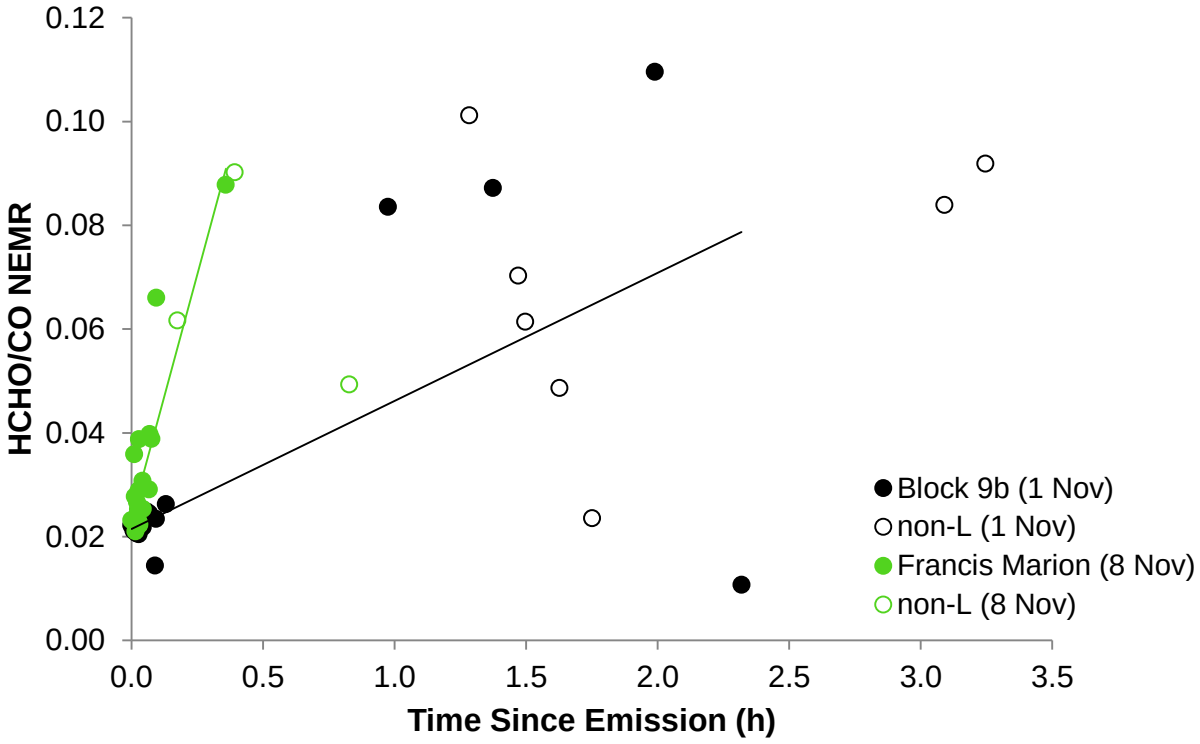

Figure 3.21. ΔHCHO/ΔCO NEMR ratios vs. time since emission (h). Airborne measurements were collected up to ~2.5 h downwind. Fires which we were able to collect downwind data, Block 9b (1 Nov, black) and Francis Marion (8 Nov, green), are included here. The y-intercept of observed trendlines is forced to the average ER(HCHO) at time *t*=0 for each particular fire. Solid circles reflect data that was considered Lagrangian while open circles labeled "non-L" represent non-Lagrangian samples collected on that respective day.

CHAPTER 4: CONCLUSIONS

4.1 *The South Carolina Regional Emissions and Aging Measurements campaign*

The final phase of our study of southeastern US prescribed fire emissions succeeded in greatly expanding the range of weather and fuel conditions probed and the scope of smoke measurements collected. Our previous work probed the emissions from frequently burned loblolly pine stands during a wet Spring. The results reported here include data for infrequently burned longleaf pine stands during a dry Fall (October-November of 2011). The recent data shows very large differences in emission factors for numerous species when compared to the previous phases of the study conducted in ecosystems that are nominally "the same" in many simplified global vegetation schemes. Thus, the results now give a much improved picture of the real variability in emissions at least for prescribed fires in pine forest understory fuels. However, further work would be needed to increase the ability to predict the emissions a priori from such a variable phenomenon with reasonable accuracy.

The expanded suite of measurements resulted in data for 97 trace gas species including their emission factors from 7 prescribed fires - from both airborne and ground-based platforms. The measurements reported here include data for a large suite of terpene compounds emitted by actual wildland fires for the first time. The known chemistry of the terpenes and their variable measured initial abundance is consistent with our observations of post-emission formation of ozone and small organic trace gases. In particular, we report the first pseudo-Lagrangian

measurements of methanol formation in the sampled plumes (an approximate doubling) and also the most dramatic post-emission increases in HCHO published to date (an approximate tripling). The monoterpenes observed are known precursors of methanol and formadehyde, but other NMOC, both measured and unmeasured likely contributed. If secondary methanol production in biomass burning plumes is common, then the global methanol source from biomass burning should be scaled upwards. Perhaps surprisingly, given the high variability in NMOC emissions, the ΔHCN/ΔCO emission ratio fell within a fairly narrow range that included the ΔHCN/ΔCO ratio for fires in many other ecosystems, further confirming the value of HCN as a biomass burning indicator/tracer. The SC results also support an earlier finding that C_3-C_4 alkynes may be of use as biomass burning indicators on the time-scale of hours to a day. It was possible to measure the photochemical production of ozone in four of the plumes. Slower O_3 production was observed on a cloudy day with low co-emissions of NO_x and the fastest O_3 production was observed on a sunny day when the plume almost certainly incorporated significant additional NO_x by passing over the Columbia, SC metro area. In the mixed BB/FF plume $\Delta O_3/\Delta CO$ reached levels from 10-90% within one hour and total O_3 was as high as 104 ppb. With population increasing both in the Southeast U.S. and in developing countries where biomass burning is common globally, the aggressive ozone increase in mixed emissions could be an increasingly significant public health issue.

4.2 *Future Work*

The findings reported here open multiple doors toward opportunities for future work. While this work had doubled what we know about RSC, further improving characterization of smoldering combustion is necessary to better our understanding of flaming vs. smoldering combustion processes. As this work confirms the emissions of monoterpenes from biomass burning, we should next confirm biomass burning as a source of additional terpenes not measured in SCREAM, such as terpinene. The emission of additional terpenes from BB would increase their percentage of total NMOC along with their potential to contribute to SOA. Additionally, we can improve characterization of smoldering combustion by searching for emission trends amongst similar RSC fuel types (ex. logs, stumps, litter, etc.). High variability in ground-based data may possibly be explained from assessing ground emissions based on sample type. Other areas of future work include emissions measurements from other important fire types in the United States including crop/agricultural fires, which were not discussed here. Lastly, we emphasize the importance of alkynes as potential biomass burning tracers for future campaigns. If exclusively emitted from biomass burning, C_3-C_4 alkynes may serve as easy to measure, relatively long-lived tracers to help discern biomass burning from urban emissions sources.

5 REFERENCES

Achtemeier, G. L.: Measurements of moisture in smoldering smoke and implications for fog, Int. J. Wildland Fire, 15, 517-525, doi:10.1071/WF05115, 2006.

Akagi, S. K., Yokelson, R. J., Wiedinmyer, C., Alvarado, M. J., Reid, J. S., Karl, T., Crounse, J. D., and Wennberg, P. O.: Emission factors for open and domestic biomass burning for use in atmospheric models, Atmos. Chem. Phys., 11, 4039-4072, 2011.

Akagi, S. K., Craven, J. S., Taylor, J. W., McMeeking, G. R., Yokelson, R. J., Burling, I. R., Urbanski, S. P., Wold, C. E., Seinfeld, J. H., Coe, H., Alvarado, M. J., and Weise, D. R.: Evolution of trace gases and particles emitted by a chaparral fire in California, Atmos. Chem. Phys., 12, 1397-1421, 2012.

Alvarado, M. J. and Prinn, R. G.: Formation of ozone and growth of aerosols in young smoke plumes from biomass burning: 1. Lagrangian parcel studies, J. Geophys. Res., 114, D09306, doi: 10.1029/2008JD011144, 2009.

Andreae, M. O., Browell, E. V., Garstang, M, et al.: Biomass burning emissions and associated haze layers over Amazonia, J. Geophys. Res., 93, 1509-1527, 1988.

Andreae, M. O., Anderson, B. E., Blake, D. R., Bradshaw, J. D., Collins, J. E., Gergory, G. L., Sachse, G. W., and Shipham, M. C.: Influence of plumes from biomass burning on atmospheric chemistry over the equatorial and tropical South Atlantic during CITE 3, J. Geophys Res., 99, 12793-12808, doi: 10.1029/94JD00263, 1994.

Andreae, M. O., Artaxo, P., Fischer, H., Freitas, S. R., Grégoire, J. –M., Hansel, A., Hoor, P., Kormann, R., Krejci, R., Lange, L., Lelieveld, J., Lindinger, W., Longo, K., Peters, W., de Reus, M., Scheeren, B., Silva Dias, M. A. F., Ström, J., van Velthoven, P. F. J, and Williams, J.: Transport of biomass burning smoke to the upper troposphere by deep convection in the equatorial region, Geophys. Res. Lett., 28 (6), 951-954, 2001.

Andreae, M. O., Rosenfeld, D., Artaxo, P., Costa, A. A., Frank, G. P., Longo, K. M., and Silva Dias, M. A. F.: Smoking rain clouds over the Amazon, Science, 303, 1337-1342, 2004.

Archibald, A.T., Cooke, M. C., Utembe, S. R., Shallcross, D. E., Derwent, R. G., and Jenkin, M. E.: Impacts of mechanistic changes on HO_x formation and recycling in the oxidation of isoprene, Atmos. Chem. Phys., 10, 8097-8118, 2010.

Atkinson, R. and Arey, J.: Gas-phase tropospheric chemistry of biogenic volatile organic compounds: a review, Atmos. Environ.,37, S197–S219, 2003.

Bertschi, I. T., Yokelson, R. J., Ward, D. E., Christian, T. J., and Hao, W. M.: Trace gas emissions from the production and use of domestic biofuels in Zambia measured by open-path Fourier transform infrared spectroscopy, J. Geophys. Res., 108, D13, 8469, doi:10.1029/2002JD002158, 2003a.

Bertschi, I. T., Yokelson, R. J., Ward, D. E., Babbitt, R. E., Susott, R. A., Goode, J. G., and Hao, W. M.: Trace gas and particle emissions from fires in large diameter and belowground biomass fuels, J. Geophys. Res. 108, D13, 8472, doi:10.1029/2002JD002100, 2003b.

Beswick, K. M., Gallagher, M. W., Webb, A. R., Norton, E. G. and Perry, F.: Application of the Aventech AIMMS20AQ airborne probe for turbulence measurements during the

Convective Storm Initiation Project, Atmos. Chem. Phys., 8, 5449–5463, doi:10.5194/acp-8-5449-2008, 2008.

Biswell, H. H.: Prescribed burning in California wildlands vegetation management, Berkeley, CA: University of California Press; p. 255, 1989.

Blake, N. J., Streets, D. G., Woo, J.-H., Simpson, I. J., Green, J., Meinardi, S., Kita, K., Atlas, E., Fuelberg, H. E., Sachse, G., Avery, M. A., Vay, S. A., Talbot, R. W., Dibb, J. E., Bandy, A. R., Thornton, D. C., Rowland, F. S., and Blake, D. R.: Carbonyl sulfide and carbon disulfide: Large-scale distributions over the western Pacific and emissions from Asia during TRACE-P, J. Geophys. Res., 109, D15S05, doi:10.1029/2003JD004259, 2004.

Bond, T. C., Streets, D. G., Yarber, K. F., Nelson, S. M., Woo, J., and Klimont, Z.: A technology-based global inventory of black and organic carbon emissions from combustion, J. Geophys. Res., 109, D14203, doi:10.1029/2003JD003697, 2004.

Bouvier-Brown, N. C., Holzinger, R., Palitzsch, K., Goldstein, A. H.: Large emissions of sesquiterpenes and methyl chavicol quantified from branch enclosure measurements, Atmos. Environ., 43, 389-401, 2009.

Broske, R., Kleffmann, J., and Wiesen, P.: Heterogeneous conversion of NO_2 on secondary organic aerosol surfaces: A possible source of nitrous acid (HONO) in the atmosphere?, Atmos. Chem. Phys., 3, 469-474, 2003.

Burling, I. R., Yokelson, R. J., Akagi, S. K., Urbanski, S. P., Wold, C. E., Griffith, D. W. T., Johnson, T. J., Reardon, J., and Weise, D. R.: Airborne and ground-based measurements

of the trace gases and particles emitted by prescribed fires in the United States, Atmos. Chem. Phys., 11, 12197-12216, 2011.

Burling, I. R., Yokelson, R. J., Griffith, D. W. T., Johnson, T. J., Veres, P., Roberts, J. M., Warneke, C., Urbanski, S. P., Reardon, J., Weise, D. R., Hao, W. M., and de Gouw, J.: Laboratory measurements of trace gas emissions from biomass burning of fuel types from the southeastern and southwestern United States, Atmos. Chem. Phys., 10, 11115-11130, 2010.

Canagaratna, M. R., Jayne, J. T., Jimenez, J. L., Allan, J. D., Alfarra, M. R., Zhang, Q., Onasch, T. B., Drewnick, F., Coe, H., Middlebrook, A., Delia, A., Williams, L. R., Trimborn, A. M., Northway, M. J., DeCarlo, P. F., Kolb, C. E., Davidovits, P., and Worsnop, D. R.: Chemical and microphysical characterization of ambient aerosols with the Aerodyne aerosol mass spectrometer, Edited by A. Viggiano, Mass Spectrometry Reviews, 26, 185-222, 2007.

Capouet, M., Peeters, J., Noziere, B., and Muller, J.-F.: Alpha-pinene oxidation by OH: simulations of laboratory experiments, Atmos. Chem. Phys., 4, 2285-2311, 2004.

Carter, M. C., and Foster, C. D.: Prescribed burning and productivity in southern pine forests: a review, Forest Ecology and Management, 191, 93-109, 2004.

Christian, T., Kleiss, B., Yokelson, R. J., Holzinger, R., Crutzen, P. J., Hao, W. M., Saharjo, B. H., and Ward, D. E.: Comprehensive laboratory measurements of biomass-burning emissions: 1. Emissions from Indonesian, African, and other fuels, J. Geophys. Res., 108, D23, 4719, doi:10.1029/2003JD00304, 2003.

Christian, T. J., Yokelson, R. J., Carvalho Jr., J. A., Griffith, D. W. T., Alvarado, E. C., Santos, J. C., Neto, T. G. S., Veras, C. A. G., and Hao, W. M.: The tropical forest and fire emissions experiment: Trace gases emitted by smoldering logs and dung from deforestation and pasture fires in Brazil, J. Geophys. Res., 112, D18308, doi: 10.1029/2006JD008147, 2007.

Christian, T. J., Yokelson, R. J., Cárdenas, B., Molina, L. T., Engling, G., and Hsu, S. -C.: Trace gas and particle emissions from domestic and industrial biofuel use and garbage burning in central Mexico, Atmos. Chem. Phys., 10, 565-584, 2010.

Cochrane, M. A., Moran, C. J., Wimberly, M. C., Baer, A. D., Finney, M. A., Beckendorf, K. L., Eidenshink, J., and Zhu, Z.: Estimation of wildfire size and risk changes due to fuels treatments, Int. J. of Wildland Fire, 21, 4, 357-367, 2012.

Crounse, J. D., DeCarlo, P. F., Blake, D. R., Emmons, L. K., Campos, T. L., Apel, E. C., Clarke, A. D., Weinheimer, A. J., McCabe, D. C., Yokelson, R. J., Jimenez, J. L., and Wennberg, P. O.: Biomass burning and urban air pollution over the Central Mexican Plateau, Atmos. Chem. Phys., 9, 4929-4944, 2009.

Crutzen, P. J. and Andreae, M. O.: Biomass burning in the tropics: Impact on atmospheric chemistry and biogeochemical cycles, Science, 250, 1669-1678, 1990.

Crutzen, P. J., and Andreae, M. O.: Biomass burning in the tropics: Impact on atmospheric chemistry and biogeochemical cycles, Science, 250, 1669-1678, 2000.

Deeming, J. E., Burgan, R. E. and Cohen, J. D.: The 1978 National Fire-Danger Rating System, Gen. Tech. Rep. INT-39, USDA Forest Service, Ogden, UT., 1978.

Drewnick, F., Hings, S. S., DeCarlo, P., Jayne, J. T., Gonin, M., Fuhrer, K., Weimer, S., Jimenez, J. L., Demerjian, K. L., Borrmann, S., and Worsnop, D. R.: A new Time-of-Flight Aerosol Mass Spectrometer (TOF-AMS)— instrument description and first field deployment, Aerosol Sci. Tech., 39, 637-658, 2005.

Ebeling, J. M. and Jenkins, B. M.: Physical and chemical properties of biomass fuels, Trans. ASAE, 28, 898-902, 1985.

Eck, T. F., Holben, B. N., Reid, J. S., O'Neill, N. T., Schafer, J. S., Dubovik, O., Smirnov, A., Yamasoe, M. A., and Artaxo, P.: High aerosol optical depth biomass burning events: A comparison of optical properties for different source regions, Geophys. Res. Lett., 30, 2035, doi:10.1029/2003GL017861, 2003.

Ferek, R. J., Reid, J. S., Hobbs, P. V., Blake, D. R., and Liousse, C.: Emission factors of hydrocarbons, halocarbons, trace gases, and particles from biomass burning in Brazil, J. Geophys. Res., 103, D24, 32107-32118, doi: 10.1029/98JD00692, 1998.

Finlayson-Pitts, B. J. and Pitts Jr., J. N.: Chemistry of the Upper and Lower Atmosphere, Academic Press., San Diego, USA, p.583,1040, 2000.

Fishman, J., Wozniak, A. E., and Creilson, J. K.: Global distribution of tropospheric ozone from satellite measurements using the empirically corrected tropospheric ozone residual technique: Identification of the regional aspects of air pollution, Atmos. Chem. Phys., 3, 893–907, 2003.

Forster, P., Ramaswamy, V., Artaxo, P., et al.: Changes in Atmospheric Constituents and in Radiative Forcing, in Climate Change 2007: The Physical Science Basis, contribution of

Working Group I to the Fourth Assessment Report of the Intergovernmental Panel on Climate Change, edited by: Solomon, S. D., Qin, M., Manning, Z., Chen, M., Marquis, K. B., Averyt, M. T., and Miller, H. L., Cambridge University Press, Cambridge, United Kingdom and New York, NY, USA, 129–134, 2007.

Fry, J. L., Kiendler-Scharr, A., Rollins, A. W., Brauers, T., Brown, S. S., Dorn, H.-P., Dube, W. P., Fuchs, H., Mensah, A., Rohrer, F., Tillmann, R., Wahner, A., Wooldridge, P. J., and Cohen, R. C.: SOA from limonene: role of NO_3 in its generation and degradation, Atmos. Chem. Phys., 11, 3879-3894, 2011.

Goode, J. G., Yokelson, R. J., Ward, D. E., Susott, R. A., Babbitt, R. E., Davies, M. A., and Hao, W. M.: Measurements of excess O_3, CO_2, CO, CH_4, C_2H_4, C_2H_2, HCN, NO, NH_3, HCOOH, CH_3COOH, HCHO, and CH_3OH in 1997 Alaskan biomass burning plumes by airborne Fourier transform infrared spectroscopy (AFTIR), J. Geophys. Res., 105, D17, 22147- 22166, doi:10.1029/2000JD900287, 2000.

Grieshop, A. P., Logue, J. M., Donahue, N. M., and Robinson, A. L.: Laboratory investigation of photochemical oxidation of organic aerosol from wood fires – Part 1: Measurement and simulation of organic aerosol evolution, Atmos. Chem. Phys., 9, 1263–1277, 2009.

Griffin, R. J., Cocker III, D. R., and Seinfeld, J. H.: Estimate of global atmospheric organic aerosol from oxidation of biogenic hydrocarbons, Geophys. Res. Lett., 26, 17, 2721-2724, 1999.

Griffith, D. W. T.: Synthetic calibration and quantitative analysis of gas-phase FTIR spectra, Appl. Spectrosc., 50, 59-70, 1996.

Guenther, A., Karl, T., Harley, P., Wiedinmyer, C., Palmer, P. I., and Geron, C.: Estimates of global terrestrial isoprene emissions using MEGAN (Model of Emissions of Gases and Aerosols from Nature), Atmos. Chem. Phys., 6, 3181-3210, 2006.

Haines T.K., Cleaves D.A.: The legal environment for forestry prescribed burning in the south: Regulatory programs and voluntary guidelines, So. J. Applied Forestry 23, 170–74. 1999.

Hamilton, J. F., Rami Alfarra, M., Wyche, K. P., Ward, M. W., Lewis, A. C., McFiggans, G. B., Good, N., Monks, P. S., Carr, T., White, I. R., and Purvis, R. M.: Investigating the use of secondary organic aerosol as seed particles in simulation chamber experiments, Atmos. Chem. Phys., 11, 5917-5929, 2011.

Hanst, P. L., Spiller, L. L., Watts, D. M., Spence, J. W., and Miller, M. F.: Infrared measurements of fluorocarbons, carbon tetrachloride, carbonyl sulfide and other atmospheric trace gases, J. of the Air Pollution Control Association, 25, 1220-1226, 1975.

Hardy, C. C., Ottmar, R. D., Peterson, J. L., Core, J. E., and Seamon, P.: Smoke management guide for prescribed and wildland fire; 2001 ed., PMS 420-2, National Wildifre Coordinating group, Boise, ID. 226 p., 2001.

Hennigan, C. J., Miracolo, M. A., Engelhart, G. J., May, A. A., Presto, A. A., Lee, T., Sullivan, A. P., McMeeking, G. R., Coe, H., Wold, C. E., Hao, W.-M., Gilman, J. B., Kuster, W. C., de Gouw, J., Schichtel, B. A., J. L. Collett Jr., Kreidenweis, S. M., and Robinson, A. L.: Chemical and physical transformations of organic aerosol from the photo-oxidation of

open biomass burning emissions in an environmental chamber, Atmos. Chem.Phys., 11, 7669–7686, doi:10.5194/acp-11-7669-2011, 2011.

Hobbs, P. V., Reid, J. S., Herring, J. A., Nance, J. D., Weiss, R. E., Ross, J. L., Hegg, D. A., Ottmar, R. D., and Liousse, C.: Particle and trace-gas measurements in smoke from prescribed burns of forest products in the Pacific Northwest. Paper presented at the Biomass Burning and Global Change, Vol. 1, New York, USA, 1996.

Hobbs, P. V., Reid, J. S., Kotchenruther, R. A., Ferek, R. J., and Weiss, R.: Direct Radiative Forcing by Smoke from Biomass Burning, Science, 275 (5307), 1777-8, 1997.

Hobbs, P.V., Sinha, P., Yokelson, R. J., Christian, T. J., Blake, D. R., Gao, S., Kirchstetter, T.W., Novakov, T., and Pilewskie, P.: Evolution of gases and particles from a savanna fire in South Africa, J. Geophys. Res., 108, D13, 8485, doi:10.1029/2002JD002352, 2003.

Holzinger, R., Williams, J., Salisbury, G., Klupfel, T., de Reus, M., Traub, M., Crutzen, P. J., and Lelieveld, J.: Oxygenated compounds in aged biomass burning plumes over the Eastern Mediterranean: evidence for strong secondary production of methanol and acetone, Atmos. Chem. Phys., 5, 39-46, 2005.

Holzinger, R., Williams, J., Herrmann, F., Lelieveld, J., Donahue, N. M., and Rockmann, T.: Aerosol analysis using a Thermal-Desorption Proton-Transfer-Reaction Mass Spectrometer (TD-PTR-MS): a new approach to study processing of organic aerosols, Atmos. Chem. Phys., 10, 2257-2267, 2010.

Jacob, D. J., Field, B. D., Jin, E. M., Bey, I., Li, Q., Logan, J. A., Yantosca, R. M., and Singh, H. B.: Atmospheric budget of acetone, J. Geophys. Res.,107(D12), 4110, doi:10.1029/2001JD000694, 2002.

Jacob, D. J., Field, B. D., Li, Q., Blake, D. R., de Gouw, J., Warneke, C., Hansel, A., Wisthaler, A., Singh, H. B., and Guenther, A.: Global budget of methanol: Constraints from atmospheric observations, J. Geophys. Res., 110, D08303, doi:10.1029/2004JD005172, 2005.

Jacob, D. J., Crawford, J. H., Maring, H., Clarke, A. D., Dibb, J. E., Emmons, L. K., Ferrare, R. A., Hostetler, C. A., Russell, P. B., Singh, H. B., Thompson, A. M., Shaw, G. E., McCauley, E., Pederson, J. R., and Fisher, J. A.: The Arctic Research of the Composition of the Troposphere from Aircraft and Satellite (ARCTAS) mission: Design, execution, and first results, Atmos. Chem. Phys., 10, 5191–5212, doi:10.5194/acp-10-5191-2010, 2010.

Johnson, T. J., Masiello, T., and Sharpe, S. W.: The quantitative infrared and NIR spectrum of CH_2I_2 vapor: vibrational assignments and potential for atmospheric monitoring, Atmos. Chem. Phys., 6, 2581–2591, doi:10.5194/acp-6-2581-2006, 2006.

Johnson, T. J., Profeta, L. T. M., Sams, R. L., Griffith, D. W. T., and Yokelson, R. J.: An infrared spectral database for detection of gases emitted by biomass burning, Vib. Spectrosc., 53, 97–102, 2010.

Jost, C., Trentmann, J., Sprung, D., Andreae, M. O., McQuaid, J. B., and Barjat, H.: Trace gas chemistry in a young biomass burning plume over Namibia: observations and model simulations, J. Geophys. Res., 108, D13, 8482, doi:10.1029/2002JD002431, 2003.

Kanakidou, M., Seinfeld, J. H., Pandis, S. N., Barnes, I., Dentener, F. J., Facchini, M. C., Van Dingenen, R., Ervens, B., Nenes, A., Nielsen, C. J., Swietlicki, E., Putaud, J. P., Balkanski, Y., Fuzzi, S., Horth, J., Moortgat, G. K., Winterhalter, R., Myhre, C. E. L., Tsigaridis, K., Vignati, E., Stephanou, E. G., and Wilson, J.: Organic aerosol and global climate modelling: A review. *Atmos. Chem. Phys*, 5, 1053-1123, doi:10.5194/acp-5-1053-2005, 2005.

Karl, T. G., Christian, T. J., Yokelson, R. J., Artaxo, P., Hao, W. M., and Guenther, A.: The tropical forest and fire emissions experiment: Method evaluation of volatile organic compound emissions measured by PTR-MS, FTIR, and GC from tropical biomass burning, Atmos. Chem. Phys., 7, 5883–5897, 2007.

Kauffman, J. B.: Death rides the forest: perceptions of fire, land use, and ecological restoration of western forests, Conserv. Biol., 18(4), 878-882, 2004.

Kaufman, Y. J., Justice, C. O., Flynn, L. P., Kendall, J. D., Prins, E. M., Giglio, L., Ward, D. E., Menzel, W. P., and Setzer, A. W.: Potential global fire monitoring from EOS-MODIS, J. Geophys. Res., 103, 32215-32238, 1998.

Keeley, J.E., Aplet, G.H., Christensen, N. L., Conard, S. G., Johnson, E. A., Omi, P. N., Peterson, D. L., and Swetnam, T. W.: Ecological foundations for fire management in

North American Forest and shrubland ecosystems, General Technical Report PNW–GTR–779, Portland: U.S. Forest Service, 2009.

Keene, W. C., Lobert, J. M., Crutzen, P. J., Maben, J. R., Scharffe, D. H., Landmann, T., Hely, C., and Brain, C.: Emissions of major gaseous and particulate species during experimental burns of southern African biomass, J. Geophys. Res., 111, D04301, doi:10.1029/2005jd006319, 2006.

Lane, P. N. J., Sheridan, G. J., Noske, P. J., Sherwin, C. B.: Phosphorus and nitrogen exports from SE Australian forests following wildfire. Journal of Hydrology, 361, 186–198. doi:10.1016/J.JHYDROL.2008.07.041, 2008.

Lapina, K., Honrath, R. E., Owen, R. C., Val Martin, M., and Pfister, G.: Evidence of significant large-scale impacts of boreal fires on ozone levels in the midlatitude Northern Hemisphere free troposphere, Geosphys. Res. Lett., 33, L10815, doi:10.1029/2006GL025878, 2006.

Lee, A., Goldstein, A. H., Kroll, J. H., Ng, N. L., Varutbangkul, V., Flagan, R. C., and Seinfeld, J. H.: Gas-phase products and secondary aerosol yields from the photooxidation of 16 different terpenes, J. Geophys. Res., 111, D17305, doi:10.1029/2006JD007050, 2006.

Lee S., W. Liu, Y. Wang, Russell, A., and Edgerton, E. S.: Source Apportionments of PM2.5: Comparing PMF and CMB Results for 4 Southeast US Sites, Atmos. Environ., 42, 4126-4137, 2008.

Lefer, B. L., Talbot, R. W., Harriss, R. C., Bradshaw, J. D., Sandholm, S. T., Olson, J. O., Sachse, G. W., Collins, J., Shipham, M. A., Blake, D. R., Klemm, K. I., Klemm, O.,

Gorzelska, K., and Barrick, J.: Enhancement of acidic gases in biomass burning impacted air masses over Canada, J. Geophys. Res., 99, D1, 1721-1737, 1994.

Lelieveld, J., Butler, T. M., Crowley, J. N., Dillon, T. J., Fischer, H., Ganzeveld, L., Harder, H., Lawrence, M. G., Martinez, M., Taraborrelli, D., and Williams, J.: Atmospheric oxidation capacity sustained by a tropical forest, Nature, 452, 737-740, 2008.

Lenschow, D., Paluch, I., Bandy, A., Thornton, D., Blake, D., and Simpson, I.: Use of a mixed-layer model to estimate dimethylsulfide flux and application to other trace gas fluxes, J. Geophys. Res., 104(D13), doi:10.1029/1998JD100090, 1999.

Li, Q., Jacob, D. J., Yantosca, R. M., Heald, C. L., Singh, H. B., Koike, M., Zhao, Y., Sachse, G. W., and Streets, D. G.: A global three-dimensional model analysis of the atmospheric budgets of HCN and CH_3CN: Constraints from aircraft and ground measurements, J. Geophys. Res., 108 (D21), 8827, doi: 10.1029/2002JD003075, 2003.

Lobert, J. M., D. H. Scharffe, W. M. Hao, T. A. Kuhlbusch, R. Seuwen, P. Wameck, and P. J. Crutzen, Experimental evaluation of biomass burning emissions: Nitrogen and carbon containing compounds, in Global Biomass Burning: Atmospheric, Climatic and Biospheric Implications, edited by J. S. Levine, pp. 289-304, MIT Press, Cambridge, Mass., 1991.

Maksymiuk, C. S., Gayahtri, C., Gil, R. R., and Donahue, N. M.: Secondary organic aerosol formation from multiphase oxidation of limonene by ozone: mechanistic constraints via two dimensional heteronuclear NMR spectroscopy, Phys. Chem. Chem. Phys., 11, 7810–7818, doi:10.1039/b820005j, 2009.

Mason, S. A., Field, R. J., Yokelson, R. J., Kochivar, M. A., Tinsley, M. R., Ward, D. E., and Hao, W. M.: Complex effects arising in smoke plume simulations due to inclusion of direct emissions of oxygenated organic species from biomass combustion, J. Geophys. Res., 106(D12), 12527-12539, 2001.

McMeeking, G. R., Kreidenweis, S. M., Lunden, M., Carrillo, J., Carrico, C. M., Lee, T., Herckes, P., Engling, G., Day, D. E., Hand, J., Brown, N., Malm, W. C., and Collett Jr., J. L. :Smoke-impacted regional haze in California during the summer of 2002, Agricultural and Forest Meteorology, 137, 25-42, 2006.

McMeeking, G. R., Kreidenweis, S. M., Baker, S., Carrico, C. M., Chow, J. C., Collet Jr., J. L., Hao, W. M., Holden, A. S., Kirchstetter, T. W., Malm, W. C., Moosmüller, H., Sullivan, A. P., and Wold, C. E.: Emissions of trace gases and aerosols during the open combustion of biomass in the laboratory, J. Geophys. Res., 114, D19210, doi:10.1029/2009JD011836, 2009.

Moteki, N., and Kondo, Y.: Effects of mixing state of black carbon measurements by laser-induced incandescence, Aerosol Sci. Tech., 41, 4, 398-417, 2007.

Muller, J.-F., Capouet, M., Wallens, S., and Stavrakou, T., Vinckier, C., Vankerckhoven, H., Van den Bergh, V., Coeckerberghs, H., Compernolle, F., Peeters, J., Vereecken, L., Fantechi, G., Hermans, I., Coeck, C., Nguyen, T. L., Jacobs, P., Arijs, E., Amelynck, C., and Schoon, N.: Anthropogenic and biogenic influences on the oxidation capacity of the atmosphere, SPSDII Report, Belgian Science Policy Office, 2005.

Naeher, L. P., Achtemeier, G. L., Glitzenstein, J. S., Streng, D. R. and Macintosh, D.: Real-time and time-integrated $PM_{2.5}$ and CO from prescribed burns in chipped and non-chipped plots: firefighter and community exposure and health implications, J. Expos. Sci. Environ. Epidemiol., 16, 351-361, doi:10.1038/sj.jes.7500497, 2006.

Neary, D. G., Ryan, K. C., DeBano, L. F., Landsberg, J. D., and Brown, J. K.: Chapter 1: Introduction, in: Wildland fire and ecosystems, 2005, Neary, D. G., Ryan, K. C., and DeBano, L. F. (Eds.), Department of Agriculture, Forest Service, Rocky Mountain Research Station, Ogden, UT., 1-17, 2005.

Paine, T. D., Blanche, C. A., Nebeker, T. E., Stephen, F. M.: Composition of loblolly pine resin defenses: comparison of monoterpenes from induced lesion and sapwood resin, Can. J. For. Res., 17, 1202-1206, 1987.

Pan, X., Underwood, J. S., Xing, J. -H., Mang, S. A., and Nizkorodov, S. A.: Photodegradation of secondary organic aerosol generated from limonene oxidation by ozone studied with chemical ionization mass spectrometry, Atmos. Chem. Phys., 9, 3851-3865, 2009.

Paulot, F., Crounse, J. D., Kjaergaard, H. G., Kürten, A., St. Clair, J. M., Seinfeld, J. H., Wennberg, P. O.: Unexpected epoxide formation in the gas-phase photooxidation of isoprene, Science, 325, 730-733, 2009.

Park, R. J., Jacob, D. J., and Logan, J. A.: Fire and biofuel contributions to annual mean aerosol mass concentrations in the United States, Atmos. Environ., 41, 7389-7400, 2007.

Peeters, J., Nguyen, T. L., Vereecken, L.: HO_x radical regeneration in the oxidation of isoprene, Phys. Chem. Chem. Phys., 11, 5935-5939, 2009.

Pfister, G. G., Emmons, L. K., Hess, P. G., Honrath, R., Lamarque, J.-F., Val Martin, M., Owen, R. C., Avery, M. A., Browell, E. V., Holloway, J. S., Nedelec, P., Purvis, R., Ryerson, T. B., Sachse, G. W., and Schlager, H.: Ozone production from the 2004 North American boreal fires, J. Geophys, Res., 111, D24S07, doi:10.1029/2006JD007695, 2006.

Pfister, G., Emmons, L., and Wiedinmyer C.: Impacts of the Fall 2007 California wildfires on surface ozone: Integrating local observations with global model simulations, Geophys. Res. Lett., 35, L19814, doi:10.1029/2008GL034747, 2007.

Ramanathan, V., and Carmichael, G.: Global and regional climate changes due to black carbon, Nature, 1, 221-227, 2008.

Rappold, A.G., Stone, S.L., Cascio, W.E., Neas, L.M., Kilaru, V.J., Carraway, M.S.,Szykman, J.J., Ising, A., Cleve, W.E., Meredith, J.T., Vaughan-Batten, H., Deyneka, L., and Devlin, R.B.: Peat bog wildfire smoke exposure in rural North Carolina is associated with cardio-pulmonary emergency department visits assessed through syndromic surveillance, Environ. Health Perspect., 119, 1415-1420, http://dx.doi.org/10.1289/ehp.1003206, 2011.

Reid, J. S., Hobbs, P. V., Ferek, R. J., Martins, J. V., Blake, D. R., Dunlap, M. R., and Liousse, C.: Physical, chemical, and radiative characteristics of the smoke dominated regional hazes over Brazil, J. Geophys. Res., 103, 32059-32080, 1998.

Reid, J. S., Koppmann, R., Eck, T. F., and Eleuterio, D. P.: A review of biomass burning emissions part II: intensive physical properties of biomass burning particles, Atmos. Chem. Phys., 5, 799-825, 2005a.

Reid, J. S., Eck, T. F., Christopher, S. A., Koppmann, R., Dubovik, O., Eleuterio, D. P., Holben, B. N., Reid, E. A., and Zhang, J.: A review of biomass burning emissions part III: intensive optical properties of biomass burning particles, Atmos. Chem. Phys., 5, 827-849, 2005b.

Rein, G., Cohen, S. and Simeoni, A.: Carbon emissions from smouldering peat in shallow and strong fronts, Proceedings of the Combustion Institute, 32, 2489-2496, doi:10.1016/j.proci.2008.07.008, 2009.

Roberts, J. M., Veres, P. R., Cochran, A. K., Warneke, C., Burling, I. R., Yokelson, R. J., Lerner, B., Gilman, J. B., Kuster, W. C., Fall, R., and de Gouw, J.: Isocyanic acid in the atmosphere and its possible link to smoke-related health effects, Proc. Natl. Acad. Sci. U. S. A., 108(22), 8966–8971, doi:10.1073/pnas.1103352108, 2011.

Rosenfeld, D.: TRMM observed first direct evidence of smoke from forest fires inhibiting rainfall, Geophys. Res. Lett., 26 (20), 3105–3108, 1999.

Rothman, L. S., Gordon, I. E., Barbe, A., Benner, D. C., Bernath, P. F., Birk, M., Boudon, V., Brown, L. R., Campargue, A., Champion, J. P., Chance, K., Coudert, L. H., Dana, V., Devi, V. M., Fally, S., Flaud, J. M., Gamache, R. R., Goldman, A., Jacquemart, D., Kleiner, I., Lacome, N., Lafferty, W. J., Mandin, J. Y., Massie, S. T., Mikhailenko, S. N., Miller, C. E., Moazzen-Ahmadi, N., Naumenko, O. V., Nikitin, A. V., Orphal, J., Perevalov, V. I., Perrin, A., Predoi-Cross, A., Rinsland, C. P., Rotger, M., Simecková, M., Smith, M. A. H., Sung, K., Tashkun, S. A., Tennyson, J., Toth, R. A., Vandaele, A. C. and Vander Auwera, J.: The HITRAN 2008 molecular spectroscopic database, J. Quant. Spectrosc. Radiat. Transfer, 110, 533-572, 2009.

Saathoff, H., Naumann, K. –H., Mohler, O., Jonsson, A. M., Hallquist, M., Kiendler-Scharr, A., Mentel, T. F., Tillmann, R., and Schurath, U.: Temperature dependence of yields of secondary organic aerosols from the ozonolysis of α-pinene and limonene, Atmos. Chem. Phys., 9, 1551-1577, 2009.

Sandberg, D. V., Ottmar, R. D., Peterson, J. L., and Core, J.: Wildland fire on ecosystems: effects of fire on air, Gen. Tech. Rep. RMRS-GTR-42-vol. 5, Ogden, UT., U.S., Department of Agriculture, Forest Service, Rocky Mountain Research Station, 2002.

Sander, S. P., Finlayson-Pitts, B. J., Friedl, R. R., Golden, D. M., Huie, R. E., Keller-Rudek, H., Kolb, C. E., Kurylo, M. J., Molina, M. J., Moortgat, G. K., Orkin, V. L., Ravishankara, A. R., and Wine, P. W.: Chemical kinetics and photochemical data for use in atmospheric studies, Evaluation Number 15 (JPL Publication 06-2), Jet Propulsion Laboratory, Pasadena, CA, 2006.

Seiler, W. and Crutzen, P. J.: Estimates of gross and net fluxes of carbon between the biosphere and the atmosphere from biomass burning, Climatic Change, 2, 207-247, 1980.

Seinfeld, J. H. and Pandis, S. N.: Atmospheric Chemistry and Physics— From Air Pollution to Climate Change, John Wiley & Sons, New York, USA, 1998.

Sharpe, S. W., Johnson, T. J., Sams, R. L., Chu, P. M., Rhoderick, G. C., and Johnson, P. A.: Gas-phase databases for quantitative infrared spectroscopy, Appl. Spectrosc., 58, 1452–1461, 2004.

Simpson, I. J., Akagi, S. K., Barletta, B., Blake, N. J., Choi, Y., Diskin, G. S., Fried, A., Fuelberg, H. E., Meinardi, S., Rowland, F. S., Vay, S. A., Weinheimer, A. J., Wennberg,

P. O., Wiebring, P., Wisthaler, A., Yang, M., Yokelson, R. J., and Blake, D. R.: Boreal forest fire emissions in fresh Canadian smoke plumes: C1-C10 volatile organic compounds (VOCs), CO2, CO, NO2, NO, HCN, and CH3CN, Atmos. Chem. Phys., 11, 6445-6463, 2011.

Singh, H. B., Kanakidou, M., Crutzen, P. J., and Jacob, D. J.: High concentrations and photochemical fate of oxygenated hydrocarbons in the global atmosphere. Nature, 378, 50–54, 1995.

Sinha, P., Hobbs, P. V., Yokelson, R. J., Blake, D. R., Gao, S., and Kirchstetter, T. W.: Emissions from miombo woodland and dambo grassland savanna fires, J. Geophys. Res., 109, D11305, doi:10.1029/2004JD004521, 2004.

Stephens, M., Turner, N., and Sandberg, J.: Particle identification by laser-induced incandescence in a solid-state laser cavity, Appl. Opt., 42(19), 3726–3736, 2003.

Stephens, S. L., Martin, R. E., and Clinton, N. E.: Prehistoric fire area and emissions from California's forests, woodlands, shrublands, and grasslands, Forest Ecology and Management 251, 205–216, 2007.

Sudo, K. and Akimoto, H.: Global source attribution of tropospheric ozone: Long-range transport from various source regions, J. Geophys. Res. 112, D12302, doi:10.1029/2006JD007992, 2007.

Susott, R. A., Olbu, G. J., Baker, S. P., Ward, D. E. Kauffman, J. B., and Shea, R. W.: Carbon, hydrogen, nitrogen, and thermogravimetric analysis of tropical ecosystem biomass, in:

Global Biomass Burning: Atmospheric, Climatic, and Biospheric Implications, edited by: Levine, J. S., pp. 249-259, MIT Press, Cambridge, MA, 1996.

Tabazadeh, A., Yokelson, R. J., Singh, H. B., Hobbs, P. V., Crawford, J. H., and Iraci, L. T.: Heterogeneous chemistry involving methanol in tropospheric clouds, Geophys. Res. Lett., 31, L06114, doi:10.1029/2003GL018775, 2004.

Tereszchuk, K. A., González Abad, G., Clerbaux, C., Hurtmans, D., Coheur, P.-F., and Bernath, P. F.: ACE-FTS measurements of trace species in the characterization of biomass burning plumes, Atmos. Chem. Phys., 11, 12169-12179, doi:10.5194/acp-11-12169-2011, 2011.

Trentmann, J., Yokelson, R. J., Hobbs, P. V., Winterrath, T., Christian, T. J., Andreae, M. O., and Mason, S. A.: An analysis of the chemical processes in the smoke plume from a savanna fire, J. Geophys. Res., 110, D12301, doi:10.1029/2004JD005628, 2005.

Val Martín, M., Honrath, R. E., Owen, R. C., Pfister, G., Fialho, P., and Barata, F.: Significant enhancements of nitrogen oxides, black carbon, and ozone in the North Atlantic lower free troposphere resulting from North American boreal wildfires, J. Geophys. Res., 111, D23S60, doi:10.1029/2006JD007530, 2006.

van der Werf, G. R., Randerson, J. T., Giglio, L., Collatz, G. J., Mu, M., Kasibhatla, P. S., Morton, D. C., DeFries, R. S., Jin, Y., and van Leeuwen, T. T.: Global fire emissions and the contribution of deforestation, savanna, forest, agricultural, and peat fires (1997-2009), Atmos. Chem. Phys., 10, 11707-11735, doi:10.5194/acp-10-11707-2010, 2010.

Vermote, E., Ellicott, E., Dubovik, O., Lapyonok, T., Chin, M., Giglio, L., and Roberts, G.: An approach to measure global biomass burning emissions of organic and black carbon from MODIS fire Radiative power, J. Geophys. Res., 114, D18205, doi:10.1029/2008JD011188, 2009.

Vrehoussis, M., Kanadidou, M., Mihalopoulos, N., Crutzen, P. J., Lelieveld, J., Perner, D., Berresheim, H., and Baboukas, E.: Role of the NO3 radicals in oxidation processes in the eastern Mediterranean troposphere during the MINOS campaign, Atmos. Chem. Phys., 4, 169-182, 2004.

Walser, M. L., Park, J., Gomez, A. L., Russell, A. R., and Nizkorodov, S. A.: Photochemical Aging of Secondary Organic Aerosol Particles Generated from the Oxidation of d-Limonene, J. Phys. Chem. A, 111, 1907–1913, doi:10.1021/jp066293l, 2007.

Ward, D. E. and Radke, L. F.: Emissions measurements from vegetation fires: A Comparative evaluation of methods and results, Fire in the Environment: The Ecological, Atmospheric and Climatic Importance of Vegetation Fires, Crutzen, P. J. and Goldammer, J. G. (Eds.), John Wiley, New York, 53-76, 1993.

Watson, J. G.: Visibility: Science and regulation, J. Air Waste Manage. Assoc., 52, 628-713, 2002.

Wiedinmyer, C., and Hurteau, M. D.: Prescribed fire as a means of reducing forest carbon emissions in the Western United States, Environ. Sci. Technol., 44, 1926-1932, 2010.

Wofsy, S. C., Sachse, G. W., Gregory, G. L., Blake, D. R., Bradshaw, J. D., Sandholm, S. T., Singh, H. B., Barrick, J. A., Harriss, R. C., Talbot, R. W., Shipham, M. A., Browell, E.

V., Jacob, D. J., and Logan, J. A.: Atmospheric chemistry in the Arctic and subarctic: Influence of natural fires, industrial emissions, and stratospheric inputs, J. Geophys Res., 97, 16731-16746, 1992.

Xu, X., Bingemer, H. G., and Schmidt, U.: The flux of carbonyl sulfide and carbon disulfide between the atmosphere and a spruce forest, Atmos. Chem. Phys., 2, 171-181, doi:10.5194/acp-2-171-2002, 2002.

Yoder, J., Tilley, M., Engle, D., and Fuhlendorf, D. Economics and prescribed fire law in the United States, Applied Economic Perspectives and Policy, 25, 218-233, doi: 10.1111/1467-9353.00055, 2003.

Yokelson, R. J., Griffith, D. W. T., Burkholder, J. B., and Ward, D. E.: Accuracy and advantages of synthetic calibration of smoke spectra, in: Optical Remote Sensing for Environmental and Process Monitoring, Air Waste Manage. Assoc., Pittsburgh, PA, 365–376, 1996.

Yokelson, R. J., Ward, D. E., Susott, R. A., Reardon, J., and Griffith, D. W. T.: Emissions from smoldering combustion of biomass measured by open-path Fourier transform infrared spectroscopy, J. Geophys. Res., 102, D15, 18865–18877, 1997.

Yokelson, R. J., Goode, J. G., Ward, D. E., Susott, R. A., Babbitt, R. E., Wade, D. D., Bertschi, I., Griffith, D. W. T., and Hao, W. M.: Emissions of formaldehyde, acetic acid, methanol, and other trace gases from biomass fires in North Carolina measured by airborne Fourier transform infrared spectroscopy, J. Geophys. Res., 104, D23, 30109–30126, doi:10.1029/1999JD900817, 1999.

Yokelson, R. J., Bertschi, I. T., Christian, T. J., Hobbs, P. V., Ward, D. E., and Hao, W. M.: Trace gas measurements in nascent, aged, and cloud-processed smoke from African savanna fires by airborne Fourier transform infrared spectroscopy (AFTIR), J. Geophys. Res., 108, 8478, doi:10.1029/2002JD002322, 2003.

Yokelson, R. J., Karl, T., Artaxo, P., Blake, D. R., Christian, T. J., Griffith, D. W. T., Guenther, A., and Hao, W. M.: The Tropical Forest and Fire Emissions Experiment: overview and airborne fire emission factor measurements, Atmos. Chem. Phys., 7, 5175-5196, 2007a.

Yokelson, R. J., Urbanski, S. P., Atlas, E. L., Toohey, D. W., Alvarado, E. C., Crounse, J. D., Wennberg, P. O., Fisher, M. E., Wold, C. E., Campos, T. L., Adachi, K., Buseck, P. R., and Hao, W. M.: Emissions from forest fires near Mexico City, Atmos. Chem. Phys., 7, 5569-5584, 2007b.

Yokelson, R. J., Christian, T. J., Karl, T. G., and Guenther, A.: The tropical forest and fire emissions experiment: laboratory fire measurements and synthesis of campaign data, Atmos. Chem. Phys., 8, 3509-3527, 2008.

Yokelson, R. J., Crounse, J. D., DeCarlo, P. F., Karl, T., Urbanski, S., Atlas, E., Campos, T., Shinozuka, Y., Kapustin, V., Clark, A. D., Weinheimer, A., Knapp, D. J., Montzka, D. D., Holloway, J., Weibring, P., Flocke, F., Zheng, W., Toohey, D., Wennberg, P. O., Wiedinmyer, C., Mauldin, L., Fried, A., Richter, D., Walega, J., Jimenez, J. L., Adachi, K., Buseck, P. R., Hall, S. R., and Shetter, R.: Emissions from biomass burning in the Yucatan, Atmos. Chem. Phys., 9, 5785-5812, 2009.

Yokelson, R. J., Burling, I. R., Urbanski, S. P., Atlas, E. L., Adachi, K., Buseck, P. R., Wiedenmyer, C., Akagi, S. K., Toohey, D. W., and Wold, C. E.: Trace gas and particle emissions from open biomass burning in Mexico, Atmos. Chem. Phys., 11, 6787-6808, 2011.

Yokelson, R. J., Burling, I. R., Gilman, J., Warneke, C., Stockwell, C. E., de Gouw, J., Akagi, S. K., Urbanski, S. P., Veres, P., Roberts, J. M., Kuster, W., Reardon, J., Griffith, D. W. T., Johnson, T. J., and Weise, D. R.: Merging field and laboratory measurements to estimate the emission factors for known and unknown trace gases emitted by some prescribed fires in the US., in preparation for Atmos. Chem. Phys., 2012.

6 APPENDIX

6.1 *SCREAM Acknowledgements*

This work was supported by the Strategic Environmental Research and Development Program (SERDP) project RC-1649 and administered partly through Forest Service Research Joint Venture Agreement 08JV11272166039, and we thank the sponsors for their support. Shawn Urbanski and some of the Twin Otter flight hours were supported by Joint Fire Science Program grant 08-1-6-09. We appreciate the efforts of "Jim's crew" to measure the consumption of wildland fuels for this study. Adaptation of the USFS Twin Otter for research flights was supported primarily by NSF grant ATM 0513055. Special thanks to our pilot Bill Mank and Twin Otter mechanic Steve Woods. We greatly appreciate the collaboration and efforts of John Maitland and forestry staff at Fort Jackson and we thank the Columbia dispatch office of the South Carolina Forestry Commission for assistance in locating fires to sample.